Fakultät für Medizin

Urologische Klinik und Poliklinik

Therapeutic targeting of signal transduction pathways in bladder cancer

Anuja Sathe

Vollständiger Abdruck der von der Fakultät für Medizin der Technischen Universität München zur Erlangung des akademischen Grades eines

Doctor of Philosophy (Ph.D.)

genehmigten Dissertation.

Vorsitzender: Univ.-Prof. Dr. Roland M. Schmid

Betreuer: Univ.-Prof. Dr. Jürgen E. Gschwend

Prüfer der Dissertation:

1. apl Prof. Dr. Margitta Retz
2. apl. Prof. Dr. Dieter Saur

Die Dissertation wurde am 27.05.15 bei der Fakultät für Medizin der Technischen Universität München eingereicht und durch die Fakultät für Medizin am 26.08.15 angenommen.

"Down to their innate molecular core, cancer cells are hyperactive, survival-endowed, scrappy, fecund, inventive copies of ourselves."

-Siddhartha Mukherjee, The Emperor of All Maladies: A Biography of Cancer, 2010

Abstract

Therapeutic targeting of signal transduction pathways represents a new treatment strategy, which can potentially improve the prognosis of advanced bladder cancer (BLCA). We characterized AKT and CDK 4/6 as novel treatment targets. AKT inhibition was effective only in cells possessing hotspot helical domain mutations in *PIK3CA*. This sensitivity correlated with a DUSP1-dependent ERK 1/2 dephosphorylation and was mediated via an increase in apoptosis. CDK 4/6 inhibition was effective only in cells expressing RB and led to a reduction in E2F target genes and cell cycle progression. This sensitivity correlated with a reduction in total RB expression. *In vitro* data was also extended to a three-dimensional, *in vivo* xenograft model. Mutant *PIK3CA*, found in 20-25%, and RB expression, found in 75-80% BLCA, can potentially be used as stratifying and predictive biomarkers for response to AKT and CDK 4/6 inhibition respectively.

Keywords: Bladder cancer, signal transduction, target therapy, personalized medicine, biomarkers, PI3K/AKT, CDK 4/6, RB

Acknowledgments

This thesis would not have been possible without the help of many people. First and foremost, I wish to thank my thesis adviser, Prof. Dr. Gschwend, for giving me the opportunity to work in the department. Many thanks also to Prof. Dr. Retz for her support on the thesis committee.

I would like to express my heartfelt and sincere gratitude to Dr. Roman Nawroth, my thesis supervisor. I had the opportunity to work on a project that was very interesting and well-designed. His supervision through the years has helped me to learn many aspects of scientific methodology, scientific writing and critical thinking. His attention to thoroughness in experiment design, reproducibility and repeatibility of data, controlling experimental conditions and troubleshooting are lessons for life. I am very thankful for the many discussions we have had that widened my scientific outlook immensely. He has been an excellent mentor who was approachable for the planning and discussion of my work at all stages of the thesis. I am most grateful that he encouraged me to think independently to generate hypotheses and let me pursue them with his guidance. I am also thankful for the teaching and supervision opportunities that he created for me and helped me to execute.

I also wish to acknowledge the support of Dr. Marcus V. Cronauer and Ms. Felicitas Genze at the University of Ulm for their guidance in establishing the chorioallantoic membrane assay.

I also extend my gratitude to the Wilhelm-Sander Stiftung and the Siegfried-Gruber-Stiftung for financial support for this project.

Thanks also to Dr. Per Sonne Holm for helpful advice and discussions. I would also like to thank Claude Kraemer, Ferdinand Guerth and Nicole Koshy for their technical support in experimental methods. Many thanks are due to Monika Moissl and Klaus Mantwill for their patient assistance and advice in all things everyday in the lab. I also wish to thank Angelika Lolic for her help around the lab. I extend my regards to all the past and present members of the Nawroth and Holm groups. The atmosphere in the lab has always been very friendly and co-operative, which made it an excellent place to work.

Many thanks also to all the wonderful friends I made at the graduate school. Your presence has contributed greatly in making Munich an incredible place to be in. Lastly, I want to thank my family for always encouraging me to pursue my academic goals. Your love and support mean a lot.

Contents

List of Figures

List of Tables

List of Symbols and Abbreviations

µl	microlitre
ml	millilitre
l	litre
nm	nanometer
µm	micrometer
cm	centimeter
m	meter
ng	nanogram
µg	microgram
mg	milligram
nM	nanomolar
µM	micromolar
mM	millimolar
fmol	femtomole
nmol	nanomole
µmol	micromole
mmol	millimole
N	normal
V	volt
°C	degree Celsius
s	second
min	minute
w/v	weight/volume
4E-BP1	Eukaryotic translation initiation factor 4E-binding protein 1
7-AAD	7-aminoactinomycin D
AGC	Protein kinase A, G and C

AKT	v-akt murine thymoma viral oncogene
APS	ammonium persulfate
ASP	Allele specific
ATP	Adenosine triphosphate
BAD	Bcl-2-associated death promoter
BCA	bicinchoninic acid
Bcl-2	B-cell lymphoma 2
BLCA	Bladder cancer
BSA	Bovine serum albumin
$CaCl_2$	Calcium chloride
CAM	Chorioallantoic membrane
CCLE	Cancer cell line Encylopedia
cDNA	Complementary DNA
CDK	Cyclin dependent kinases
CDKI	Cyclin dependent kinase inhibitor
CI	Combination index
CIS	Carcinoma in situ
CML	Chronic myelogenous leukemia
$C0_2$	Carbon dioxide
COSMIC	Catalogue of somatic mutations in cancer
CpG	Cytosine-Phosphate-Guanine
CREB	cAMP response element-binding protein
CST	Cell Signalling technology
ctrl	Control
Deptor	DEP-domain-containing mTOR-interacting protein
DSS	Disease specific survival
DMEM	Dulbecco's Modified Eagle's Medium
DMSO	dimethylsulfoxide
DNA	Deoxyribonucleic acid
DTT	dithiothreitol
DUSP1	Dual-specificity phosphatase-1

EAU	European Association for Urology
EDTA	ethylenediaminetetraacetic acid
EdU	5 ethynyl 2'-deoxyuridine
eIF4E	eukaryotic translation initiation factor 4E
EGFR2	Epidermal growth factor receptor type 2
ERK	Exracellular signal-regulated kinase
FBS	Fetal bovine serum
FDA	Food and drug administration
FGFR3	Fibroblast growth factor receptor-3
FOXO	Forkhead
GC	Gemcitabine, cisplatin
G-PCR	G-protein coupled receptor
GSK	Glycogen synthase kinase
GTP	Guanine triphosphate
GU	Genomically unstable
H_2O_2	Hydrogen peroxide
HCl	Hydrogen chloride
HD	Helican domain
HDAC	histone deacetylase
HRP	Horseradish peroxidase
HM	Hydrophobic motif
HSP	Heat shock protein
IC	Inhibitory concentration
IgG	Immunoglobulin G
IHC	Immunohistochemistry
IRS-1	Insulin receptor substrate-1
KD	Kinase domain
LOH	Loss of heterozygosity
MAPK	Mitogen activated protein kinase
mLST8	mammalian lethal with Sec13 protein 8
mTOR	Mechanistic target of rapamycin

mTORC1	mTOR complex 1
mTORC2	mTOR complex 2
MVAC	Methotrexate, vinblastine, adriamycin, cisplatin
MMP	matrix metalloproteinase
MIBC	muscle invasive bladder cancer
miRNA	microRNA
mSIN1	mammalian stress-activated protein kinase-interacting protein 1
NaCl	Sodium chloride
NaOH	Sodium hydroxide
NEAA	Non-essential amino acids
NAC	Neoadjuvant chemotherapy
NMIBC	Non-muscle invasive bladder cancer
OS	Overall survival
P	Phosphate
PAGE	Polyacrylamide gel electrophoresis
PBS	Phosphate buffered saline
PCR	Polymerase chain reaction
PD-L1	Programmed death-ligand 1
PDK1	protein dependent kinase 1
PFS	Progression free survival
pH	potentia hydrogenii
PH	Pleckstrin homology
PHLPP	PH domain and Leucine rich repeat Protein Phosphatases
PI	phosphatidylinositol
PI3K	phosphoinositide 3-kinase
PLND	Pelvic lymph node dissection
PP2A	Protein phosphatase 2 A
PRAS40	Proline-rich Akt substrate 40
PTEN	phosphatase and tensin homolog
PVDF	Polyvinylidene fluoride
qPCR	Quantitative polymerase chain reaction

Raptor	regulatory associated protein of mTOR
Ras	Rat sarcoma
RB	Retinoblastoma
RC	Radical cystectomy
RCF	Relative Centrifugal Force
RFS	Recurrence free survival
RFU	Relative fluorescence units
Rictor	rapamycin-insensitive companion of mTOR
RNA	Ribonucleic acid
RPMI	Roswell Park Memorial Institute
RTK	Receptor tyrosine kinase
S6K1	Ribosomal protein S6 kinase beta-1
SCC	Squamous cell carcinoma
S.D.	Standard deviation
SDS	Sodium dodecyl sulfate
S.E.	Standard error of the mean
Ser	Serine
SH2	Src homology domain-2
siRNA	Small interfering RNA
TBS	Tris buffered saline
TBST	Tris buffered saline with Tween-20
TCGA	The Cancer Genome Atlas
TEMED	Tetramethylethylenediamine
Thr	Threonine
TKI	Tyrosine kinase inhibitor
TNM	Tumor, Node, Metastasis
TP53	Tumor protein p53
Tris	Tris(hydroxymethyl)-aminomethane
TSC	Tuberous sclerosis complex
TURBT	Transurethral resection of the bladder tumor
UroA	Urobasal A

UroB	Urobasal B
VEGF	Vascular endothelial growth factor
WB	Immunoblotting
WT	Wild type

1 Introduction

Bladder cancer (BLCA) includes neoplastic lesions arising from the tissues of the urinary bladder. Advanced BLCA is a complex, heterogeneous and aggressive disease. Current treatment strategies have had limited success in the management of patients with advanced BLCA. The majority of these patients continue to have poor clinical outcomes.

1.1 Epidemiology of bladder cancer

BLCA was diagnosed in 429000 new patients in 2012 and led to 165000 deaths worldwide (Ferlay et al., 2015). It is the ninth most common cancer and the second most common genitourinary cancer. Men are affected more than women with a worldwide sex ratio of 3.5:1 and it is the sixth most common cancer affecting men. BLCA is mainly a disease of older age groups, with 80% cases occurring in patients over 60 years. Most risk factors associated with the development of BLCA are environmental. Cigarette smoking is the most well-established of these and is associated with more than 50% of cases (Freedman et al., 2011). Smoking for 20 years is associated with an approximately 2-fold higher risk of developing BLCA, while smoking for 60 years increases the risk around 5.5 fold. Increased risk of BLCA also correlates with the number of daily cigarettes smoked (Brennan et al., 2000). Around 20% of cases are associated with an occupational exposure to carcinogens such as aromatic amines, polycyclic and chlorinated hydrocarbons. This exposure is likely to occur in industries that process dyes, rubber, textiles, metals, paints, leather and petroleum (Burger et al., 2013). The presence of arsenic in drinking water and previous pelvic radiation therapy are other associated risk factors (Witjes et al., 2014). Chronic inflammation of the bladder resulting from calculi, prolonged catheterization or chronic infections can also contribute to the development of the disease (Sharma et al., 2009). The endemic presence of *Schistosoma haematobium*, a parasite that infects the bladder to cause chronic cystitis, contributes to the high incidence of the disease in northern Africa (Mostafa et al., 1999).

It has also been observed that a positive family history of BLCA in first degree relatives increases the risk of disease development by two fold (Aben et al., 2002). This has prompted the investigation into genetic causes of BLCA. Current data indicate that some familial cases of BLCA might be explained by genetic predispositions that affect individual susceptibility to external carcinogens. This includes genetic variations in *NATS* and *GSTM1* that metabolize carcinogens, as well as *SLC14A* that can influence urine concentration and the contact of carcinogens with the urothelium (Burger et al.,

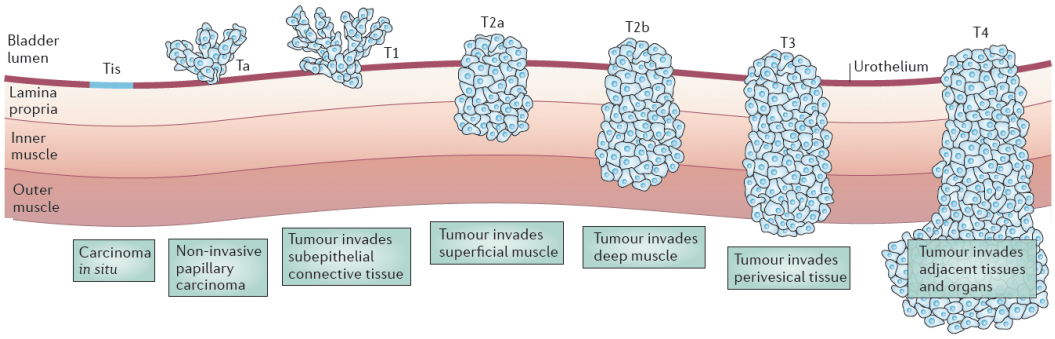

Figure 1.1: **Tumor staging of BLCA.** Ta includes papillary non-invasive tumors. Localized epithelial dysplasia constitutes CIS. Tumors are staged as T1, T2, T3 or T4 as they invade into the sub-epithelial connective tissue, muscle layer, perivesical tissue or surrounding organs respectively. Modified with permission from Knowles and Hurst, 2015.

2013).

1.2 Pathology and staging of bladder cancer

Over 95% of bladder tumors are of epithelial origin. The majority of these are urothelial carcinomas that affect the specialized 3 to 6 layer thick urothelium (or transitional epithelium) lining the bladder (Epstein et al., 1998). Apart from a pure urothelial histology, these tumors can also show squamous or glandular differentiation or have micropapillary, nested, small cell or spindle cell variants. Other than urothelial carcinomas, epithelial tumors can also be squamous, adeno or undifferentiated carcinomas. Squamous cell carcinomas (SCC) are typically associated with cases arising from *S. haematobium* infection. Non-epithelial tumors are rare and include sarcoma, lymphoma, melanoma, paraganglioma, etc.

Disease staging of BLCA is determined by the tumor, node and metastasis (TNM) classification (Witjes et al., 2013)(Figure 1.1). Non- invasive tumors that are papillary in nature are classified as Ta. Flat tumors bearing malignant cellular features, but localized to the epithelium, are classified as carcinoma in situ (CIS). Tumors that invade into the sub-epithelial connective tissue are classified as T1 and those that extend into the muscle layer of the bladder are staged as T2. T3 tumors are those that invade the perivesical tissue, while T4 tumors extend into surrounding organs such as the prostate stroma, seminal vesicles, uterus, vagina, pelvic or abdominal wall. Hence, Ta and T1 tumors are referred to as non-muscle invasive BLCA (NMIBC), T2 tumors represent organ confined muscle invasive BLCA (MIBC), while T3 and T4 tumors are considered to be non-organ confined MIBC. Absence of metastasis to regional lymph nodes is regarded as N0. Involvement of single or multiple pelvic nodes that include

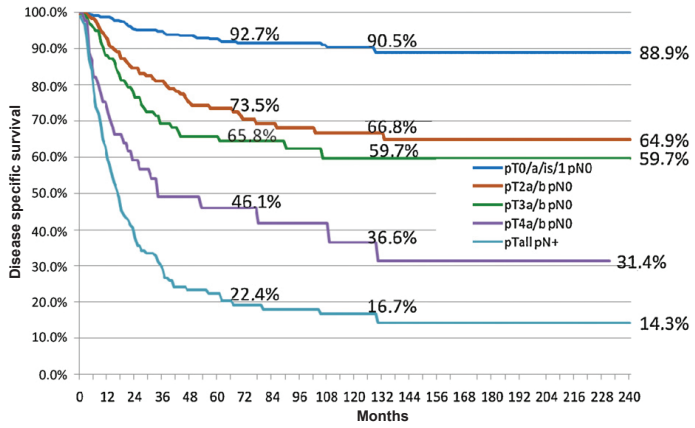

Figure 1.2: **Prognostic factors for RC.** Tumor stage and lymph node involvement are independent prognostic factors for the outcome of RC. Modified with permission from Hautmann et al., 2012.

the hypogastric, obturator, external iliac or presacral nodes is classified as N1 or N2 respectively. Metastasis to the common iliac lymph nodes is classified as N3. M0 indicates the absence of distant organ metastasis, while M1 includes tumors that metastasize to distant organs such as the liver, lung, mediastinum, bone or skin, etc.

1.3 Management of advanced bladder cancer

NMIBC accounts for around 70% of all BLCA. The standard treatment of these tumors is a combination of surgery, using transurethral resection of the bladder tumor (TURBT), and intravesical immunotherapy. These tumors tend to recur and patients require extensive follow up and monitoring, making BLCA the most expensive malignancy to treat from diagnosis until death (Botteman et al., 2003). However, their overall prognosis is excellent with a 5-year survival over 90%. About 10-15% of NMIBC can progress to MIBC (Anastasiadis and de Reijke, 2012).

The standard of care for localized MIBC is radical cystectomy (RC). This includes the surgical removal of the bladder, distal ureters and regional lymph nodes, together with the prostate and seminal vesicles in males, and the urethra, adjacent vagina and uterus in females (Witjes et al., 2013). The tumor stage and lymph node status are independent prognostic factors for the outcome of RC (Hautmann et al., 2012)(Figure 1.2). In a series of 1100 patients that underwent RC with pelvic lymph node dissection (PLND), node negative Ta or CIS tumors had a disease-specific survival (DSS) of 88.9% at 20 years of follow-up. This reduced to 64.9%, 59.7% and 31.4% with node negative T2, T3 and T4 tumors respectively. Lymph node involvement,regardless of tumor stage, led to a DSS of only 14.3%. In order to improve the outcome of RC, perioperative chemotherapy has been used in the treatment of MIBC. Using neoadjuvant chemotherapy (NAC) has the advantage that chemotherapy is delivered early in the disease course when the

burden of micrometastasis might be low and tolerance might be better. A response to NAC can also result in the shrinkage of the surgical margins at the time of RC. The current European association of Urology (EAU) guidelines recommend cisplatin based NAC in patients with MIBC. However the overall survival (OS) improvement at 5 years is only 5-8%. Hence, non-responders are subjected to unnecessary toxicities as well as a delay in RC (Witjes et al., 2013, Rosenberg et al., 2005).

Despite treatment, almost half of the patients with MIBC relapse and present with metastatic disease. Additionally, around 10-15% patients present with metastasis at the time of diagnosis (Rosenberg et al., 2005). Historically, the OS of patients with metastatic disease was only around 3-6 months in the absence of chemotherapy regimens (Sternberg and Vogelzang, 2003). Since the 1980s, cisplatin based combination therapy has been used for the treatment of metastatic disease. The standard regimen used is methotrexate, vinblastine, adriamycin and cisplatin (MVAC) that leads to a median survival of about 12-15 months. However, this regimen is also associated with mucosal and hematological toxicity, with a treatment related mortality of up to 3%. This has led to the development of alternate regimens (Bellmunt and Petrylak, 2012). Doublet gemcitabine and cisplatin (GC) chemotherapy when compared to MVAC has a similar efficacy with a median OS of 14 months and 15.2 months respectively (von der Maase et al., 2005). However, GC has a lower toxicity profile as compared to MVAC and is also recommended for standard use in the treatment of metastatic disease. Present data does not support the recommendation of chemotherapeutic agents such as paclitaxel, docetaxel, ifosfamide, topotecan, etc. as second line regimens after the failure of MVAC or GC based treatment. Vinflunine was demonstrated to offer a modest benefit of a median OS of 6.9 months as compared to 4.6 months with best supportive care (BSC) (Bellmunt et al., 2013). It is approved in Europe as a second line chemotherapy for patients with metastatic disease (Witjes et al., 2013).

Quantification of temporal trends has revealed that no significant changes have occurred in the survival or mortality rates of BLCA from 1973-2009 (Abdollah et al., 2013). It is thus strikingly clear that the prognosis of muscle invasive and metastatic BLCA remains poor to this day. More than a quarter of a century since the advent of cisplatin based chemotherapy, these patients continue to have limited treatment options. There is an urgent, unmet need for the development of novel treatment strategies to improve their clinical outcome.

1.4 Target therapy in cancer

The past few decades have seen an explosion in our understanding of the molecular biology of cancer. Normal cells become cancerous via a complex multistep process that leads to the acquisition of specific molecular alterations. These alterations occur due to different genetic and epigenetic mechanisms that lead to the gain or loss of function of key cellular regulators of different processes (Hanahan and Weinberg, 2011). As a result of these changes, cancer cells possess the remarkable property of unregulated growth and proliferation. This results from a self-sufficiency in growth signaling

together with a resistance to anti-proliferative and apoptotic signals. A limitless replicative potential makes the cancer cell immortal and an altered cellular metabolism helps it to proliferate. Additionally these cells can interact with tumor stromal cells to sustain angiogenesis, evade attack from the immune system and can ultimately metastasize to other organs.

Classical chemotherapy used in the treatment of cancer is cytotoxic to all rapidly dividing cells. Thus, apart from cancer cells, it also affects other normal cells of the body including gastrointestinal epithelium, skin cells, hematological cells, etc. which can lead to multiple side effects. In recent decades, target therapy is emerging as a promising component of cancer treatment. Unlike chemotherapy, these agents selectively target specific cellular molecules that are the regulators of tumor cell survival and proliferation. Target therapy can thus selectively attack cancer cells as compared to normal cells and avoid the systemic side effects seen with chemotherapy. Additionally, it also has the potential to provide a better therapeutic effect by interfering with specific molecular drivers of tumor growth (Gerber, 2008).

The first clinical application of target therapy was in the use of tyrosine kinase inhibitors (TKIs) in chronic myelogenous leukemia (CML). The molecular basis for CML is the presence of a translocation between chromosomes 9 and 22, the so called 'Philadelphia chromosome', that leads to the constitutive activation of the BCR-Abl tyrosine kinase. Targeting this kinase by TKIs such as Imatinib has led to a 5 year survival rate of 89% for CML patients (Druker, 2008). Target therapy has also been used with some success in breast cancer. Around 20-30% of invasive breast cancers overexpress ErbB2 (Her2) that encodes the human epidermal growth factor receptor type 2 (EGFR2), which regulates cell growth and survival. Targeting this overexpression in breast cancer by using Trastuzumab, an anti-Her2 monoclonal antibody, was the first US Food and drug administration (FDA) approval for target therapy in solid tumors (Hudis, 2007). The ten-year OS of Her2 positive early stage breast cancer treated with Trastuzumab in combination with chemotherapy is 84%, as compared to 75% with chemotherapy alone (Slamon et al., 2011). Both these examples highlight the presence of an identifiable molecular target, which is selectively altered in cancer cells and important to their malignant potential, as a requirement for target therapy. Success of target therapy also relies on the ability of agents to effectively inhibit this molecule. The molecular make up of each individual tumor is unique. Hence, an important prerequisite for target therapy is the presence of the molecular alteration in an individual's cancer. This is the rationale of personalized or precision medicine, where a patient's tumor genetics are analyzed and targeted treatment is offered only in the presence of suitable alterations.

1.5 Molecular biology of bladder cancer

A two pathway model has been proposed to explain the divergence of molecular alterations that produce NMIBC and MIBC as distinct clinical entities (Wu, 2005). NMIBCs are genomically more stable with a near diploid karyotype while MIBCs are aneuploid and genomically unstable. Both subtypes commonly show deletion of chromosome 9.

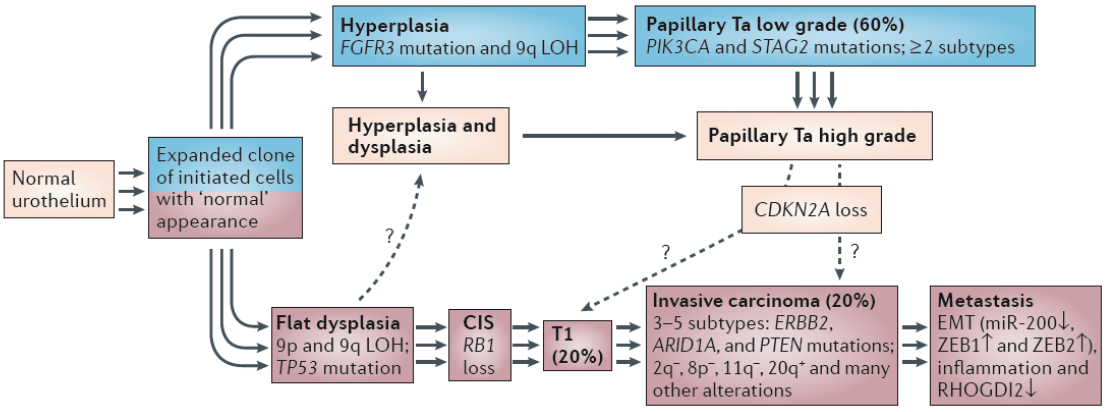

Figure 1.3: **Molecular pathogenesis of BLCA.** The pathogenesis of BLCA proceeds via multiple pathways to produce a disease that has molecular and clinical heterogeneity. Modified with permission from Knowles and Hurst, 2015.

Candidate tumor suppressor genes affected by this deletion include *CDKN2A*, *CDKN2B*, *TSC1*, *PTCH1*, and *DBC1* (Knowles and Hurst, 2015). NMIBC arises from epithelial hyperplasia that commonly possesses mutations in *FGFR3*, *HRAS*, *PIK3CA*, *STAG2* and produces papillary tumors. In contrast, MIBCs arise from flat dysplasia and CIS lesions that possess alterations in *ECC2*, *ATM*, *FANCA* that regulate DNA repair, as well as *STAG1*, *STAG2*, *NIPBL*, *SMC1A*, *SMC1B*, *SMC3* and *ESPL1* that regulate chromatin adhesion and segregation. These molecular alterations are proposed to promote frequent chromosomal aberrations including the deletion of chromosomes 8p, 2q and 5q. Unlike NMIBCs, MIBCs frequently have molecular alterations in p53 and RB. The somatic mutation frequency in MIBC is higher than the average frequency across several other cancer types (Kandoth et al., 2013). Invasion and metastasis are regulated by alterations in MMP9, E-cadherin, VEGF, δNp63, among others that occur only in MIBCs. NMIBCs and MIBCs also show distinct patterns of DNA methylation, with non-CpG island hypomethylation occurring in NMIBC and extensive CpG island hypermethylation in MIBC (Wolff et al., 2010). An extensive analysis of MIBC (131 chemotherapy naive T2-T4a, Nx, Mx) tumors, including whole exome sequencing, and expression analysis of mRNA, miRNA and proteins, was recently described by the Cancer Genome Atlas (TCGA) (The Cancer Genome Atlas Research, 2014) . Thirty two genes showed significant levels of recurrent alteration including *TP53*, *MLL2*, *ARID1A*, *KDM6A*, *PIK3CA*, *EP300*, *CDKN1A*, *RB1*, *ERCC2*, *FGFR3*, *STAG2*, *ERBB3*, *FBXW7*, *RXRA*, *ELF3*, *NFE2L2*, *TSC1*, *KLF5*, *TXNIP*, *FOXQ1*, *CDKN2A*, *RHOB*, *FOXA1*, *PAIP1*, *BTG2*, *HRAS*, *ZFP36L1*, *RHOA* and *CCND3*. This study also found that mutations in chromatin regulatory elements are found at a higher frequency in BLCA than in any other epithelial cancer in the TCGA cohort.

Recent data has identified distinct molecular sub-types, based on gene expression signatures, in both NMIBC and MIBC. 5 subgroups were identified in a BLCA cohort consisting of tumors of all grades and stages (Sjodahl et al., 2012). These subgroups

were termed as urobasal (Uro) A, UroB, genomically unstable (GU), squamous cell carcinoma like (SCCL) or basal (sharing features with basal like breast cancers), and infiltrated (showing infiltration of non-tumor cells). These molecular sub-types also cut across pathologic stages, suggesting that they arise as divergent properties of tumors within the same pathologic classification. Ta tumors dominated UroA subtype but were also present across the other sub-types. T1 tumors were present in both the UroB and GU sub-types. MIBC tumors were distributed across all sub-types. FGFR3, CCND1 and p63 showed higher expression in UroA and UroB. The presence of *TP53* mutations and *CDKN2A* deletions in the largely MIBC UroB tumors, together with the presence of *FGFR3* mutations, represents a potential evolution from UroA tumors. FGFR3, CCND1 and p63 showed a lower expression in GU tumors which was accompanied by higher levels of ERBB2 and E-Cadherin. KRT5, KRT6, KRT14 and EGFR were highly expressed in the SCCL or basal tumors. UroA had the best prognosis, GU and infiltrated were intermediate, while UroB and SCCL or basal tumors had the worst prognosis. Three other studies that consisted of only MIBC cohorts have demonstrated similar findings (Damrauer et al., 2014, Choi et al., 2014, The Cancer Genome Atlas Research, 2014). One of these reports also discovered a molecular subtype that possesses an activated wild type p53 gene signature and correlates with response to NAC (Choi et al., 2014). It is thus emerging that unlike the simplified two pathway model, multiple pathogenic pathways and sub-pathways operate in BLCA (Knowles and Hurst, 2015) (Figure 1.3). This molecular diversity resembles the complex heterogeneity that is seen in BLCA patients in their clinical progression and treatment response.

1.6 Target therapy in bladder cancer

No molecular target therapy has been approved for BLCA treatment to date. Recent studies examining the molecular biology of BLCA have led to the identification of signaling pathways that are frequently altered, suggesting that they might be important drivers of tumorigenesis. Some of these pathways are also amenable to inhibition with the help of small molecule inhibitors that are already in clinical development.

Multi-TKIs such as Sunitinib and Sorafenib have shown minimal benefit in clinical trials of BLCA (Gallagher et al., 2010, Dreicer et al., 2009). Gefitinib, an EGFR inhibitor, was associated with high toxicity (Philips et al., 2008). Trastuzumab was tested in a trial where patients were prospectively screened for Her2 overexpression. A 57% response was observed in Her2 positive patients (Hussain et al., 2007). Although a trial with Bevacizumab, a monoclonal antibody directed against vascular endothelial growth factor (VEGF), failed to meet its endpoint; it had a partial response rate of 53% and a complete response of 19% respectively (Hahn et al., 2011). Rapamycin analogues (rapalogues) that selectively target mechanistic target of rapamycin 1 (mTORC1) were tested in different clinical trials for BLCA with overall disappointing results. However, some of the trials had a small fraction of partial or complete responders (Gerullis et al., 2011, Seront et al., 2012, Milowsky et al., 2013, Niegisch et al., 2015). Promising results were recently seen using immunotherapy in metastatic BLCA. This trial had a

52% overall response rate with the use of MPDL3280A, an antibody directed against PD-L1 that is involved in the immune checkpoint pathway. Several clinical trials are currently ongoing that target FGFR, PI3K, EGFR2, Aurora kinase A, Polo-like kinase 1, Heat shock protein (HSP) 27 and HSP90 (Carneiro et al., 2015).

The TCGA data when integrated for mutation and copy number analysis reveal that three signaling pathways are most commonly altered in MIBC, signifying that they might represent important driver events in tumorigenesis. These are the p53/Rb pathway (93%), RTK/Ras/PI3K pathway (72%) and chromatin remodeling by histone modification (89%) or SWI/SNF nucleosome remodeling (64%) (Network, 2014). According to this data set, 69% of all MIBC tumors possess molecular targets for therapy. Another study has also demonstrated that about 60% of high-grade BLCA patients possess actionable molecular alterations (Iyer et al., 2013). Despite these data, the results of most clinical trials have been disappointing. However, it should be noted that the majority of these trials were conducted without any molecular pre-stratification of patients. The molecular heterogeneity of BLCA has been demonstrated in multiple independent studies (Knowles and Hurst, 2015). It is thus likely that the success of target therapy in BLCA depends not only on the selection of a suitable target, but also on the application of these treatments to a suitable patient population. Hence, more thorough pre-clinical studies are needed that assess not only the therapeutic value of a potential target, but also develop molecular markers for patient stratification and response prediction.

1.7 Targeting the PI3K signaling pathway in bladder cancer

The phosphoinositide 3-kinase (PI3K)/ v-akt murine thymoma viral oncogene (AKT)/ mechanistic target of rapamycin (mTOR) signaling pathway is the most frequently altered pathway in cancer cells. *PIK3CA*, which encodes for the p110α subunit of the PI3K, is the second most commonly mutated oncogene and the phosphatase and tensin homolog (*PTEN*) is the most commonly altered tumor suppressor gene (Dienstmann et al., 2014). Molecular alterations in upstream receptor tyrosine kinases (RTKs) or RAS as well as in downstream signaling molecules such as AKT or tuberous sclerosis complex (TSC) can also lead to over activation of this pathway. This can influence a number of downstream molecular events that are pro-oncogenic.

1.7.1 The PI3K signaling pathway

PI3Ks are classified according to their structural homology and substrate preference into three different classes (Engelman et al., 2006). Class I PI3Ks phosphorylate phosphatidylinositol-4, 5 bisphosphate (PI-4,5-P2) to produce phosphatidylinositol-3,4,5-trisphosphate (PIP3). Class II PI3Ks can phosphorylate phosphatidylinositol (PI) to form phosphatidylinositol-3-phosphate (PI-3-P), phosphatidylinositol-3, 4-biphosphate

(PI-3,4-P2) and PIP3. Class III PI3Ks can generate PI-3-P from PI. Class 1 PI3Ks have been extensively studied in cancer biology and are classified into two types. Class 1A are activated via RTK stimulation at the cell membrane, while class 1B PI3K activation is mediated via the G-protein coupled receptors (GPCRs). Structurally, the class 1A PI3Ks are heterodimers that consist of a p85 regulatory sub-unit and a p110 catalytic sub-unit. The p85 sub-unit has three different isoforms, p85α, p85β and p55γ, and contains a p110-binding domain and two Src-homology 2 (SH2) domains. The SH2 domains of the p85 sub-units can bind to the phopshotyrosine motifs of activated RTKs. This interaction is important in recruiting the PI3K to the plasma membrane as well as in relieving the suppression of the p110 catalytic sub-unit. The isoforms of the p110 sub-unit include p110α , p110β, p110γ and p110δ . They contain an N-terminal adapter domain that interacts with the p85 regulatory subunit, a Ras-binding domain (RBD) that mediates activation by the small GTPase Ras, a C2 domain, a helical domain (HD) and a C-terminal catalytic or kinase domain (KD) (Arcaro and Guerreiro, 2007). Stimulation of RTKs thus leads to the p85 subunit mediated activation of the p110 catalytic function that results in the formation of PIP3 from PIP2. The formation of PIP3 functions as a second messenger that initiates further signaling cascades. Phosphatase and tensin homolog (PTEN) inactivates PIP3 formation and stops these signaling events.

PIP3 recruits molecules such as AKT (also known as protein kinase B or PKB) and PDK1 owing to the affinity of their pleckstrin homology (PH) domains for PIP3 (Franke, 2008). After recruitment to the plasma membrane, AKT is phosphorylated at two distinct sites, threonine 308 in the T loop of the kinase domain by PDK1, and serine 473 in the hydrophobic motif in the C-terminal tail by mTORC2. This dual phosphorylation results in conformational changes that enable subsequent substrate binding and is necessary for the complete activation of the kinase activity of AKT. mTORC2 is a complex of six different proteins, the kinase mTOR; rapamycin-insensitive companion of mTOR (Rictor); mammalian stress-activated protein kinase interacting protein (mSIN1); protein observed with Rictor-1 (Protor-1); mammalian lethal with Sec13 protein 8 (mLST8, also known as GbL); and DEP-domain-containing mTOR-interacting protein (Deptor) (Laplante and Sabatini, 2009). Dephosphorylation of AKT by phosphatases such as PP2A and members of the PHLPP family result in its negative regulation. When inactive, AKT exists in a 'PH-in' confirmation state where the PH and regulatory domains are folded to cover parts of the kinase domain. Interaction of the PH domain with PIP3 moves the PH and regulatory domains away from the kinase domain, leading to a 'PH-out' conformation. This allows access to PDK1 and mTORC2 for AKT phosphorylation (Huang and Kim, 2006).

1.7.2 Downstream effectors of AKT

AKT is an oncogenic serine/threonine kinase belonging to the AGC family of kinases and a central node within the PI3K signaling cascade. It has the potential to regulate multiple downstream effectors that control important cellular processes. A major downstream effector of AKT signaling is the mTOR pathway. mTORC1 is a complex

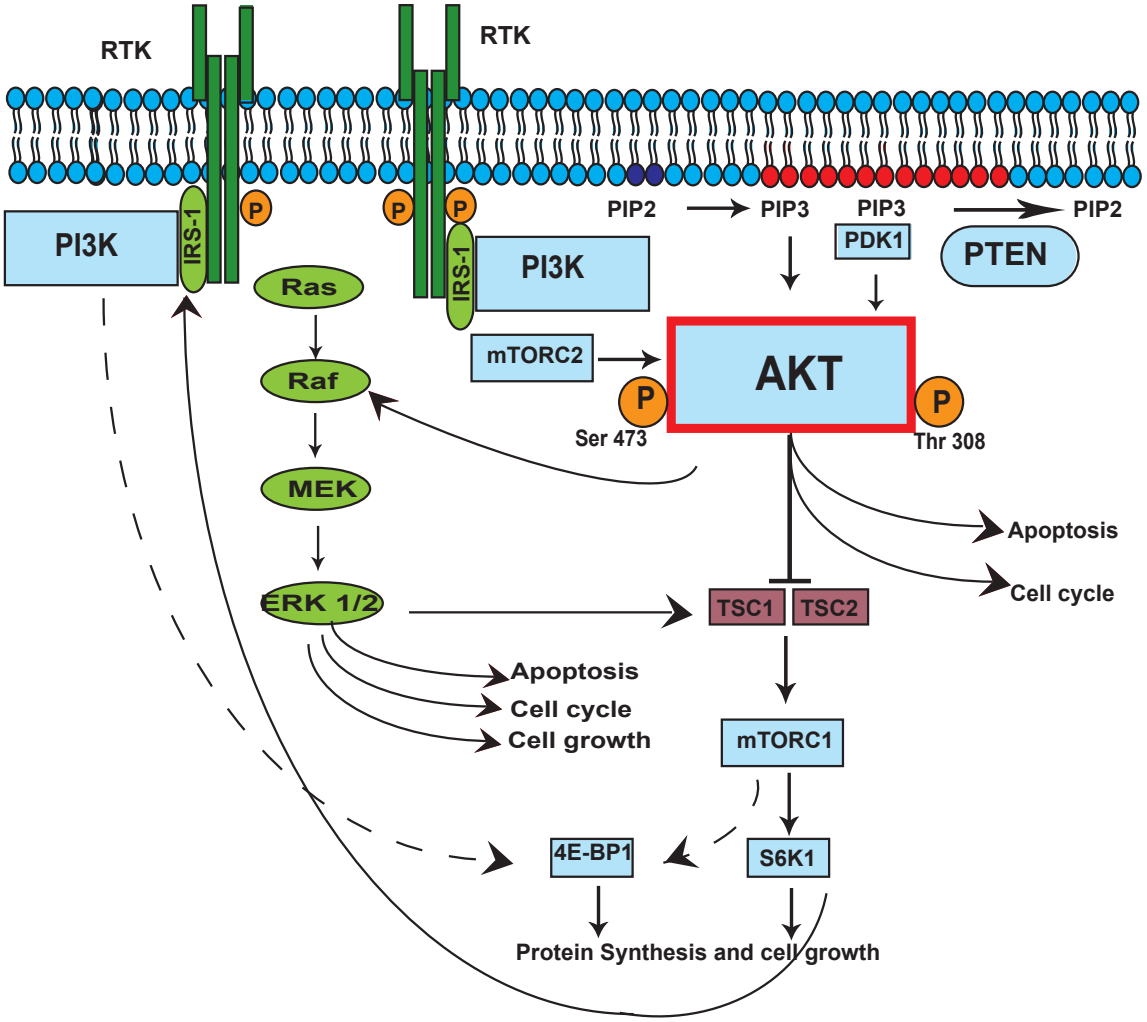

Figure 1.4: **The PI3K/AKT/mTOR pathway.** PI3K activation results in the formation of PIP3 that recruits AKT to the plasma membrane. Activation of AKT by PDK1 and mTORC2 leads to the phosphorylation of downstream targets that regulate multiple cellular processes. In BLCA, mTORC1 controls only S6K1 phosphorylation and does not regulate 4E-BP1 phosphorylation. The PI3K pathway also has cross-talk at different levels with the MAPK pathway. Adapted from Franke T.F., 2008 and Nawroth et al. 2011.

consisting of the mTOR kinase (which is also a component of the mTORC2 complex that activates AKT), regulatory-associated protein of mTOR (Raptor); mammalian lethal with Sec13 protein 8 (mLST8, also known as GbL); proline rich AKT substrate 40 kDa (PRAS40); and DEP-domain-containing mTOR-interacting protein (Deptor) (Laplante and Sabatini, 2009). It is negatively regulated by the tuberous sclerosis complex (TSC), which is composed of TSC1 and TSC2. AKT mediated phosphorylation of PRAS40 and TSC2 inactivates the TSC, relieves this inhibition, and leads to the activation of mTORC1. The two important substrates of mTORC1 are ribosomal protein S6 kinase beta-1 (S6K1) and eukaryotic translation initiation factor 4E-binding protein 1 (4E-BP1) that control protein translation. Phosphorylated S6K1 is necessary for the translation of 5' terminal oligopyrimidine mRNAs while phosphorylation of 4E-BP1 prevents its binding to eIF4E and promotes cap dependent translation. These two downstream effectors can control the protein synthesis within the cell and ultimately exert control over cell growth (Mamane et al., 2006). However, it has been previously demonstrated by our group that mTORC1 regulates only S6K1 and does not influence 4E-BP1 phosphorylation in BLCA (Nawroth et al., 2011). Additionally, S6K1 can regulate a negative feedback loop that acts on IRS-1, an adapter molecule of RTKs, to control the activity of PI3K (Figure 1.4).

AKT can also regulate cell cycle progression and proliferation via multiple additional substrates including GSK3β, p21Cip1 and p27Kip1 (Manning and Cantley, 2007). AKT mediated regulation of apoptosis and cell survival occurs through different substrates such as MDM2, Bad, Bax, Bim and the FOXO proteins. It can also influence the transcription of multiple genes by regulating transcription factors such as CREB, YB-1, the GATA and FOXO families. Regulation of hypoxia inducible factor (HIF)-1α, eNOS and the Rho GTPase family can control angiogenesis and cell migration. AKT can also influence cellular metabolism by regulating glucose transporters and the phosphorylation of GSK3β and FOXO proteins. Hence, AKT is able to influence multiple properties of a cancer cell including its growth, proliferation, apoptosis, metabolism, invasion and metastasis.

The PI3K signaling pathway also interacts at multiple levels with the RAS-RAF-MEK-ERK component of the MAPK pathway, which is also initiated through activated RTKs, GPCRs or protein kinase C (PKC) (Mendoza et al., 2011). Signaling in this pathway is also upregulated in cancer cells. Activated RAS can directly stimulate PI3K, independently from its regulation by the p85 sub-unit. ERK can also activate mTOR signaling via its regulation of TSC2. Phosphorylation of RAF by AKT can inhibit its activity and reduce ERK signaling. Both pathways also converge on common effectors such as BAD, FOXO proteins, GSK3β, and c-Myc that regulate cell growth, survival and proliferation.

1.7.3 AKT structure and its isoforms

The structure of AKT consists of an N-terminal PH domain, a central kinase catalytic (CAT) domain, a linker region (LINK) connecting the PH and the CAT domain, and a regulatory hydrophobic motif (HM) in the C-terminal extension (EXT) (Kumar and Madison, 2005) (Figure 1.5). AKT has three isoforms AKT 1, 2 and 3 encoded by dis-

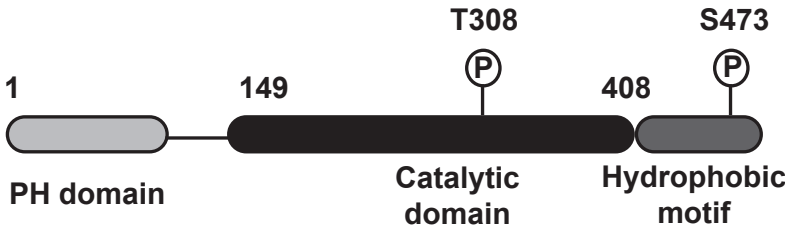

Figure 1.5: **Structure of AKT.** AKT structure includes a PH domain, a linker region, a kinase domain and a hydrophobic motif. Amino acid positions are numbered according to AKT1. Adapted from Kumar and Madison, 2005.

tinct genes. They share considerable structural homology with around 80%, 90% and 70% identical PH domains, CAT domains and EXT respectively. The LINK is poorly conserved among the three isoforms with only a 17-64% homology in structure (Kumar and Madison, 2005). Despite their structural similarities, these isoforms might have distinct functional roles that can be regulated by their response to stimulation, tissue distribution, sub-cellular localization and downstream substrate specificity (Gonzalez and McGraw, 2009). Results from AKT isoform specific knockout mice have suggested non-redundant roles for AKT1 in embryonic development, cell growth and survival, AKT2 in glucose homeostasis and AKT3 in neuronal development. The three isoforms were also demonstrated to possess distinct functions in breast cancer, prostate cancer and glioma cells (Dummler and Hemmings, 2007). Small molecule inhibitors of AKT can differ in the degree to which they inhibit AKT1, AKT2 and AKT3. It is thus imperative to understand the functional consequences of isoform specific inhibition in particular model systems to determine the most effective strategy of tumor inhibition. Isoform specific inhibitors can potentially minimize side effects that result from the inhibition of their physiological functions. For example, targeting only AKT1 in a tumor that relies on it for cell proliferation could prevent the AKT2 inhibition induced adverse effects on glucose metabolism.

1.7.4 Targeting the PI3K pathway in cancer

Targeting the PI3K/AKT/mTOR signaling network offers a chance to inhibit cellular mechanisms that are integral to the function of tumor cells. Six different types of agents that target this pathway at different nodes are currently in clinical trials. They include Class I PI3K inhibitors, isoform selective PI3K inhibitors, mTORC1 selective inhibitors (rapalogues), active site mTOR inhibitors, dual PI3K/mTOR inhibitors and AKT inhibitors (Fruman and Rommel, 2014).

Targeting the PI3K pathway can result in signaling events or changes in gene expression that can compensate for the inhibitory effect (Klempner et al., 2013). For example, inhibition of mTORC1 reduces S6K1 phosphorylation that results in a feedback activation of IRS1 and PI3K signaling (Carracedo et al., 2008). PI3K inhibition can cause a FOXO mediated feedback uregulation of multiple molecules such as Bcl-2,

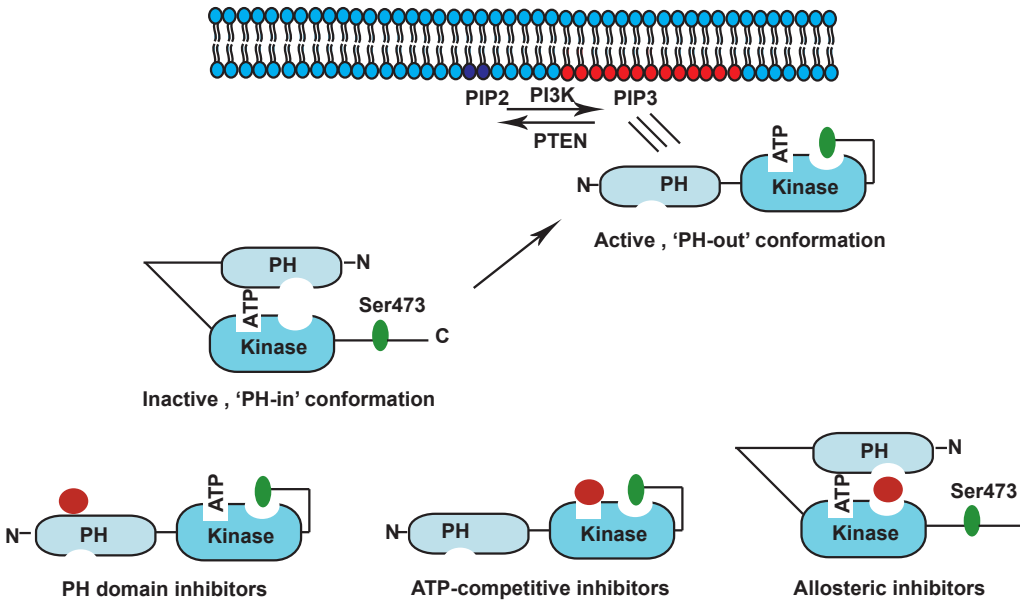

Figure 1.6: **Mechanism of action of AKT inhibitors.** PH3 domain inhibitors prevent the binding of AKT with PIP3, ATP-competitive inhibitors target the kinase domain and activation of AKT while allosteric inhibitors prevent an active conformation of AKT. Adapted from Mattmann et al., 2011.

IGF-1R, phosphoSTAT3, p-c-Jun, EGFR, etc. that can promote cell growth (Muranen et al., 2012). The multiple levels of cross-talk between PI3K and MAPK signaling can also result in the compensatory activation of the MAPK pathway after PI3K inhibition. This activation can result in increased cell proliferation with a resistance to apoptosis (Mendoza et al., 2011). Hence, complex feedback signaling networks and cross talk with other pathways provide potential escape routes and resistance mechanisms to the inhibition of the PI3K pathway.

1.7.5 AKT inhibitors

Small molecule inhibitors of AKT have been designed to target different areas within the AKT molecule and have varying mechanism of action (Mattmann et al., 2011) (Figure 1.6).

ATP-competitive kinase inhibitors

Several inhibitors, such as A-443654, A-674563 and GSK690693, have been developed that target the ATP binding pocket of AKT. However, these compounds have a problem with target selectivity due to the homology of the kinase domain with other members of the AGC kinase family. Some of these compounds are no longer being pursued in the pipeline of several drug companies owing to toxicity (Kumar and Madison, 2005, Mattmann et al., 2011). Biochemical studies have shown that treatment with

ATP-competitive AKT inhibitors leads to an unexpected hyperphosphorylation of AKT. This phenomenon has been explained by an inhibitor induced increase in membrane localization of AKT as well as an increased reactivity to phosphorylation by PDK1 and mTORC2 (Okuzumi et al., 2009). Although downstream AKT substrates were demonstrated to be dephosphorylated despite the AKT hyperphosphorylation, it is possible that dissociation of the inhibitor from AKT might promote increased catalytic activity of AKT leading to oncogenic effects.

PH-domain inhibitors

These inhibitors prevent the binding of PIP3 to the PH domain and hence prevent activation of AKT. However, they can potentially target other molecules that share the PH domain structure and might not be selective for AKT (Mattmann et al., 2011). Perifosine is proposed to have a similar mechanism of action and is in an advanced stage of clinical development. However, it is not a specific AKT inhibitor and can also inhibit the MAPK and JNK pathways. Despite promising pre-clinical data, disappointing results have been obtained with perifosine in trials of prostate, breast, pancreatic, head and neck cancer and melanoma (Gills and Dennis, 2009).

Allosteric inhibitors

Allosteric inhibitors are proposed to lock AKT in its 'PH-in' confirmation by binding to sites at the PH domain and/or the hinge region. This stabilization results in inhibiting AKT activity without affecting its ATP dependent kinase activity (Mattmann et al., 2011, Barnett et al., 2005). This specific inhibitor binding location also enabled the development of isoform specific inhibitors directed against only AKT1 or AKT2, or both AKT 1 and 2 (Lindsley et al., 2005). Subsequent modifications have led to the development of MK-2206, an allosteric inhibitor dependent on the presence of the PH domain, which was selective for AKT against over 250 examined kinases. It inhibits all three AKT isoforms with IC50s of 8, 12 and 65 nM for AKT 1, 2 and 3 respectively (Hirai et al., 2010). It has been extensively studied in different pre-clinical models and led to effective suppression of tumor growth and proliferation. Its safety was established in a phase 1 trial in 2011 (Yap et al., 2011). MK-2206 is currently a part of over 50 phase 2 or 3 clinical trials in different cancers including breast, colorectal, endometrial, ovarian, lung, head and neck cancer (https://clinicaltrials.gov/).

1.7.6 PI3K signaling in bladder cancer

Multiple studies have confirmed that the PI3K/AKT/mTOR pathway is frequently altered in BLCA. Mutations in *PIK3CA* (encoding for the p110α subunit of the PI3K) are present in 21-25% of MIBCs (Network, 2014, Iyer et al., 2013, Platt et al., 2009). Most *PIK3CA* mutations in different cancers are located in the KD. The spectrum of *PIK3CA* mutations is different in BLCA where around 75% of all mutations occur in the hotspot region of the HD, commonly as E545K or E542K (Platt et al., 2009, Knowles et al.,

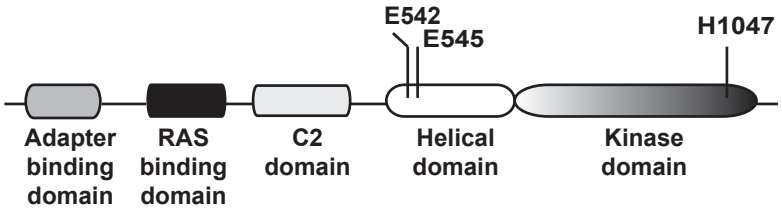

Figure 1.7: ***PIK3CA* mutations.** *PIK3CA* mutations in BLCA are commonly found at hotspot locations in the HD of the p110α. Adapted from Arcaro and Guerreiro, 2007.

2009)(Figure 1.7). A small fraction of mutations, referred to as 'rare mutants', also occur in non-hotspot regions of the HD or in other *PIK3CA* regions. *PIK3R1* mutations (encoding for the p85 subunit of the PI3K), that can lead to deregulation of PI3K signaling, are also found in 1-5% (Network, 2014, Ross et al., 2013b). Although mutations in *PTEN* occur at a low frequency of 3-4% (Iyer et al., 2013, Network, 2014), loss of PTEN expression is a common event in BLCA and is found in as many as 39-94% patients (Platt et al., 2009, Calderaro et al., 2014, Cappellen et al., 1997, Aveyard et al., 1999, Tsuruta et al., 2006). Decreased expression of TSC1 or TSC2 is also common with a loss of heterozygosity (LOH) in 40-50% and 15% of BLCA respectively (Knowles et al., 2003, Platt et al., 2009). Activating mutations in *AKT1* are a rare event occurring in 2-3% (Iyer et al., 2013, Askham et al., 2010). Moreover, hyper activation of the PI3K signaling pathway can also result from molecular alterations in upstream components including RTKs such as the ERRB family of proteins (found in 2% to 11%) and FGFR3 (found in 3% to 11%), as well through the activation of RAS (found in 1% to 5%). Integrated analysis of genetic alterations in the RTK/RAS/PI3K/AKT/mTOR pathway reveals that this signaling network is altered in 72% of BLCA (Network, 2014). This high frequency of alterations and the development of several small molecule inhibitors makes the PI3K signaling pathway a strong contender for target therapy in BLCA.

Only rapalogues that selectively target mTORC1 have been tested so far in clinical trials for BLCA. There are reports of four different clinical trials that used rapalogues as a second line treatment in patients with metastatic BLCA, after the failure of platinum based chemotherapy (Gerullis et al., 2011, Seront et al., 2012, Milowsky et al., 2013, Niegisch et al., 2015). The overall results from all the trials were disappointing and expected efficacy of rapalogues was not observed. However, some of the trials had a small fraction of patients that responded to rapalogues and a retrospective molecular analysis has been performed from these responders. In one study, loss of PTEN expression correlated with resistance to rapalogues, while a complete responder in another study had an inactivating mutation in *TSC1* (Iyer et al., 2012, Seront et al., 2012). In a clinical trial of different solid tumors treated with a combination of a rapalogue and pazopanib, a multi-TKI, an exceptional responder with BLCA had mutations in mTOR (Wagle et al., 2014). While these associations offer interesting insights into the molecular determinants of sensitivity to rapalogues, it should be remembered that they are

case reports of single patients in a small cohort. The association between alterations in PTEN and *TSC1* and sensitivity to rapalogues could not be confirmed mechanistically using cell line models (Seront et al., 2013, Guo et al., 2013).These findings need to be studied further to enable the development of a robust clinical biomarker and the molecular determinants of sensitivity to rapalogues currently remain unclear. However, these data support the hypothesis that response to inhibitors targeting the PI3K network might be dependent on specific molecular alterations that activate signaling within this pathway.

A detailed *in vitro* analysis using chemical and genetic inhibition of different components in the PI3K pathway has led to several insights into its signaling in BLCA (Nawroth et al., 2011). In this study, rapalogues as well as shRNAs directed against mTOR were unable to dephosphorylate 4EBP1 in BLCA cell lines and led to a reduction in only S6K1 phosphorylation. However, an inhibition of both 4EBP1 and S6K1 was required for an optimal reduction in BLCA proliferation. The absence of 4E-BP1 regulation might reflect a possible mechanism for the disappointing results of rapalogue trials. Inhibition of both S6K1 and 4E-BP1 phosphorylation was observed only when using a dual inhibitor of PI3K and mTOR. Hence, the present model of PI3K signaling in BLCA supports a PI3K dependent regulation of 4E-BP1, either alone or in combination with mTOR. Furthermore, treatment of cells with both rapalogues and dual PI3K/mTOR inhibitors led to AKT rephosphorylation via an S6K1- mediated feedback loop. This reactivation of AKT correlated with a decrease in caspase activity in these cells and a lack of apoptosis. Given the importance of AKT in modulating various processes such as cell growth, proliferation, angiogenesis, metabolism, migration and invasion, this reactivation represents a potential route for cells to escape the action of PI3K and mTOR inhibitors. Hence, targeting AKT directly might be necessary to observe maximum therapeutic potential of inhibiting the PI3K signaling pathway in BLCA. AKT inhibition might also be effective only in cells with specific molecular alterations that influence PI3K signaling.

1.8 Targeting the CDK 4/6-RB pathway in bladder cancer

Uncontrolled proliferation is a hallmark feature of cancer cells and the deregulation of cell cycle signaling is a common occurrence.

1.8.1 Cell cycle progression

Cell division is a tightly regulated process that consists of different sequential stages. DNA replication occurs in the S phase and mitotic division occurs in the M phase, where a single cell produces two daughter cells (van den Heuvel, 2005). G1 is a gap phase between the M and the S phase where cells are sensitive to external growth promoting stimuli and prepare for entry into the S phase. G2 is a gap phase following the S phase where the cell prepares for the M phase. Non-proliferating cells are those that

have reversibly withdrawn from the cell cycle and are present in the resting G0 phase. Cells that enter the G1 phase commit irreversibly to enter the S phase after passing the restriction or R point. This sequential progression of the cell cycle is tightly regulated by a network of cyclin dependent kinases (CDKs) (Malumbres and Barbacid, 2009). CDK activity is controlled by binding to the cyclin proteins which are regulated temporally in the cell cycle thus allowing specific phases to proceed. Cyclin D/CDK4, cyclin D/ CDK6 and cyclin E/CDK2 control the G1 to S transition by regulating the entry of cells through the R point. Cyclin A/CDK2 and cyclin B/CDK1 drive the progression through the G2 and the M phases. Specific checkpoint mechanisms are also present that control for any errors in DNA synthesis or chromosomal segregation, to prevent their transmission to daughter cells. When activated, these molecules regulate CDK activity by means of CDK inhibitors (CDKIs) that can produce a cell cycle arrest, during which these defects can be repaired. When such a repair is unsuccessful, cells are programmed to undergo senescence or apoptosis to prevent further transmission of errors in the genetic code. Molecular alterations in the regulatory machinery can allow cells to accumulate genetic or chromosomal defects that are a characteristic feature of malignant cells. Genetic alterations in various molecules involved in cell cycle regulation also allow the uncontrolled proliferation of cancer cells.

1.8.2 Signal transduction in the CDK 4/6-RB pathway

Signaling events initiated by growth promoting external stimuli act in the early part of the G1 phase to push resting G0 cells to proliferate. This external control extends only till the later part of the G1 phase until the R point is reached. Beyond this point, the progress through the cell cycle can be controlled only by the internal cell cycle machinery and is insensitive to external stimuli. The retinoblastoma (RB) protein is responsible for the regulation of the R point and the G1-S transition to allow cell proliferation (Knudsen and Wang, 2010) (Figure 1.8). In the absence of external mitogenic stimuli, RB family proteins (RB, p107 and p130) are hypophosphorylated and inhibit the expression of E2F target genes such as *CCNE2*, *CCNA2*, *CDK1*, *CDK2* and *DHFR* that control further cell cycle progression. This occurs by their direct binding with E2F and blocking its activation domain, or by active repression of gene transcription by modifying chromatin structure through the recruitment of histone deacetylase (HDAC), methyltransferase, Polycomb proteins, SWI/SNF factors. RB family proteins are a substrate of the CDKs. When mitogenic stimuli are present, the formation and assembly of D-type cyclins (cyclin D1, cyclin D2 and cyclin D3) and CDK 4 or CDK 6 complexes is increased. This results in activation of the kinase activity of CDK 4/6 and phosphorylation of the RB family of proteins in the early and mid G1 phase. This phosphorylation removes the inhibitory effect on the transcription of E2F targets and allows cells to progress through the cell cycle and proliferate. The CDKIs interfere with the binding of CDKs to cyclins and result in their inhibition. The INK4 family of proteins that includes CDKN2A (p16INK4A), CDKN2B (p15INK4B), CDKN2C (p18INK4C) and CDKN2D (p19INK4D) inhibit the activity of CDK 4/6 in response to anti-proliferative signals and thus prevent RB phosphorylation and subsequent cell cycle progression. In

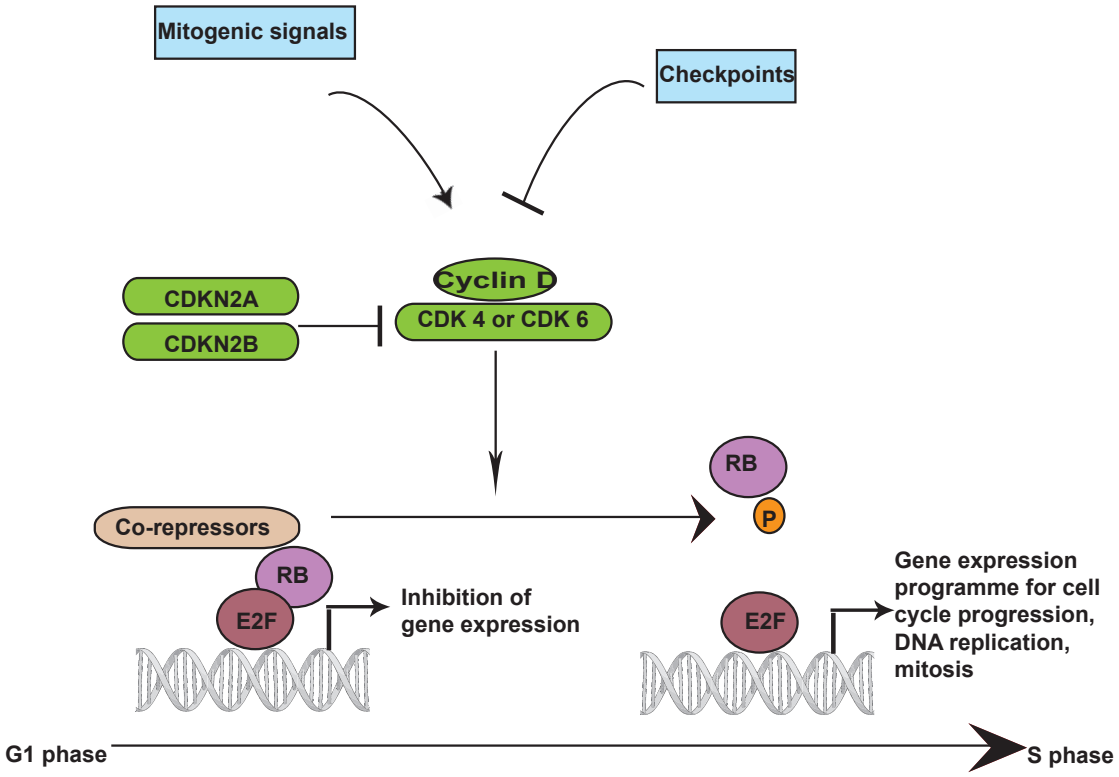

Figure 1.8: **The CDK 4/6 RB network.** The CDK 4/6-RB pathway regulates the G1-S transition. Phosphorylation of RB by CDK 4/6 results in its dissociation from the E2F complex. This allows the transcription of genes that enable the cell cycle to proceed. CDKN2A (p16INK4A) and CDKN2B (p15INK4B) negatively regulate the activity of CDK 4/6. Adapted from Asghar et al., 2015.

the late G1 phase, RB phosphorylation is also regulated by the cyclin E/CDK2 complex that can be inhibited by the Cip/Kip family of CDKIs such as CDKN1A (p21Cip1) and CDKN1B (p27Kip1).

Loss of RB function allows deregulation of the cell cycle machinery and is a common event in cancer cells (Giacinti and Giordano, 2006). In fact the RB protein was the first tumor suppressor that was identified . This loss of function occurs most frequently through inactivating mutations, which are commonly found in retinoblastoma, a childhood cancer. RB inactivation can also result from binding with viral oncoproteins like in cervical cancer. Overexpression of cyclin D, CDK4 or CDK6 as well as the loss of function of CDKN2A or CDKN2B can all result in the hyperphosphorylation of RB, which results in uncontrolled cell proliferation.

1.8.3 CDK 4/6 inhibitors in cancer treatment

The deregulation of the cell cycle can be targeted for cancer treatment with the use of CDK inhibitors. These inhibitors can prevent RB phosphorylation, repress E2F transcription and prevent S phase entry leading to reduced cell proliferation. The first (eg. flavopiridol) and second (eg. dinaciclib) generation of CDK inhibitors were non-specific and inhibited several CDKs. This low specificity was responsible for disappointing results in clinical trials and was also accompanied by high toxicities (Asghar et al., 2015). Newer inhibitors have been developed that are more selective and act against specific CDKs. There are three specific CDK 4/6 inhibitors that have been reported to date: PD-0332991, LEE011 and LY2835219 (Fry et al., 2001, Gelbert et al., 2014, Rader et al., 2013). While all these inhibitors are speculated to bind to the ATP-binding cleft in CDK 4/6 and function as ATP-competitive kinase inhibitors, no structural analyses have been published to date. These CDK 4/6 inhibitors have been tested in pre-clinical models of several cancer types including breast, ovarian, lung, prostate, renal, colon and liver cancer, as well as in haematological malignancies. Most reports have shown an accumulation of cells in the G0/G1 phase after treatment that is effective only in the absence of RB mutations. This reflects a specific mechanism of action of the inhibitors that relies on the RB regulated G1-S transition of the cell cycle (Asghar et al., 2015). PD-0332991 is being examined in over 60 clinical trials in oncology (https://clinicaltrials.gov/). It was recently granted FDA breakthrough therapy designation in the treatment of estrogen receptor (ER) positive metastatic breast cancer in combination with hormone therapy (Dhillon, 2015).

1.8.4 CDK 4/6 as a target in bladder cancer

Integrated network analysis from TCGA data has demonstrated that the cell cycle is deregulated in up to 93% of BLCA. This includes molecules such as *TP53*, *ATM*, *MDM2* as well as members of the RB signaling pathway (Network, 2014). This high frequency of molecular alterations provides a rationale for the therapeutic targeting of cell cycle regulation in BLCA. CDK 4/6 inhibitors have shown promising results in a variety

of cancers and have an established safety profile. Specific CDK 4/6 inhibitors have not been examined to date in BLCA. Inhibiting the CDK 4/6-RB network using these inhibitors represents a novel experimental treatment strategy in BLCA.

1.9 Aims and objectives

Target therapies directed against specific signaling networks have the potential to improve the dismal prognosis of patients with advanced BLCA. The two most frequently altered signaling pathways in BLCA are the RTK/PI3K/AKT/mTOR pathway and the cell cycle regulation pathway. This high frequency of alterations provides a rationale for examining their potential for therapeutic targeting. In this work, we aimed to:

(I) characterize the potential of AKT as a target for BLCA treatment.

(II) characterize the potential of CDK 4/6 as a target for BLCA treatment.

(III) identify stratifying and predictive biomarkers for response to these treatments to enable their personalized application in the clinic.

We had the following objectives to address these aims:

(i) Using BLCA cell lines that mimic the molecular alterations and heterogeneity found in BLCA.

(ii) Determining the biochemical effects of AKT or CDK 4/6 inhibition on signal transduction in these cell lines.

(iii) Analyzing the functional consequences of AKT or CDK 4/6 inhibition on cell viability, apoptosis and cell cycle proliferation in these cell lines.

(iv) Investigating the influence of specific molecular alterations on sensitivity to AKT or CDK 4/6 inhibition.

(v) Utilising genetic manipulation strategies to identify the molecular determinants of treatment response.

(vi) Determining the molecular mechanism underlying treatment response.

(vii) Extrapolating the *in vitro data* to a three-dimensional, *in vivo* xenograft model.

2 Materials

2.1 Multiple use equipment

Multiple use equipment	Source
3M durapore surgical tape	3M, Saint Paul, MN, USA
Analytical balance AT250	Mettler Toledo, Giessen, Germany
Analytical balance Sartorius 2254	Sartorius, Goettingen, Germany
Autoclave Sytec DX-65	Systec GmbH, Linden, Germany
Automatic film processor Curix CP1000	Agfa Healthcare, Mortsel, Belgium
Bag sealer Folio FS3602	Severin Elektrogeraete GmBH, Sundern, Germany
BD FACSCalibur Flow Cytometry System	BD Biosciences, San Jose, CA, USA
Biological safety cabinet Herasafe KS12	Thermo Scientific, Waltham, MA, USA
BVC professional laboratory fluid aspirator	Vacuubrand Gmbh, Wertheim, Germany
Centrifuge 5810R	Eppendorf GmbH, Hamburg, Germany
Centrifuge ROTINA 35R	Hettich, Tuttlingen, Germany
Chemidoc XRS Imaging System	BioRad, Hercules, CA, USA
CO_2 incubator HERA Cell240	Thermo Scientific, Waltham, MA, USA
CO_2 incubator HERA Cell240i	Thermo Scientific, Waltham, MA, USA
Cold light source Leica L2	Leica Microsystems GmbH, Wetzlar, Germany
Cryogenic Freezing Container, 1 Deg C	Nalgene, Rochester, NY, USA
Dremel 300	Dremel, Racine, WI, USA
Electrophoresis Power Supply EPS 601	Amersham Pharmacia Biotech., Uppsala, Sweden
Embedding center Leica EG1150	Leica Microsystems GmbH, Wetzlar, Germany
Glassware	Schott AG, Mainz, Germany
Heating and drying oven Heraeus FunctionLine B6	Thermo Scientific, Waltham, MA, USA
Heating and drying oven Heraeus FunctionLine UT20	Thermo Scientific, Waltham, MA, USA
Heating block thermostat BT100	Kleinfeld Labortechnik, Gehrden, Germany
Ice machine Manitowoc	Manitowoc Ice, Manitowoc, WI, USA

Multiple use equipment	Source
Intellimixer RM-2L	Elmi Ltd. Laboratory Equipment, Calabasas, CA, USA
Magnetic Stirrer	Heidolph Instruments GmbH, Schwabach, Germany
Microcentrifuge 5430R	Eppendorf GmbH, Hamburg, Germany
Microcentrifuge QikSpin QS7000 personal	Edwards Instrument Co., Narellan NSW, Australia
Micropipettes PIPETMAN P2,P10, P20, P200, P1000	Gilson Inc., Middleton, WI , USA
Microplate reader Vmax Kinetic	Molecular Devices, Sunnyvale, CA, USA
Microscope AxioVert.135	Carl Zeiss, Oberkochen, Germany
Microscope AxioVert.A1	Carl Zeiss, Oberkochen, Germany
Microscope camera AxioCam ERc 5s	Carl Zeiss, Oberkochen, Germany
Microtome RM 2255	Leica Microsystems GmbH, Wetzlar, Germany
Mini Protean System	BioRad, Hercules, CA, USA
Mini Trans-blot cell transfer system	BioRad, Hercules, CA, USA
Mini-PROTEAN Tetra Cell gel system	BioRad, Hercules, CA, USA
Minishaker IKA MS2	IKA Works Inc., Staufen, Deutschland
Multilabel plate reader VICTOR X3	Perkin Elmer, Waltham, MA, USA
Neubauer chamber	LO Laboroptik, Lancing, England
Orbital shaker K15	Edmund Buehler GmbH, Hechingen, Germany
PerfectBlue Gelsystem Mini M	PEQLAB Biotechnologie GmbH, Erlangen, Deutschland
pH Meter 691	Metrohm, Filderstadt, Germany
Power supply PowerPac HC	BioRad, Hercules, CA, USA
Pressure cooker	Fissler & Fissler, Idar-Oberstein, Germany
Spectrophotometer Nanodrop 2000c	Thermo Scientific, Waltham, MA, USA
Stereo microscope Stemi DV4	Carl Zeiss, Oberkochen, Germany
Surgical instruments	Timesco, Essex, United Kingdom
Thermal cycler C1000 CFX96	Bio-Rad, Hercules, CA, USA
Thermal cycler MJ Research PTC-200	BioRad, Hercules, CA, USA
Tissue processor Leica ASP200 S	Leica Microsystems GmbH, Wetzlar, Germany
Vortex-Genie 2	Scientific Industries, Inc., Bohemia, NY, USA
Water bath W350	Memmert, Schwabach, Germany
Water purification system, Purelab	ELGA Lab water, Celle, Germany

Table 2.2: List of multiple use equipment.

2.2 Disposable equipment

Disposable equipment	Source
Amersham hybond-P PVDF-Membrane	GE-Healthcare, Buckinghamshire, England
Cell culture plates 96 well, 6 well, 10 cm, 20 cm	Corning Incorporated, Corning, NY, USA
Cell lifter Sigma	Sigma-Aldrich Chemie GmbH, Munich, Germany
Chromatography paper Whatman	GE-Healthcare, Buckinghamshire, England
Conical bottom polystyrene tubes	Elkay, Hampshire, United Kingdom
Conical tubes 15 ml and 50 ml Falcon	Greiner GmbH, Frickenhausen, Germany
Cryogenic vials 1.8 ml Nunc	Thermo Scientific, Waltham, MA, USA
Embedding cassettes Rotilabo	Carl Roth, Karlsruhe, Germany
Hard-Shell PCR Plates 96-well	BioRad, Hercules, CA, USA
Lens cleaning paper	The Tiffen company, Hauppauge, NY, USA
Microscope coverslips	Thermo Scientific, Waltham, MA, USA
Microscope slides Superfrost plus	Thermo Scientific, Waltham, MA, USA
Microtome blades Feather R35	pfm medical AG, Cologne, Germany
Needles 27 Gauge	BD Biosciences, San Jose, CA, USA
PCR reaction tubes 0.5 ml	Biozym Scientific, Oldendorf, Germany
PCR Sealers Microseal 'B' Film	BioRad, Hercules, CA, USA
Pipette tips with and without filter	Sarstedt, Nuembrecht, Germany
Reaction tubes 0.5 ml, 1.5 ml, 2 ml	Sarstedt, Nuembrecht, Germany
Round bottom polystyrene tubes	Corning Incorporated, Corning, NY, USA
Silicone sheet, 0.5 mm thick	Sahlberg GmbH & Co., KG, Munich, Germany
Serological pipettes	Greiner Bio-One International AG, Kremsmuenster, Austria
Sterile filter Nalgene 0.25 µm, 0.45 µm	Thermo Scientific, Waltham, MA, USA
Syringes 1 ml Omnifix	B.Braun Melsungen AG, Melsungen, Germany
White polystyrene 96 well plates	Corning Incorporated, Corning, NY, USA
X-ray film CEA RP New	Agfa Healthcare, Mortsel, Belgium

Table 2.4: List of disposable equipment.

2.3 Chemicals, reagents and enzymes

Chemicals, reagents and enzymes	Source
2-mercaptoethanol	Sigma-Aldrich Chemie GmbH, Munich, Germany
70% Ethanol	BrueggemannAlcohol Heilbronn GmbH, Heilbornn, Germany
7-aminoactinomycin D (AAD)	Life Technologies, Carlsbad, CA, USA
96% Ethanol	Otto Fischar GmbH, Saarbruecken, Germany
Agarose Ultrapure	Thermo Scientific, Waltham, MA, USA
Ammonium persulfate (APS)	Sigma-Aldrich Chemie GmbH, Munich, Germany
Ampicillin	Sigma-Aldrich Chemie GmbH, Munich, Germany
Boric acid	Sigma-Aldrich Chemie GmbH, Munich, Germany
Bovine serum albumin (BSA)	Sigma-Aldrich, St. Louis, MO, USA
Bromophenol blue	Serva Electrophoresis GmbH, Heidelberg, Germany
Cisplatin	Sigma-Aldrich Chemie GmbH, Munich, Germany
Color Prestained Protein Standard, Broad Range	New England Biolabs, Ipswich, MA, USA
Complete Mini - Protease Inhibitor	Roche, Basel, Switzerland
DAKO REAL antibody diluent	Dako, Hamburg, Germany
Developing and fixation solutions Vision X GV60	Roentgen bender GmbH & Co. KG, Baden-Baden, Germany
Dimethyl sulfoxide (DMSO)	Sigma-Aldrich Chemie GmbH, Munich, Germany
Dithiothreitol (DTT)	Cell-Signaling, Cambridge, England
DNA ladder 2-Log (0.1 to 10 kb)	New England Biolabs GmbH, Frankfurt, Germany
DNA Loading buffer (6x)	Thermo Scientific, Waltham, MA, USA
Dulbecco's Modified Eagle's Medium (DMEM)	Biochrom, Berlin, Germany
E. coli, DH10B	Dr. P. S. Holm, Experimental Urology, Klinikum rechts der Isar, TUM
Ethanol absolute	Merck Chemicals GmbH, Hessen, Germany
Ethidiumbromide, 10 mg ml^{-1}	Sigma-Aldrich Chemie GmbH, Munich, Germany

Chemicals, reagents and enzymes	Source
Ethylenediaminetetraacetic acid (EDTA), 0.5 M	AppliChem, Darmstadt, Germany
Fertilized eggs from white Leghorn chickens	Brueterei Sued, Regenstauf, Germany
Fetal Bovine Serum (FBS)	Biochrom, Berlin, Germany
Formaldehyde solution, 36.5-38%	Sigma-Aldrich Chemie GmbH, Munich, Germany
Fugene HD	Promega Corporation, Madison, WI, USA
Glycine	Sigma-Aldrich Chemie GmbH, Munich, Germany
GoTaq qPCR master mix	Promega, Madison, WI, USA
GoTaq Green PCR master mix	Promega, Madison, WI, USA
Haematoxylin solution, Mayer's	Krankenhausapotheke, Klinikum rechts der Isar, Munich, Germany
Human serum	Life technologies, Carlsbad, CA, USA
Hydrogen chloride (HCl)	Merck Chemicals GmbH, Hessen, Germany
Hydrogen peroxide (H_2O_2)	Merck Chemicals GmbH, Hessen, Germany
Isocitrate monohydrate	Sigma-Aldrich Chemie GmbH, Munich, Germany
Isopropanol	Sigma-Aldrich Chemie GmbH, Munich, Germany
Kanamycin	Sigma-Aldrich Chemie GmbH, Munich, Germany
Lipofectamine 2000	Invitrogen, Carlsbad, CA, USA
Lipofectamine RNAimax	Invitrogen, Carlsbad, CA, USA
Luminol	Sigma-Aldrich Chemie GmbH, Munich, Germany
LY2835219	Selleck Chemicals, Houston, TX, USA
Matrigel Phenol red free	BD Biosciences, San Jose, CA, USA
Methanol	Sigma-Aldrich Chemie GmbH, Munich, Germany
MK-2206 HCl	Active Biochem, Bonn, Germany
Mounting medium Entellan-new	Merck Chemicals GmbH, Hessen, Germany
Non-essential amino acids (NEAA), 100x	Biochrom, Berlin, Germany
Opti-MEM	Invitrogen, Carlsbad, CA, USA
p-Coumaric acid	Sigma-Aldrich Chemie GmbH, Munich, Germany
PD-0332991 isethionate	Sigma-Aldrich Chemie GmbH, Munich, Germany

Chemicals, reagents and enzymes	Source
Phosphate buffered saline (PBS), 1x, 10x	Biochrom, Berlin, Germany
Phosphatase inhibitor Mix II	Serva Electrophoresis GmbH, Heidelberg, Germany
Precision Plus Protein Standard	Bio-Rad, Hercules, CA, USA
Restriction enzymes and buffers	Thermo Scientific, Waltham, MA, USA
Roswell Park Memorial Institute medium (RPMI)	Biochrom, Berlin, Germany
Rotiphorese gel 30	Carl Roth, Karlsruhe, Germany
Select agar	Sigma-Aldrich Chemie GmbH, Munich, Germany
Skimmed milk powder	Nestle, Vevey, Switzerland
SOC medium	Life Technologies, Darmstadt, Germany
Sodium acetate	Merck, Darmstadt, Germany
Sodium azide	Sigma-Aldrich Chemie GmbH, Munich, Germany
Sodium chloride (NaCl)	Merck Chemicals GmbH, Hessen, Germany
Sodium dodecyl sulfate (SDS)	Sigma-Aldrich Chemie GmbH, Munich, Germany
Sodium orthovanadate	Sigma-Aldrich Chemie GmbH, Munich, Germany
Sterile NaCl 0.9%	B.Braun Melsungen AG, Melsungen, Germany
T4 DNA Ligase	Thermo Scientific, Waltham, MA, USA
TaqDNA Polymerase	Thermo Scientific, Waltham, MA, USA
Tetramethylethylenediamine (TEMED)	Carl Roth, Karlsruhe, Germany
Tris(hydroxymethyl)-aminomethane	Merck, Darmstadt, Germany
Triton X-100	Sigma-Aldrich Chemie GmbH, Munich, Germany
Trypan blue, 0.5%	Biochrom, Berlin, Germany
Trypsin/EDTA	Biochrom, Berlin, Germany
Tryptone	Sigma-Aldrich Chemie GmbH, Munich, Germany
Tween-20	Serva Electrophoresis GmbH, Heidelberg, Germany
Yeast Extract	Sigma-Aldrich Chemie GmbH, Munich, Germany

Table 2.6: List of chemicals, reagents and enzymes

2.4 Commercial kits

Commercial kits	Source
Caspase-Glo 3/7 Assay	Promega, Madison, WI, USA
CellTiter-blue Cell Viability Assay	Promega, Madison, WI, USA
Click-iT EdU Flow Cytometry Assay	Life Technologies, Carlsbad, CA, USA
HiSpeed Plasmid Midi Kit	Qiagen, Hilden, Germany
mirVANA miRNA isolation kit	Thermo Scientific, Waltham, MA, USA
Pierce BCA Protein Assay	Thermo Scientific, Waltham, MA, USA
QIAquick gel extraction kit	Qiagen, Hilden, Germany
QIAprep Spin Miniprep Kit	Qiagen, Hilden, Germany
REAL Detection System K5001	Dako, Hamburg, Germany

Table 2.7: List of commercial kits

2.5 Buffers and solutions

All buffers and solutions were prepared using distilled H_2O.

Buffer	Components
0.05 % SDS Protein lysis buffer used in section 4.1	150 mM NaCl 50 mM Tris/HCl, pH 7.2 1% Triton X-100 0.05% SDS 5 mM EDTA Add 1 Complete Mini-Protease Inhibitor tablet and 100 µl of phosphatase inhibitor for every 10 ml of protein lysis buffer prior to use
1% SDS Protein lysis buffer used in section 4.2	10 mM Tris/HCl, pH 7.2 1% SDS 1 mM Na orthovanadate (heated until pH 10 obtained) Add 1 Complete Mini-Protease Inhibitor tablet and 100 µl of phosphatase inhibitor for every 10 ml of protein lysis buffer prior to use
Stacking gel buffer	0.5 M Tris-HCl, pH 6.8

Buffer	Components
Separating gel buffer	1.5 M Tris-HCl, pH 8.8
10x SDS page running buffer	25 nM Tris 192 mM Glycine 0.1% w/v SDS pH 8.3
10x Transfer buffer	25 nM Tris 192 mMGlycine
1x Transfer buffer	10% 10x Transfer buffer 20% Methanol
4X Protein loading buffer	0.25 M Tris-HCl, pH 6.8 8% SDS 0.04% Bromophenol blue 40% Glycerine Add 100 µl of 1 M DTT to 500 µl of 4x - protein loading buffer prior to use
10x TBS	0.5 M Tris-HCl, pH=7.6
10x TBE	1 M Tris 1 M Boric acid 0.02 M EDTA
TBS-T	1x TBS 0.001% Tween-20
Immunoblotting blocking solution	5% non-fat milk powder in TBS-T
Immunoblotting antibody dilution buffer	5% BSA in TBS-T with 0.02% Sodium Azide
Citrate buffer for heat induced epitope - retrieval	0.01 M Isocitrate monohydrate, pH 6.0
LB medium	0.01% Tryptone 0.005% Yeast extract 0.01% NaCl
LB agar	LB medium 1.5% Select agar
Chemiluminescence reagent part A	0.1 M Tris-HCl, pH 8.5 2.5 mM Luminol 0.4 mM p-Coumaric acid
Chemiluminescence reagent part B	0.1 M Tris-HCl, pH 8.5 0.18% H_2O_2

Table 2.9: List of buffers and solutions.

2.6 Antibodies

Following antibodies were used for immunoblotting (WB) or immunohistochemistry (IHC) at the respective concentrations. CST indicates Cell Signaling Technology.

Target protein, catalogue number	**Application**	**Dilution**	**Source**
4E-BP1, 9452	WB	1:1000	CST, Beverly, MA, USA
Phospho-4E-BP1 (Ser 65) 9456	WB	1:1000	CST, Beverly, MA, USA
Phospho-4E-BP1 (Thr 70) 9455	WB	1:1000	CST, Beverly, MA, USA
Phospho-4E-BP1 (Thr 37/46), (9459)	WB	1:1000	CST, Beverly, MA, USA
Akt (pan), 4685	WB	1:1000	CST, Beverly, MA, USA
Akt1, 2938	WB	1:1000	CST, Beverly, MA, USA
Akt2, 3063	WB	1:1000	CST, Beverly, MA, USA
Akt3, 4059	WB	1:1000	CST, Beverly, MA, USA
Phospho-Akt (Ser473), 3787	WB	1:1000	CST, Beverly, MA, USA
Phospho-Akt (Thr308), 2965	WB	1:1000	CST, Beverly, MA, USA
Phospho-Akt (Thr308), BS4009	IHC	1:100	Bioworld Technology Inc., St.Louis Park, MN, USA
Actin, A 2066	WB	1:1000	Sigma-Aldrich Chemie GmbH, Munich, Germany
CREB, 9197	WB	1:1000	CST, Beverly, MA, USA
Cyclin D1, 2978	WB	1:1000	CST, Beverly, MA, USA
GAPDH, 2118	WB	1:1000	CST, Beverly, MA, USA
GSK-3β, 9315	WB	1:1000	CST, Beverly, MA, USA
Phospho-GSK-3β (Ser9), 9323	WB	1:1000	CST, Beverly, MA, USA
HA-Tag, 2367	WB	1:1000	CST, Beverly, MA, USA
Ki-67 Antigen, M7240	IHC	1:100	Dako, Hamburg, Germany
MKP-1, sc-1102	WB	1:1000	Santa Cruz Biotechnology, Inc., Dallas, TX, USA
MEK1/2, 8727	WB	1:1000	CST, Beverly, MA, USA
Phospho-MEK1/2 (Ser217/221), 9154	WB	1:1000	CST, Beverly, MA, USA
p110α, 4249	WB	1:1000	CST, Beverly, MA, USA
Total Erk-1/2, 9102	WB	1:1000	CST, Beverly, MA, USA

Target protein, catalogue number	Application	Dilution	Source
Phospho-Erk-1/2 (Thr202/Tyr204), 4376	WB	1:1000	CST, Beverly, MA, USA
p70-S6Kinase, 9202	WB	1:1000	CST, Beverly, MA, USA
Phospho-p70-S6Kinase (Thr389), 9234	WB	1:1000	CST, Beverly, MA, USA
c-Raf, 9422	WB	1:1000	CST, Beverly, MA, USA
Phospho-c-Raf (Ser259), 9421	WB	1:1000	CST, Beverly, MA, USA
Phospho-c-Raf (Ser338), 9427	WB	1:1000	CST, Beverly, MA, USA
RB, 554136	WB	$2\,\mu g\,ml^{-1}$	BD Biosciences, San Jose, CA, USA
Phospho-RB (Ser 780), 8180	WB	1:1000	CST, Beverly, MA, USA
Peroxidase-conjugated Anti-Rabbit IgG , 711-036-152	WB	1:10000	Dianova GmbH, Hamburg, Germany
Peroxidase-conjugated Anti-Mouse IgG, 715-036-150	WB	1:10000	Dianova GmbH, Hamburg, Germany

Table 2.11: List of antibodies.

2.7 siRNA sequences

All small interfering RNAs (siRNAs) were synthesized by Life technologies (Darmstadt, Germany) and diluted in H_20 to a stock solution of $20\,\mu M$.

Target gene	Sequence	Modification
AKT1	UGCAGCAUCGCUUCUUUGCCGGUAU	Stealth
AKT1	GACGUGGCUAUUGUGAAGGAGGGUU	Stealth
AKT2	GGCACGGGCTAAAGTGACCATGAAT	Stealth
AKT2	CCUUGGCAAGGGAACCUUUGGCAAA	Stealth
AKT3	GGCACACACUCUAACUGAAAGCAGA	Stealth
AKT3	ACCTCAAGATGTGGATTTACCTTAT	Stealth
PIK3CA (directed against 5' UTR)	AAGAGCCCCGAGCGUUUCUGCUUUU	Stealth

Target gene	Sequence	Modification
DUSP1	GCCAUUGACUUCAUAGACUCCAUCA	Stealth
Mutant *PIK3CA* P9 13C	CTCCTGCTTAGTCATTTCAGAGAtt	Stealth
Mutant *PIK3CA* P9	CTCCTGCTTAGTGATTTCAGAGAtt	Stealth
Mutant *PIK3CA* P10	TCTCCTGCTTAGTGATTTCAGAGtt	Stealth
Mutant *PIK3CA* P16	AATCTTTCTCCTGCTTAGTGATTtt	Stealth
Negative control	Stealth RNAi siRNA Negative Control Hi GC Duplex #2 (proprietary sequence)	Stealth
CREB	GCUGGCUAACAAUGGUACCtt	None
Negative control	Silencer Negative Control No. 1 siRNA (proprietary sequence)	None

Table 2.13: List of siRNA sequences.

2.8 Primer sequences

All primers were synthesized by Life Technologies (Darmstadt, Germany) and dissolved in H_20 to 10 µM stock solutions.

Target gene	Forward primer	Reverse primer
RB1	AGCAACCCTCCTAAACCACT	TGTTTGAGGTATCCATGCTATCA
CCNA2	ACAAAGCTGGCCTGAATCAT	GTCTCTGGTGGGTTGAGGAG
CCNE2	TGTTGGCCACCTGTATTATCTGG	ATCTGGAGAAATCACTTGTTCCTATTTC
ACTB	ATCTGGCACCACACCTTCTAC-AATGAGCTGCG	CGTCATACTCCTGCTTGCTGAT-CCACATCTGC
GAPDH	TGGCATGGACTGTGGTCATGAG	ACTGGCGTCTTCACCACCATGG

Table 2.14: List of primers for qPCR.

Name	Primer sequence
pBABE forward primer	CTTTATCCAGCCCTCAC
pBABE forward primer	CCTCGGCCTCTGCATAAAT
T7	TAATACGACTCACTATAGGG
BGH	TAGAAGGCACAGTCGAGG

Table 2.15: List of primers for cloning and sequencing.

2.9 Plasmids

Plasmid	Source
pcDNA 3.1 V5 His TOPO	Life Technologies, Darmstadt,Germany
pBABE puro HA PIK3CA E545K, plasmid number 12525 (Zhao et al., 2005)	Addgene, Cambridge, MA, USA
RcCMV/Rb , plasmid number 1763 - (deposited by Bob Weinberg)	Addgene, Cambridge, MA, USA

Table 2.16: List of plasmids

2.10 Software for analysis

Name	Manufacturer
CompuSyn	Combo Syn Inc., Parasmus, NJ, USA
FlowJo	FlowJo LLC, Ashland, OR, USA
GraphPad	GraphPad Software Inc., La Jolla, CA, USA
Zen Lite 2012	Carl Zeiss, Oberkochen, Germany

Table 2.17: List of software for analysis

2.11 Cell culture

Quality control of cell lines was conducted by short tandem repeat profiling for authentication, and mycoplasma testing.

2.11.1 Cell lines

Cell line	Source
253J	Prof. Dr. WA Schulz, Heinrich-Heine-University, Duesseldorf, Germany
5637	Prof. Dr. WA Schulz, Heinrich-Heine-University, Duesseldorf, Germany
639V	Prof. Dr. WA Schulz, Heinrich-Heine-University, Duesseldorf, Germany
647V	Leibniz Institute German collection of microorganisms and cell culture, Braunschweig, Germany
HT1197	American type culture collection, Manassas, VA, USA
HT1376	American type culture collection, Manassas, VA, USA
J82	American type culture collection, Manassas, VA, USA
RT112	Leibniz Institute German collection of microorganisms and cell culture, Braunschweig, Germany
RT4	American type culture collection, Manassas, VA, USA
T24	American type culture collection, Manassas, VA, USA
UMUC3	American type culture collection, Manassas, VA, USA
VmCUB1	Prof. Dr. WA Schulz, Heinrich-Heine-University, Duesseldorf, Germany

Table 2.18: List of cell lines used

2.11.2 Media used for cell culture

Medium	Formulation
Culture medium for cells at 5 % $C0_2$	RPMI
	10% FBS
	1 % NEAA
Culture medium for cells at 10 % $C0_2$	DMEM
	10% FBS
	1 % NEAA
Freezing medium	50% RPMI or DMEM
	40% FBS
	10% DMSO

Table 2.19: List of cell culture media

3 Methods

3.1 Cell culture

3.1.1 Sub-culturing cell lines

Cells were cultured in laminar flow biological safety cabinets under sterile conditions. All cell lines were maintained in sub-confluent conditions and used in early passages. Solutions were pre-warmed to 37 °C before use. Sub-culturing of cells was carried out by aspirating existing medium, washing with PBS containing 5% 0.5 M EDTA, and incubating with trypsin at 37 °C until the cells were dissociated. Fresh medium was added to neutralize the tryspin and cells were centrifuged at 300 RCF for 5 min. They were re-suspended in fresh medium and a fraction was transferred onto new plates for culturing the subsequent passage. Cells were maintained at 37 degreeCelsius in saturated humidity. 253J, HT1197, 639V, HT1376, UMUC3 and VmCUB1 cell lines were maintained at 10% CO_2, while J82, 647V, T24, RT112, RT4 and 5637 cell lines were maintained at 5% $C0_2$.

3.1.2 Cell counting

Cells were diluted in 0.5% trypan blue and counted using a Neubauer chamber. Unstained cells were considered to be viable.

3.1.3 Cyropreservation of cells

Cells were detached from plates using PBS and trypsin as described above. Following centrifugation of cells, the pellet was re-suspended in 1 ml of freezing medium and transferred into cryovials. They were transported using a freezing container and stored at −80 °C for 48-72 hours, before transferring to liquid nitrogen. When thawing frozen cells for use, the cryovial was immersed in a water bath to ensure quick thawing of the freezing medium. Once thawed, cells were added to a tube containing fresh medium, centrifuged and sub-cultured as described in section 3.1.1.

3.2 Treatment with small molecule inhibitors and chemotherapeutic agents

MK-2206 was dissolved in DMSO and stored as a 10 mM stock solution at −20 °C. PD-0332991 esthionate and LY2835219 were dissolved in H_2O and stored as 10 mM stock solutions at −20 °C. Cisplatin was stored as a 3 mM stock solution dissolved in 0.9% NaCl at room temperature. Working concentrations were made fresh in pre-warmed medium. 1×10^6, 2×10^6 or 500-1000 cells were seeded a day before treatment with inhibitors in 10 cm, 6 well and 96 well formats respectively. For inhibitors dissolved in DMSO, the highest DMSO concentration was used as a control.

3.3 *In vitro* functional assays

3.3.1 Determination of cell viability

Cell viability was determined using the Cell-Titer blue cell viability assay as per manufacturer's protocol using 560 nm and 580 nm excitation and emission wavelengths respectively. Importantly, cell numbers were adjusted such that cells were not more than 70% confluent on the day of performing the assay (section 4.1). All experiments were performed in triplicate.

3.3.2 Determination of caspase 3/7 activity

Caspase 3/7 activity was determined using the Caspase-Glo 3/7 assay, as a readout for apoptosis. Manufacturer's protocol was followed by measuring luminescence. Absolute luminescence value was normalized to the number of living cells, which was determined by cell counting using trypan blue in parallel. All experiments were performed in triplicate.

3.3.3 Cell cycle analysis

Click-it EdU Alexa Fluor 488 flow cytometry kit was used as per manufacturer's protocol by incubating 10 µM EdU for 1-3 hours in triplicate samples. Total DNA was stained using 4 µg mL^{-1} 7-AAD. 10000 events were recorded on the flow cytometer ensuring a low speed that corresponded to less than 600 events per s. Data was analyzed using FlowJo software.

3.4 Determination of absolute IC50 values

Absolute IC50 values for the effect on cell viability were obtained using the 4 parameter logistic model using GraphPad Prism software. According to this model (Sebaugh,

2011),

$$\text{IC50} = c\left(\frac{a - 50\%\text{response}}{50\%\text{response} - d}\right)\left(\frac{1}{b}\right) \tag{3.1}$$

where a is the lower asymptote of the sigmoid curve, d is the upper asymptote, b is the slope of the linear portion of the curve and c is the concentration corresponding to the response midway between a and d.

3.5 Quantification of synergy

Efficacy of drug combinations was assessed by calculating the combination index (CI) (Chou, 2010, Chou, 2006) using the CompuSyn software. According this method, the effect of a single drug is given by the median effect equation:

$$\frac{Fa}{Fu} = \left(\frac{D}{Dm}\right)m, \tag{3.2}$$

where D is the dose of a drug, Fa is the fraction affected by this dose, Fu is the fraction unaffected by the dose, Dm is the median effect dose and m is the coefficient signifying the shape of the dose-effect relationship, with $m = 1$, > 1 and < 1 indicating hyperbolic, sigmoidal and flat curves respectively. The CI is calculated from the median effect of the constituent drugs in the combination as well as the combined effect of the combination as:

$$\text{CI} = \frac{D_1}{Dx_1} + \frac{D_2}{Dx_2} \tag{3.3}$$

where Dx in the denominator are for the D1 and D2 when drugs 1 and 2 are used alone to produce an x% effect, while the $D1$ and $D2$ in the numerator refer to the combination of 1 and 2 that also produces an x% effect. A CI value less than 1, equal to 1 and greater than 1 indicates synergism, additive effect and antagonism respectively. The dose reduction index (DRI) measures how many fold the dose of each drug in a combination can be reduced compared with the doses of each drug alone to obtain a given effect.

3.6 Immunoblotting

3.6.1 Preparation of cell lysates

Entire procedure was carried out on ice. Medium from cell culture plates was aspirated and cells were washed using ice cold PBS. Maximum possible PBS was aspirated and cold lysis buffer containing phosphatase and protease inhibitors was added onto the plate. 500 µL and 100 µL volumes of buffer were used for 10 cm and 6 well plates respectively. Cells were harvested in the lysis buffer using cell scrapers and transferred

Ingredient	Volume (ml)
H_20	2.45
1.5 M Tris pH 8.8	2.5
30% acrylamide/Bis-acrylamide solution	5
10% APS	0.05
TEMED	0.01
Total	10

Table 3.1: Formulation of a 15% polyacrylamide gel.

Ingredient	Volume (ml)
H_20	3.07
0.5 M Tris pH 6.8	1.25
30% acrylamide/Bis-acrylamide solution	0.65
10% APS	0.025
TEMED	0.005
Total	5

Table 3.2: Formulation of a polyacrylamide stacking gel.

to a microcentrifuge tube. When using lysis buffer containing 1% SDS, shear forces were applied to the lysate using a 27 gauge needle until no viscosity was observed. Lysates were centrifuged at 30000 RCF for 30 min at 4 °C in a pre-cooled centrifuge, following which the supernatant was transferred into a fresh tube. Lysates were either used immediately or stored at −80 °C.

3.6.2 Protein quantification and sample preparation

Proteins were quantified using the BCA assay as per manufacturer's protocol in a 96-well format. Briefly, all samples were prepared in duplicate together with a series of BSA standards and incubated with the working reagent for 30 min at 37 °C. Absorbance was measured at 562 nm and the protein quantity of the samples was obtained by comparison with the BSA reference standards. Proteins from all samples were adjusted to equal amounts using protein lysis buffer and a fresh mixture of 4x protein loading buffer and DTT. Samples were mixed and denatured for 5 min at 100 °C. Following denaturation, samples were either immediately used for immunoblotting or stored at −20 °C.

3.6.3 Sodium dodecyl sulfate polyacrylamide gel electrophoresis (SDS-PAGE)

Polyacrylamide gels were hand cast using gel casting chambers. 8, 10, 12 or 15% separating gels were used depending on the desired protein separation (table 3.1). Few ml of Isopropanol were used to cover the separating gel to allow polymerization and ensure a sharp demarcation. Once the separating gel was polymerized, stacking gel was prepared (table 3.2). Isopropanol was removed, stacking gel was poured and a comb was inserted. Following complete polymerization, gels were fixed into the electrophoresis assembly and 20-100 µg of protein sample was loaded onto the gel. Electrophoresis was carried out at 90 V until proteins entered the separating gel and then continued at 150 V.

3.6.4 Transfer and blocking

Following electrophoresis, proteins were transferred onto a PVDF membrane that was activated by immersing in methanol for 2-5 min. The gel and the membrane were assembled in between two layers of blotting paper and sponges, which were incubated in blotting buffer before use. Wet transfer was conducted for 1-2 hours at 100 V using transfer buffer. Following the transfer, membrane was blocked for nonspecific binding by incubating in blocking solution for 1 hour at room temperature.

3.6.5 Immunodetection

Primary antibodies were added at the required concentrations by dissolving in antibody dilution buffer and incubated at 4 °C overnight. Membranes were then washed 3-5 times in TBST and incubated for 30 min at room temperature with secondary antibody diluted in the blocking solution. After 3-5 further washing steps, proteins were detected using the ECL reaction. Chemiluminescent signal was visualized using autoradiography films.

3.7 Designing allele specific siRNAs

siRNAs can potentially distinguish between mRNA sequences that differ at a single base pair. This property can be used to design allele specific (ASP) siRNAs that discriminate between a mutant and a wild-type (WT) copy of a gene (Schwarz et al., 2006). We designed siRNAs to distinguish between the WT *PIK3CA* gene and *PIK3CA* gene with a 1633G>A (E545K) mutation (Figure 3.1). All siRNA sequences were fully complementary to the mutant sequence but possessed a mismatch with the WT sequence at position 1633 containing the nucleotide G. Previous reports indicate that successful allelic discrimination is aided by specific positions of nucleotide mismatches (Schwarz et al., 2006). Hence, we built a tiled set of siRNAs with mismatches at positions 9, 10 and 16 (named as P9, P10 and P16 respectively), which have been demonstrated

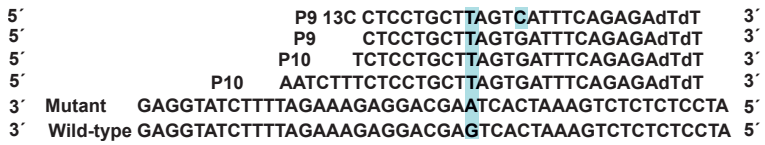

Figure 3.1: **Allele specific siRNA design.** Sequences of guide siRNA strands were designed complementary to the mutant *PIK3CA* allele, but mismatched with the WT allele. This mismatch was generated at different nucleotide positions within the siRNA.

to enable maximum discrimination. Another report also indicated that an additional mismatch at a subsequent position enhances the allelic discrimination (Ohnishi et al., 2008). Hence, we added an extra P13 mismatch in the P9 sequence (named P9 13C). dT overhangs were added to have an unpaired 5' end in the anti-sense siRNA strand, to enable its activity as the guide strand (Schwarz et al., 2003).

3.8 Transfection of nucleic acids

siRNA transfection was carried out using Lipofectamine RNAiMax as per manufacturer's protocol. 0.5×10^5 or 1×10^5 cells were reverse transfected in a 6 well format with a final siRNA concentration of 10 nM. Fugene HD was used for DNA transfection according to manufacturer's protocol. Generally, cells were seeded one day before transfection and 3 µl of Fugene HD was used to transfect 1 µg of DNA in a 6 well format. Co-transfection of DNA and siRNAs was conducted using Lipofectamine 2000 as per manufacturer's protocol using 1 µg DNA and 10 nM final concentration of siRNA in a 6-well format. All nucleic acid-transfection reagent complexes were prepared in Opti-MEM. For different cell culture plate formats, cell numbers and quantities of reagents were adjusted according the surface area. Care was taken that the transfection reagent was pipetted directly into OptiMEM, avoiding any contact with the plastic of microcentrifuge tubes. Mixing was done using gentle pipetting or inverting the tube to prevent dissociation of the complexes.

3.9 Molecular biology techniques for cloning

3.9.1 Isolation of plasmid DNA

LB medium containing the selective antibiotic (100 µg ml^{-1} Ampicillin or 50 µg ml^{-1} Kanamycin) was inoculated with single colonies of the plasmid containing bacteria and cultured at 37 °C with vigorous shaking for 16-18 hours until saturation was reached. 5 ml or 100 ml volumes were used for DNA extraction with miniprep or midiprep kits respectively, which were performed according to the manufacturer's protocol and DNA

concentration was measured using NanoDrop 2000c. Plasmid stocks were prepared by mixing 1 ml of the growth culture with 1:1 glycerol or 1:10 DMSO respectively and stored at −80 °C.

3.9.2 Generation of competent bacteria

E.coli (DH10B were streaked overnight on agar plates and sub-cultured in 5 ml LB medium. 100 µl of this culture was added to 100 ml of LB medium and incubated for 2-3 hours to ensure growth in an early log phase. Culture was centrifuged at 3200 g for 10 min at 4 °C and resuspended in cold 50 mM $CaCl_2$, followed by incubation on ice for 90 min. Cells were centrifuged again and resuspended in cold 1 ml $CaCl_2$, mixed with glycerol in a 1:4 volume and frozen immediately at −80 °C.

3.9.3 Restriction digestion

For analysis of plasmids or obtaining DNA fragments for cloning, generally 1 µg DNA was digested in required enzymes in a compatible buffer for 1 hour at 37 °C. Plasmid identity was additionally confirmed by sequencing which was performed by GATC Biotech AG, Constance, Germany.

3.9.4 Agarose gel electrophoresis

1-2% agarose gels were prepared in 1xTBE buffer with a 0.5 µg ml^{-1} final concentration of ethidium bromide. DNA was loaded using 6x loading dye. Gels were run in 1x TBE buffer at 110 V until bands were separated adequately. Bands were visualized using UV transillumination and documentation was done using the Chemidoc XRS system.

3.9.5 Gel extraction, ligation and transformation

Following agarose gel electrophoresis, the DNA fragment of interest was isolated using the Qiaquick gel extraction kit. 80 fmol of the insert was ligated to 16 fmol of the vector using T4 DNA ligase, by incubating at 15 °C for 16-18 hours. Competent bacteria were thawed on ice shortly before transformation, mixed gently with 0.8 µl of 2-Mercaptoethanol and kept on ice for 10 min. 100 µl of the ligation mixture was added to the competent cells and incubated on ice for 30 min, followed by a 45 s pulse at 42 °C and a 2 min incubation on ice. The cells were then re-suspended in pre-warmed SOC medium and incubated for 1 hour, shaking at 37 °C. Various amounts of this medium were streaked onto LB agar plates containing the selection antibiotic and incubated at 37 °C for 16-18 hours.

3.9.6 Polymerase chain reaction (PCR) screening of clones

PCR mix was prepared using the GoTaq Green PCR master mix according to manufacturer's protocol, using 10 µM of forward and reverse primers. Up to 24 single colonies

were picked using a sterile pipette tip and streaked onto a fresh LB agar plate containing the selection antibiotic. The same pipette tip was placed inside the PCR reaction mix to transfer the plasmid DNA. PCR cycling conditions were as follows: 95 °C for 2 min, with 30 cycles of 95 °C for 30 s, 60 °C for 30 s, 72 °C for 4 min, followed by 72 °C for 5 min. Restriction digestion, agarose gel electrophoresis and sequencing were performed to confirm the identity of the clone.

3.9.7 Cloning strategy for pcDNA3.1 v5 HisTOPO HA PIK3CA E545K

The HA PIK3CA E545K fragment from pBABE puro HA PIK3CA E545K was digested using BamHI and SacII, and ligated into the pcDNA 3.1 v5 His TOPO vector, which was digested using the same restriction enzymes.

3.10 Analysis of gene expression levels

3.10.1 RNA extraction

Total RNA was extracted from cultured cells using the mirVANA miRNA isolation kit as per manufacturer's protocol and stored at −80 °C. RNA quantity was determined using Nanodrop 2000c. RNA with an A260/280 and A260/230 ratio between 1.9-2 was used for downstream applications.

3.10.2 cDNA synthesis

High capacity cDNA reverse transcription kit was used following manufacturer's protocol to synthesize cDNA from 2 µg of total RNA in a 20 µl volume.

3.10.3 Quantitative polymerase chain reaction (qPCR)

qPCR was carried out using GoTaq qPCR Master mix with 50 ng of cDNA in a 10 µl volume with 0.25 µM or 0.5 µM of forward and reverse primers. Reactions were performed in triplicate using a CFX96 Real-Time PCR detection system with following cycling conditions: 94 °C for 2 min, 94 °C for 15 s, 60 °C for 30 s and 72 °C for 1 min for 44 cycles. Quality of the reaction was analyzed by agarose gel electrophoresis of the final product to confirm correct size and the absence of primer-dimer formation. A melting curve was performed with each qPCR run.

3.10.4 Relative quantification of gene expression

Two normalizer genes were used for the relative quantification of gene expression using the ΔΔ CT method (Livak and Schmittgen, 2001). According to this method,

$$\Delta\text{CT} = \text{CT(gene of interest)} - \text{CT(normalizer gene)} \tag{3.4}$$

$$\Delta\Delta\text{CT} = \Delta\text{CT(treated sample)} - \Delta\text{CT(reference control sample)} \tag{3.5}$$

$$\text{Relative gene expression} = 2^{-\Delta\Delta\text{CT}} \tag{3.6}$$

3.11 Analysis of molecular alterations in BLCA

Data from the Cancer Genome Atlas (TCGA) was analyzed by using cBioPortal (www.cbioportal.org) for the presence of mutations or copy number alterations in genes in defined signaling networks (Network, 2014, Gao et al., 2013, Cerami et al., 2012). Molecular alterations in cell lines were analyzed using the Cancer Cell Line Encyclopedia (CCLE) (www.broadinstitute.org/ccle) (Barretina et al., 2012) and the Catalogue of somatic mutations in cancer (COSMIC) (cancer.sanger.ac.uk/cosmic) (Forbes et al., 2015) public databases.

3.12 Chicken chorioallantoic membrane (CAM) assay

The CAM assay represents an *in vivo* model where tumors form three-dimensional structures on top of the CAM of fertilized embryos. Additionally, these tumors acquire blood supply from the CAM vasculature. The CAM model also has the advantage of being naturally immunodeficient (Ribatti, 2014). Fertilized white Leghorn chicken eggs were placed at 37 °C with the convexity at the bottom. This was considered to be embryonic day (ED) 1. On ED 4, eggs were turned by 180° and a small hole was made at the apex using a drill. This was enlarged to around 1.5 cm diameter using a pair of curved scissors and sealed with a piece of surgical tape. Either ED 8 or 9 was selected for seeding cell line xenografts, ensuring that the CAM was well developed. An area of the CAM was irritated using sterile lens paper until spots of bleeding were observed and was marked by placing a sterile silicone ring on top. 2×10^6 cells resuspended in 10 µl medium without additives were mixed homogenously with 10 µl of Matrigel and incubated in a heating block for 2- 5 min until adequate viscosity was reached. The entire mixture was then pipetted onto the CAM within the silicone ring, avoiding bubbles. Formation of visible tumor xenografts was confirmed on ED 11 before treatment with inhibitors. Concentration of inhibitors was calculated with respect to the circulating blood volume of the embryo (Kind, 1975) and solutions were prepared in 10 µl sterile 0.9% NaCl, which was pipetted on top of the tumor. MK-2206 was used at a final concentration of 500 nM on ED 11 and 14, while 1000 nM of PD-0332991 was used daily from ED 11 to ED 14. On ED 15, xenografts were carefully dissected from the CAM surface and transferred into a plate containing cold PBS. These tumors were then

finely dissected under a stereomicroscope to remove any residual CAM, dried on a tissue, transferred into pre-weighed PBS containing microcentrifuge tubes and weighed again. Tumor weight was obtained by calculating the difference between the two values. During the course of the assay, movement of eggs was kept to a minimum. Eggs were kept at room temperature for a minimal amount of time.

3.13 Tissue processing and immunohistochemistry (IHC)

Tissue was fixed in formaldehyde for 16-24 hours at 4 °C, followed by dehydration in the tissue processor and embedding in paraffin. 3 µm thick sections were cut using a microtome and placed sequentially onto slides that were used for subsequent IHC. Deparaffinization was carried out by incubating sections for 10 min in xylol followed by sequential rehydration with 5 min washes in isopropanol, 96% ethanol and 70% ethanol. For heat induced epitope retrieval, citrate buffer was prewarmed in a pressure cooker and sections were incubated for 7 min at 116 °C, followed by cooling in the same buffer for 10-15 min, and a TBS wash. Next, the endogenous peroxidase activity was blocked by incubating sections for 5 min in 6% H_2O_2, followed by a TBS wash. In order to block non-specific binding, sections were incubated in 5% human serum-TBS for 2 hours at room temperature, followed by three washes in TBS. Primary antibody diluted in the DAKO real antibody dilution buffer was added onto the sections for 2 hours at room temperature in a moist chamber. IgG of the same species and concentration as the primary antibody was used as a negative control. Following a TBS wash, sections were incubated for 15 min each with biotinylated secondary antibody and streptavidin peroxidase (DAKO Real detection system) with TBS washes in between. Detection was performed by incubating with the DAB peroxidase substrate and buffer (DAKO Real detection system). Counterstaining was performed with haematoxylin for 60 s. Stain was washed away in running lukewarm water, and sections were transferred to H_20. Dehydration was performed by sequential washes in an ascending alcohol series of 70% ethanol, 95% ethanol and isopropanol for 5 min each, followed by xylol for 10 min. Slides were mounted using mounting medium. For the quantification of staining, cells that were positively stained were manually counted from at least three different areas from 4 to 5 different tumors of each treatment condition.

3.14 Graphical depiction and statistical comparison

Unless stated otherwise, all data were obtained from at least three independent experiments. Graphs were plotted using Microsoft Excel depicting the arithmetic mean ± standard deviation (S.D.) or standard error of the mean (S.E.). A two-tailed Student's t test was used for comparison between data sets and $p < 0.05$ was considered to be significant. Mutual exclusivity in TCGA data was assessed by a Log Odds Ratio. A $p < 0.001$ using a Fisher Exact test was considered significant.

4 Results

We aimed to characterize the effects of AKT and CDK 4/6 inhibition in BLCA. An important readout for determining the response to these treatment strategies is their effect on cell viability. Hence, we began by defining the assay conditions to determine cell viability.

4.1 Establishment of cell viability measurement

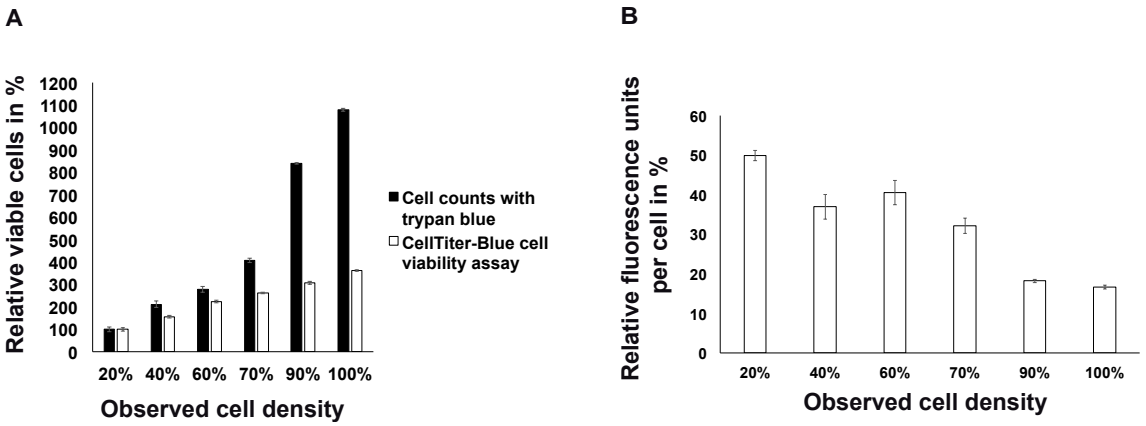

Figure 4.1: **Cell viability estimation requires sub-confluent cell culture conditions.** (A) Cell counting using trypan blue was compared with the Celltiter-blue assay at varying cell densities and (B) RFU value per cell was determined.

The ideal measure of cell viability is the determination of the number of living cells from a cell population. However, compared to cell counting, cell viability assays can enable this quantification in a high throughput manner. We directly compared the Celltiter-blue cell viability assay with manual cell counting using trypan blue, in order to establish if it is a true readout for viable cells. Cells seeded in varying densities, with an observed confluence between 20 to 100%, were compared in parallel using cell counts and the Celltiter-blue cell viability assay (Figure 4.1 A). The relative percentage of living cells as determined by cell counts correlated with the observed cell density. This relationship was also seen when using the CellTiter-blue assay for an observed cell density between 20-60%. However, in cells that were 70-100% confluent, the cell viability assay greatly underestimated the number of living cells. Normalizing the relative fluorescence units (RFU) to the number of living cells showed a relatively

constant value of RFU per cell until cells reached a 70% confluence (Figure 4.2 B). However, at 90-100% cell density the RFU per cell was 66-68% lower, which might explain the underestimation of viability at higher cell densities. Thus, the CellTiter-blue cell viability assay can substitute for cell counting only when cells are present at a sub confluent density less than 70%. This condition was maintained in all the assays which were performed.

4.2 Characterizing AKT as a therapeutic target

For characterizing the potential of AKT as a target in BLCA, we began by examining the expression and function of AKT isoforms in different BLCA cell lines. We then proceeded to analyze the effects of a suitable AKT inhibitor on cell signaling, viability, apoptosis and cell cycle proliferation and also investigated the molecular determinants of treatment response (Sathe et al., 2014).

4.2.1 Expression and function of AKT isoforms

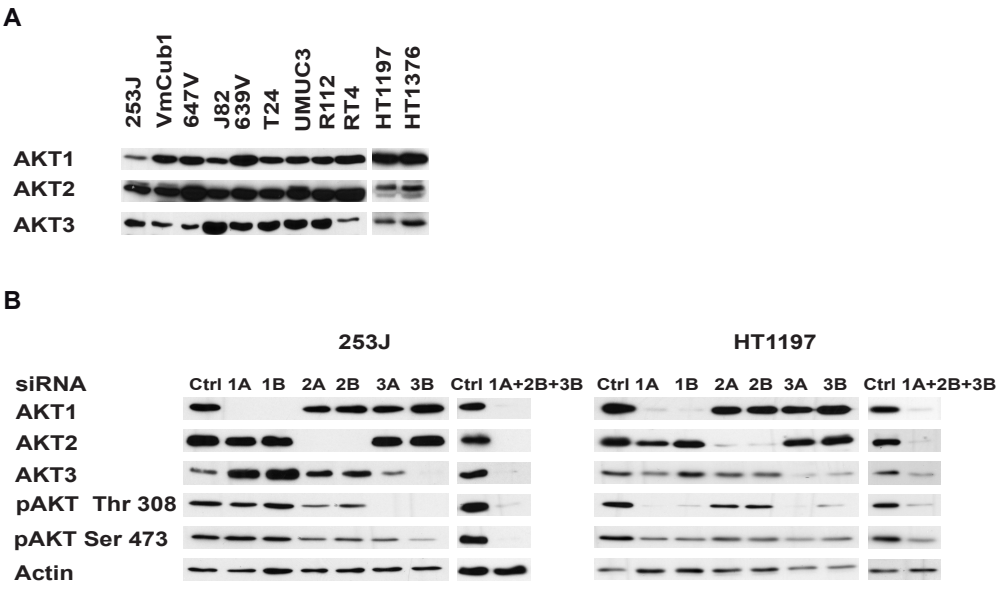

Figure 4.2: **AKT isoforms contribute heterogeneously to signaling in BLCA.** (A) Respective cell lines were analyzed for the expression of the AKT isoforms by immunoblotting. (B) Representative cell lines were transfected with two different siRNA oligonucleotides directed against each AKT isoform (A or B) or control (ctrl), and protein expression was analyzed by immunoblotting with the respective antibodies.

AKT inhibitors target the three AKT isoforms with different affinities. In order to use an appropriate inhibitor in future experiments, we analyzed the expression of the AKT

isoforms in BLCA and their contribution to signaling and maintenance of viability. All AKT isoforms were expressed in a panel of 11 BLCA cell lines (Figure 4.2 A).

In order to analyze their activation status, we silenced the expression of each isoform by using two independent siRNA oligonucleotides, as well as combined them to silence AKT expression completely. The two representative cell lines showed varying expression of phosphorylated AKT after silencing the isoforms (Figure 4.2 B). While only isoforms 2 and 3 contributed to phosphorylated AKT in the 253J cells, all three isoforms were phosphorylated in the HT1197 cells. In both the 253J and HT1197 cells, silencing each of the isoforms led to a decrease in cell viability (Figure 4.3). However, combined silencing of all three isoforms produced the greatest effect. Hence, the contribution of AKT isoforms in BLCA signaling and maintenance of viability is heterogeneous and all three isoforms should be inhibited for maximum treatment benefit.

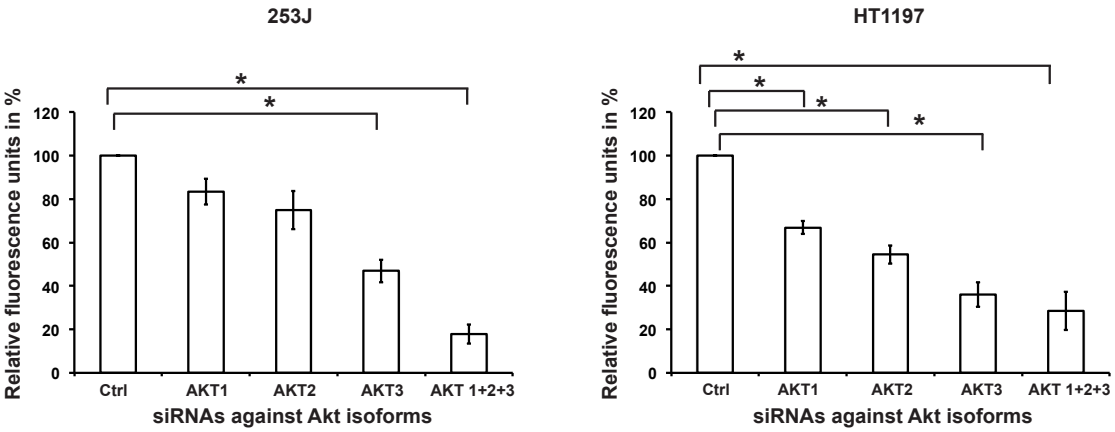

Figure 4.3: **Inhibition of all three AKT isoforms is most efficacious.** Representative cell lines were transfected with two different siRNA oligonucleotides against each AKT isoform (A or B) or control (ctrl). Cell viability of transfected cells was analyzed at 72 hours.* indicates $p < 0.05$.

We extended our data to the tumor specimens in the TCGA dataset by analyzing them for molecular alterations in the AKT isoforms (www.cbioportal.org) (Figure 4.4). Deletions in *AKT1* were noted in only 3% of tumors, suggesting that most tumors express the three isoforms. Moreover, *AKT 1*, *AKT2* and *AKT3* amplifications were observed in 3%, 6% and 3% of tumors respectively. Interestingly amplifications in *AKT1* were mutually exclusive to the occurrence of alterations in either *AKT2* or *AKT3*. Hence, the AKT isoforms show a heterogeneous distribution of molecular alterations in BLCA primary tumors.

Figure 4.4: **Genetic alterations in AKT isoforms are mutually exclusive in BLCA.** Data for 131 muscle invasive BLCA tumors from TCGA was analyzed using the cBioPortal and an Oncoprint was generated. Values denote percentage of tumors altered with mutations (green), homozygous deletion (blue) or amplification (red).

4.2.2 Biochemical effects of AKT inhibition

In order to inhibit all three AKT isoforms, we studied the biochemical effects of MK-2206, a pan-AKT allosteric inhibitor, by immunoblotting in various BLCA cells (Figure 4.5). No AKT phosphorylation was detectable in the RT4 cells. In all the other cell lines, MK-2206 treatment led to a dose dependent reduction in the serine and threonine phosphorylation of AKT. This was accompanied by a decrease in S6K1 phosphorylation, with no effect on total protein expression. However, no reduction was observed in the phosphorylation of 4E-BP1, another mTORC1 downstream target, in different amino acid residues.

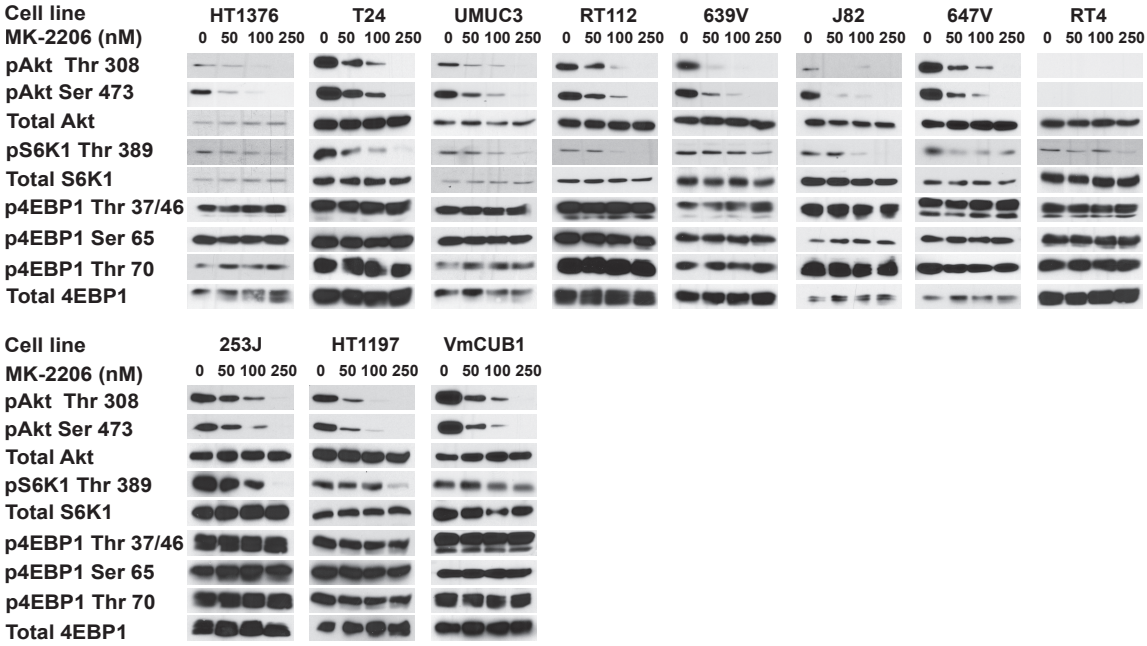

Figure 4.5: **AKT inhibition does not affect 4E-BP1 phosphorylation.** Respective cell lines were treated for 1 hour with indicated concentrations of MK-2206 and protein expression and phosphorylation was analyzed by immunoblotting.

4.2.3 Functional effects of AKT inhibition

Next, we assessed the effect of MK-2206 treatment on the viability of these cell lines. Despite a uniform biochemical response in mTORC1 downstream signaling, only three of the eleven cell lines showed a reduction in cell viability of 40-60% after treatment (Figure 4.6 A). The sensitive HT1197, 253J and VmCUB1 cells responded to MK-2206 with absolute IC50s ranging from 242, 674 and 1469 nM respectively. This response to MK-2206 was confirmed by directly determining the number of living cells in all three sensitive cell lines, which showed a 37-48% reduction (Figure 4.6 B). No such decrease was observed in the 647V, RT112 and T24 cells as representatives of the resistant cell lines.

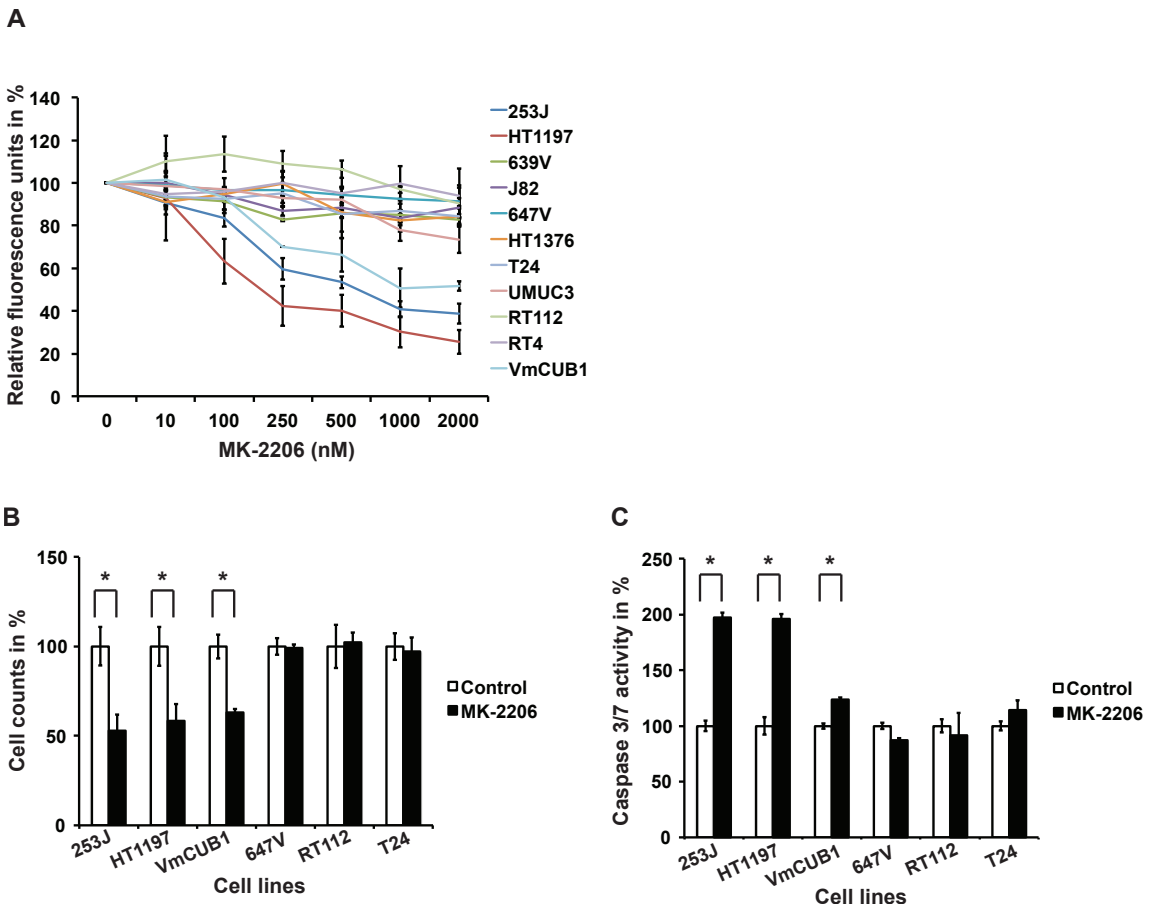

Figure 4.6: **MK-2206 increases apoptosis and reduces viability only in selected cell lines.** (A) Cell viability was assessed 72 hours after the addition of respective MK-2206 concentrations. (B) Cell counts and (C) caspase 3/7 activity were determined in the respective cell lines after 24 hours treatment with 1000 nM MK-2206.* indicates $p < 0.05$.

In order to determine the cellular mechanism that causes this decrease in cell number, we examined these representative cell lines for caspase 3/7 activity, as an indicator

of apoptosis (Figure 4.6 C). MK-2206 treatment led to a 97%, 95% and 23% increase in caspase 3/7 activity in the 253J, HT1197 and VmCUB1 cells respectively while no significant changes were seen the resistant cell lines. Additionally, we assessed the effect of MK-2206 on cell cycle progression in these cells by analyzing the EdU incorporation followed by flow cytometry (Figure 4.7). Modest but significant decreases in the S phase or increase in the G0/G1 phase were seen in not only the sensitive 253J, HT1197 and VmCUB1 cells but also the resistant 647V and T24 cells, indicating that the selective response to MK-2206 is mediated by an increase in apoptosis.

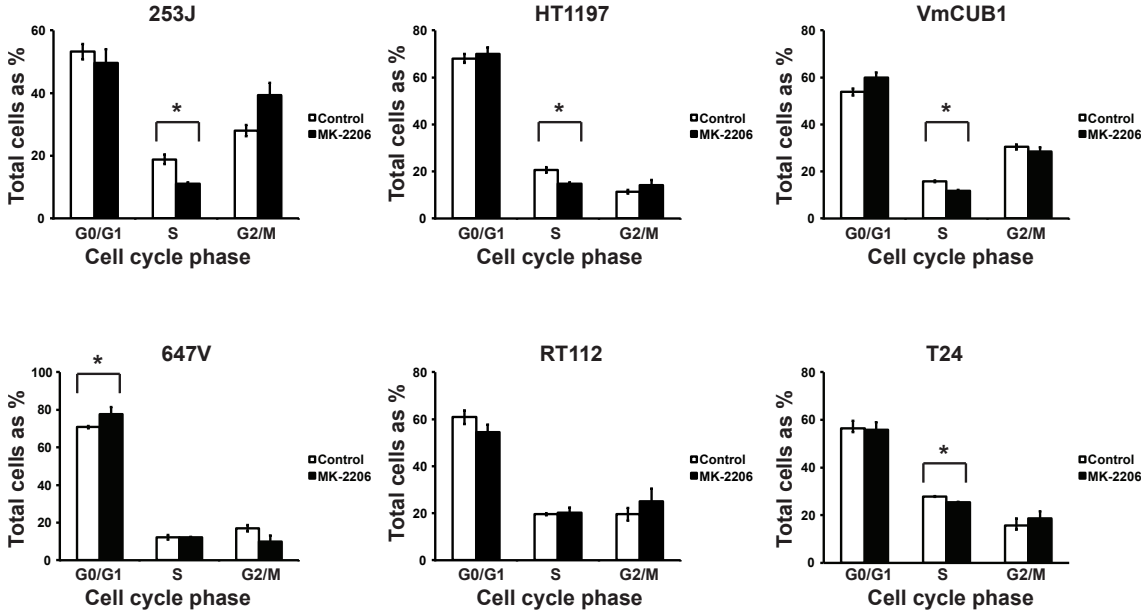

Figure 4.7: **MK-2206 has a modest effect on cell cycle progression.** Respective cell lines were treated with 1000 nM MK-2206 for 24 hours and analyzed for their cell cycle progression.* indicates $p < 0.05$.

4.2.4 Molecular correlates of response to MK-2206

Since only selected cell lines were sensitive to MK-2206, we analyzed if this response correlated with genomic alterations in relevant molecules. All the eleven cell lines in our panel were examined for alterations in *PIK3CA*, *PTEN*, *TSC1*, *RAS* and *FGFR3* using the COSMIC (cancer.sanger.ac.uk/cosmic) and CCLE (www.broadinstitute.org/ccle) public databases, as well as previously published data (Platt et al., 2009) (table 4.1). No correlations were present between the response to MK-2206 and alterations in *PTEN*, *TSC1*, *RAS* and *FGFR3*. However, all three sensitive cell lines possessed activating hotspot HD mutations in *PIK3CA*, which were not found in any of the resistant cell lines.

Cell line	*PIK3CA*	*PTEN*	*TSC1*	*RAS*	*FGFR3*	Response to MK2206
RT112	WT	WT	WT	WT	WT over expressed	Resistant
RT4	WT	WT, reduced copy number	Mutant	WT	WT over expressed	Resistant
647V	WT	WT, reduced copy number	WT	WT	WT	Resistant
HT1376	WT	WT	WT	WT	WT	Resistant
T24	WT	Mutant	WT	HRAS Mutant, KRAS WT, NRAS WT	WT	Resistant
UMUC3	WT	Homozygous deletion	WT	KRAS Mutant, NRAS WT, HRAS WT	WT	Resistant
J82	P124L rare mutant	Homozygous deletion	WT	WT	Mutant	Resistant
639V	A1066V rare mutant	Mutant	Mutant	KRAS Mutant, NRAS Mutant, HRAS WT	WT	Resistant
253J	E545G hotspot helical domain mutant	WT	WT	WT	WT	Sensitive
HT1197	E545K hotspot helical domain mutant	WT, reduced copy number	WT	NRAS Mutant, HRAS WT, KRAS WT	WT	Sensitive
VmCUB1	E542K hotspot helical domain and E674Q helical domain mutant	WT	WT	WT	WT	Sensitive

Table 4.1: **Genetic background of BLCA cell lines and their response to MK-2206.** Hotspot HD *PIK3CA* mutations correlate with sensitivity to MK-2206. WT indicates wild type.

4.2.5 Biochemical signature of MK-2206 response

Both resistant and sensitive cell lines had shown a similar biochemical response in downstream mTOR substrates after MK-2206 treatment, which cannot explain their differential sensitivity. Hence,we examined these cell lines for additional signaling events (Figure 4.8). GSK3β is a major regulator of cell proliferation and survival and a direct AKT downstream target (Rayasam et al., 2009). However, both sensitive and resistant cell lines showed a dose dependent reduction in GSK3β phosphorylation that correlated with a decrease in AKT phosphorylation. Previous data has shown that the Ras/Raf/Mek/Erk branch of the MAPK signaling pathway influences the proliferation of BLCA cells and can influence PI3K signaling at multiple levels (Nawroth et al., 2011). MK-2206 treatment in all the six cell lines resulted in an increase in RAF-1 phosphorylation at serine 338, which indicates activated MAPK signaling. No decrease in phospohrylation was observed at the serine 259 site of RAF-1, which is regarded as a direct downstream substrate of AKT. However, the sensitive and resistant cells showed opposite effects on the phosphorylation of ERK 1/2. While the sensitive 253J, HT1197 and VmCUB1 cells showed a dose dependent reduction in phosphorylated ERK 1/2, an increase was observed in the resistant 647V, RT112 and T24 cells. The uniform increase in RAF-1 phosphorylation at serine 338 indicated that this effect was independent of upstream RAF signaling.

A possible mediator could be DUSP1 (MKP-1), a phosphatase that is responsible for the dephosphorylation of ERK 1/2. In the sensitive cell lines, MK-2206 treatment led to an increase in DUSP1 expression that correlated with the observed ERK 1/2 dephosphorylation. An opposite response was seen in the resistant cells with a reduction in DUSP1 expression.

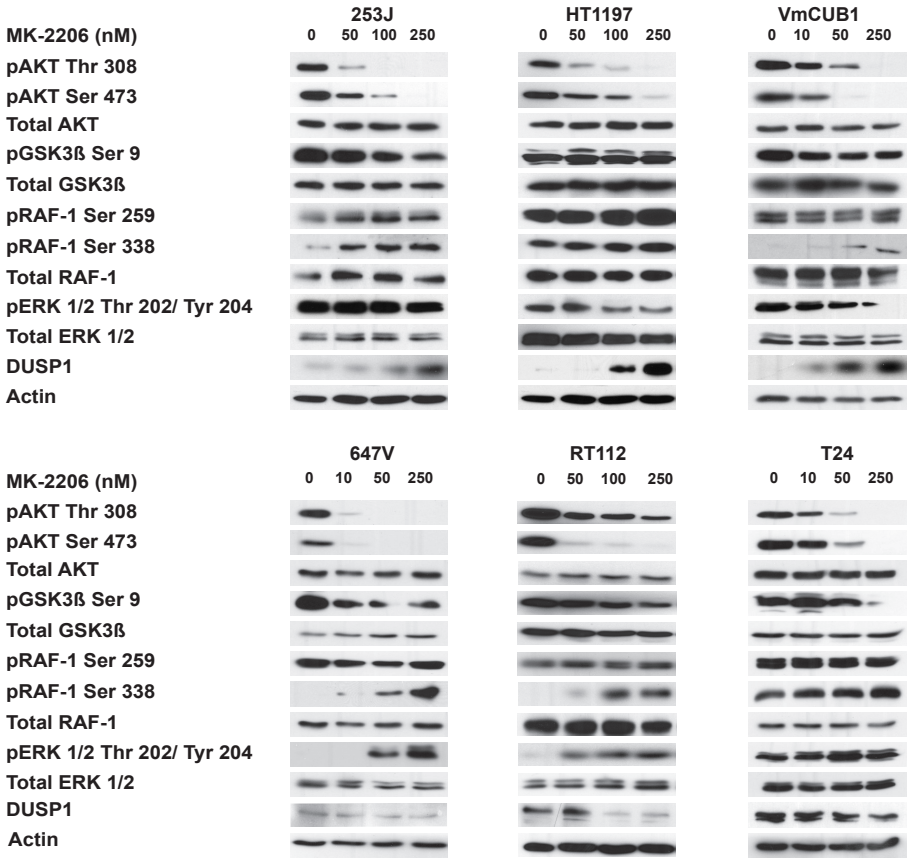

Figure 4.8: **MK-2206 sensitive cells show a reduction in ERK 1/2 phosphorylation and an increase in DUSP1 expression.** Cell lines were incubated with indicated MK-2206 concentrations for 1 hour and protein expression and phosphorylation was analyzed by immunoblotting.

To establish whether the DUSP1 mediated effect on ERK 1/2 phosphorylation is responsible for conferring sensitivity to MK-2206, we silenced its expression by using an siRNA in all the three sensitive cell lines (Figure 4.9 A). In the absence of DUSP1 expression, MK-2206 treatment in all the three cell lines led to an increase in ERK 1/2 phosphorylation. Moreover, these cells became resistant to MK-2206 (Figure 4.9 B). These results demonstrate that the increase in expression of DUSP1 that negatively regulates ERK 1/2 phosphorylation, is involved in conferring sensitivity to MK-2206.

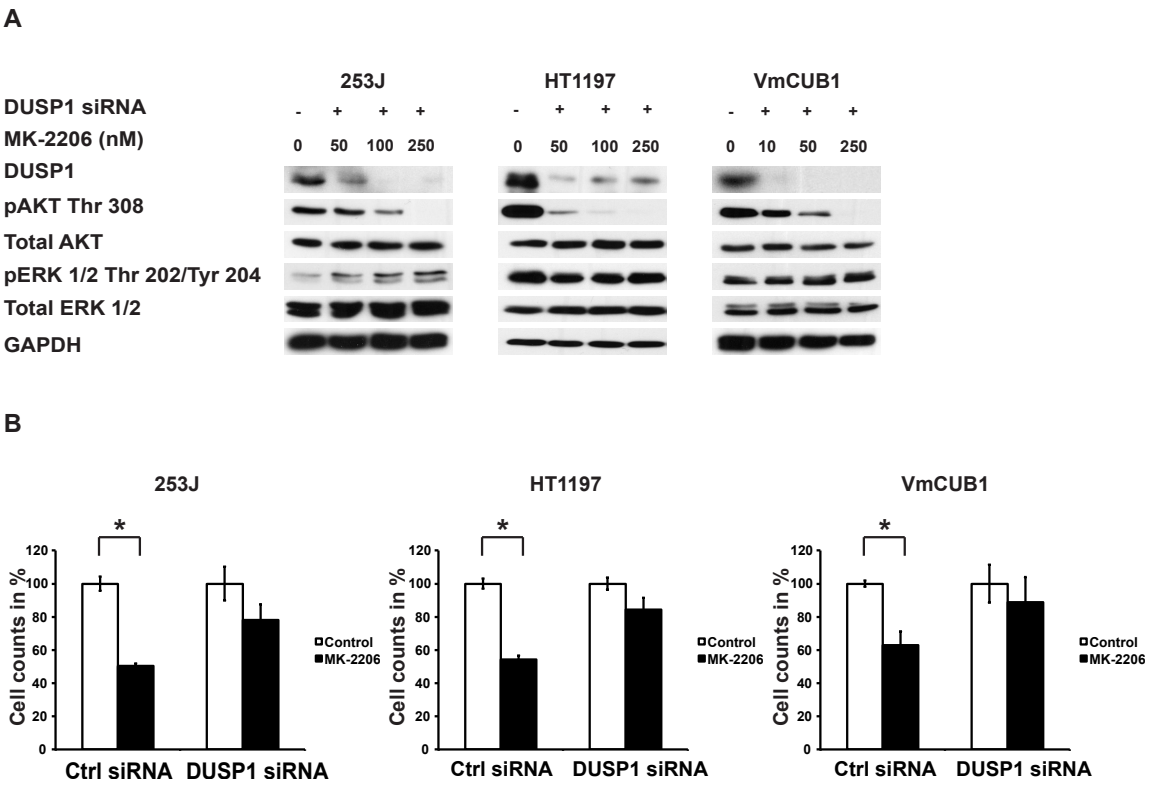

Figure 4.9: **DUSP1 mediated regulation of ERK 1/2 phosphorylation regulates sensitivity to MK-2206.** Cell lines were transfected with control (ctrl) or siRNAs directed against DUSP1. Transfected cells were treated with (A) indicated MK-2206 concentrations for 1 hour and analyzed by immunoblotting or (B) 1000 nM MK-2206 and cell viability was assessed at 72 hours. '+' indicates present and '-' indicates absent.

A possible regulator of this effect on DUSP1 expression can be CREB, which is a downstream AKT target and can control the transcription of DUSP1 (Du and Montminy, 1998, Xu et al., 2007). We silenced the expression of CREB in HT1197 cells (Figure 4.10). Despite the decrease in CREB levels, MK-2206 treatment of these cells continued to produce an increase in DUSP1 expression. The regulation of DUSP1 after AKT inhibition is thus independent of CREB.

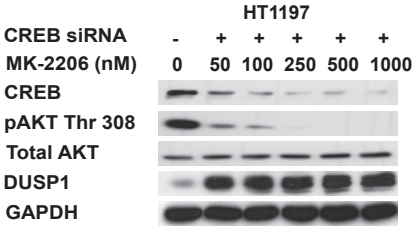

Figure 4.10: **MK-2206 induced DUSP1 expression is independent of CREB.** Cells transfected with control or CREB directed siRNA oligonucleotides were treated with indicated concentrations of MK-2206 for 1 hour and protein expression was analysed by immunoblotting. '+' indicates present and '-' indicates absent.

4.2.6 Molecular determinants of sensitivity to MK-2206

MK-2206 sensitive cells all possessed mutations in *PIK3CA*. The response of these cells was dependent on the reduction in ERK 1/2 phosphorylation after treatment. We wanted to examine if *PIK3CA* mutations were associated with this biochemical signature of response. In order to investigate this, we used two different strategies.

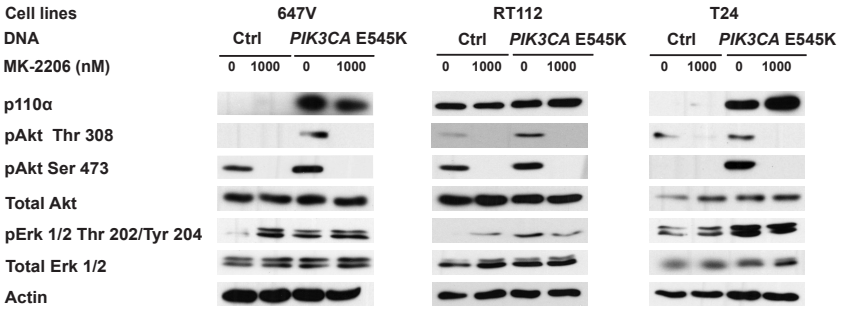

Figure 4.11: **Mutant *PIK3CA* controls the decrease in ERK 1/2 phosphorylation after AKT inhbition.** Cells were transfected with either control vector (ctrl) or mutant *PIK3CA* E545K for 72 hours and treated for 1 hour with 1000 nM MK-2206 and analyzed by immunoblotting.

First, we expressed recombinant mutant *PIK3CA* E545K in the 647V, RT112 and T24 cells that possess WT *PIK3CA* and compared the biochemical responses after MK-2206 treatment (Figure 4.11). The presence of the mutant *PIK3CA* led to an increase in both phosphorylated AKT and ERK 1/2 (comparing lanes 1 and 3). As demonstrated before (Figure 4.8), cells with a WT *PIK3CA* responded to treatment with an increase in ERK 1/2 phosphorylation. However, with expression of the *PIK3CA* mutation, MK-2206

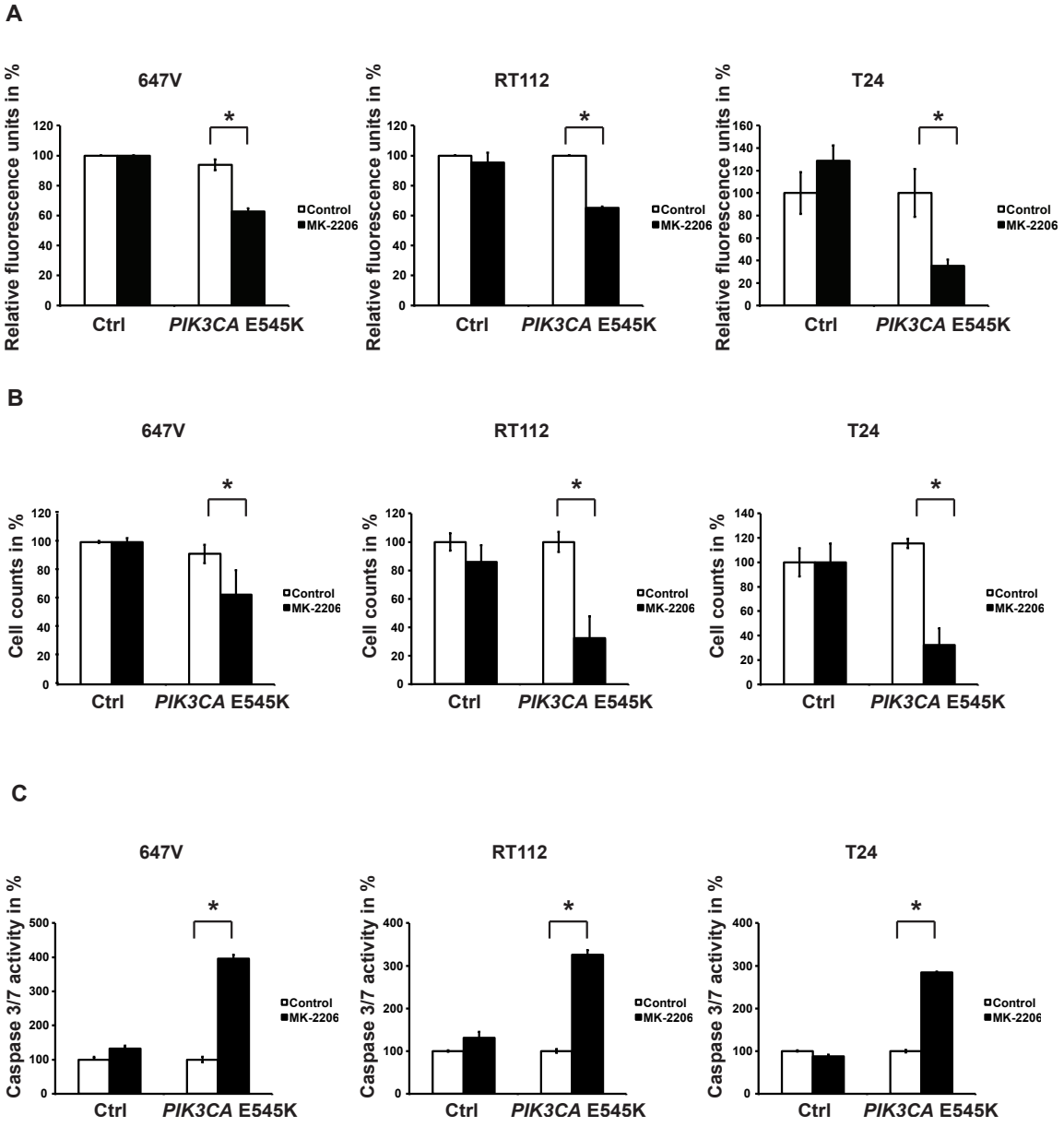

Figure 4.12: **Mutant *PIK3CA* sensitizes cells to MK-2206 by increasing apoptosis.** Cells were transfected with either control vector (ctrl) or mutant *PIK3CA* E545K for 72 hours and treated for (A) a further 72 hours to assess cell viability or for 24 hours to assess (B) cell counts and (C) caspase 3/7 activity.

treatment prevented this increase in phosphorylated ERK 1/2 in the 647V cells and led to a reduction in the RT112 and T24 cells. This resembles the response in the sensitive cells that we observed previously (Figure 4.8). Additionally, expression of the *PIK3CA* mutation conferred sensitivity to MK-2206 treatment in all three cell lines, as evidenced

by a 37-68% reduction in cell viability (Figure 4.12 A). This was confirmed by a 30-70% decrease in the number of living cells (Figure 4.12 B). A 200-300% increase in caspase 3/7 activity was also observed in these cells after MK-2206 treatment (Figure 4.12 C), confirming that sensitivity is mediated via an increase in apoptosis.

As a second strategy, we wanted to silence the expression of the *PIK3CA* mutation and determine its effect on sensitivity to MK-2206. The HT1197 cells are heterozygous for the *PIK3CA* E545K mutation (cancer.sanger.ac.uk/cosmic). One way to selectively silence the expression of this mutant without affecting the WT copy is the use of allele specific (ASP) siRNAs that can selectively target the mutant gene sequence but not the WT sequence . We designed four different ASP siRNAs on the basis of recommendations from literature (Ohnishi et al., 2008, Schwarz et al., 2006)(section 3.7). We transfected the HT1197 cells, that have the *PIK3CA* E545K mutation, and RT112 cells, that are *PIK3CA* WT, with these siRNAs and analyzed the expression of p110α by immunoblotting (Figure 4.13) . P9 C13 failed to induce a significant reduction in the expression of p110α in either cell line. P9, P10 and P16 all led to a reduction in p110α expression of the RT112 cells that are WT for *PIK3CA*. Hence, none of the four sequences were allele specific. We speculate that this is due to the prymidine:purine mismatch between the ASP siRNA and its target that has been previously described as being less efficient in allelic discrimination (Schwarz et al, 2006).

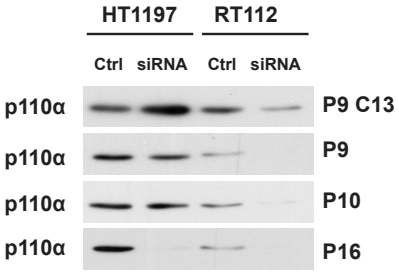

Figure 4.13: **Allele specific siRNAs.** Different siRNA sequences do not distinguish between mutant and WT *PIK3CA*.

Since we were unable to selectively silence the mutant *PIK3CA* allele, we used an siRNA directed against the 5'UTR of the gene in the 253J and HT1197 cells that possess mutant *PIK3CA* (Figure 4.14 A). We further reconstituted these cells with a recombinant WT *PIK3CA*. Hence, the mutant *PIK3CA* was effectively substituted to a WT (Figure 4.14 B). This substitution led to a reduction in both AKT and ERK 1/2 phosphorylation (comparing lanes 1 and 3). After treatment with MK-2206, cells containing the mutant *PIK3CA* responded with a reduction in ERK 1/2 phosphorylation as demonstrated previously (Figure 4.8). However, cells containing the WT *PIK3CA* showed an increase in phosphorylated ERK after treatment, resembling the response of the resistant cells that we observed previously (Figure 4.8). These cells also became resistant to MK-2206 as indicated by no significant changes in cell counts after treatment (Figure 4.14 C).

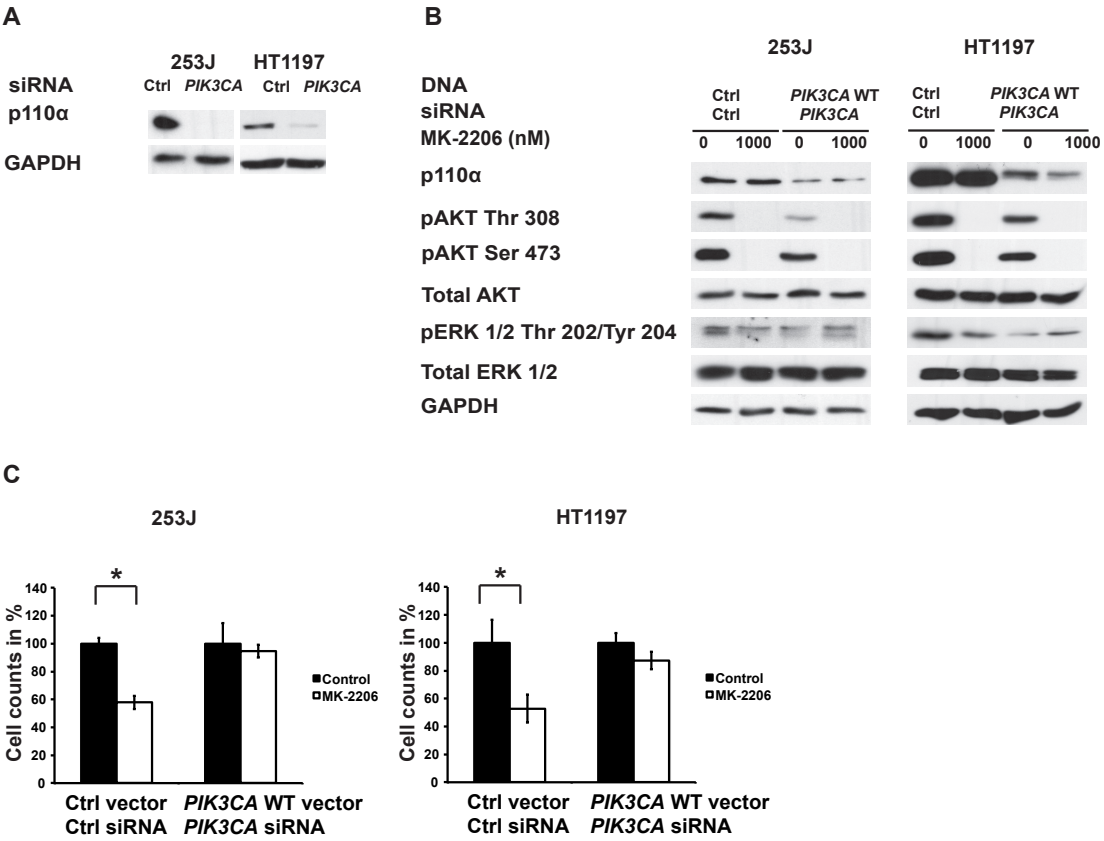

Figure 4.14: **WT *PIK3CA* leads to resistance to MK-2206.** (A) Cells were transfected with control (ctrl) or siRNA oligonucleotides against *PIK3CA* for 24 hours. (B) siRNA transfected cells were then transfected with control (ctrl) or WT *PIK3CA* containing vector for 48 hours and treated with 1000 nM MK-2206 for 1 hour for immunoblotting or (C) incubated for another 72 hours to assess cell viability. * indicates $p < 0.05$.

Taken together, both these strategies confirm that the presence of a mutant *PIK3CA* confers a response to AKT inhibition by leading to a decrease in ERK 1/2 phosphorylation after treatment. This response is mediated by an increase in apoptosis.

4.2.7 AKT inhibition in a three-dimensional xenograft model

In order to extend our *in vitro* data, we used the CAM model to grow three-dimensional *in vivo* xenografts of selected cell lines and treated them with MK-2206 (Figure 4.15 A). *PIK3CA* WT RT112 cells showed no decrease in tumor weight after MK-2206 treatment while the *PIK3CA* mutant HT1197 cells showed a 50% reduction (Figure 4.15 B). Both

cell lines showed a 50-70% decrease in AKT phosphorylation after MK-2206 treatment (Figure 4.16 A, B). However, only the HT1197 cells showed a reduction of 54% in Ki-67 expression after treatment, indicating a reduction in proliferation.

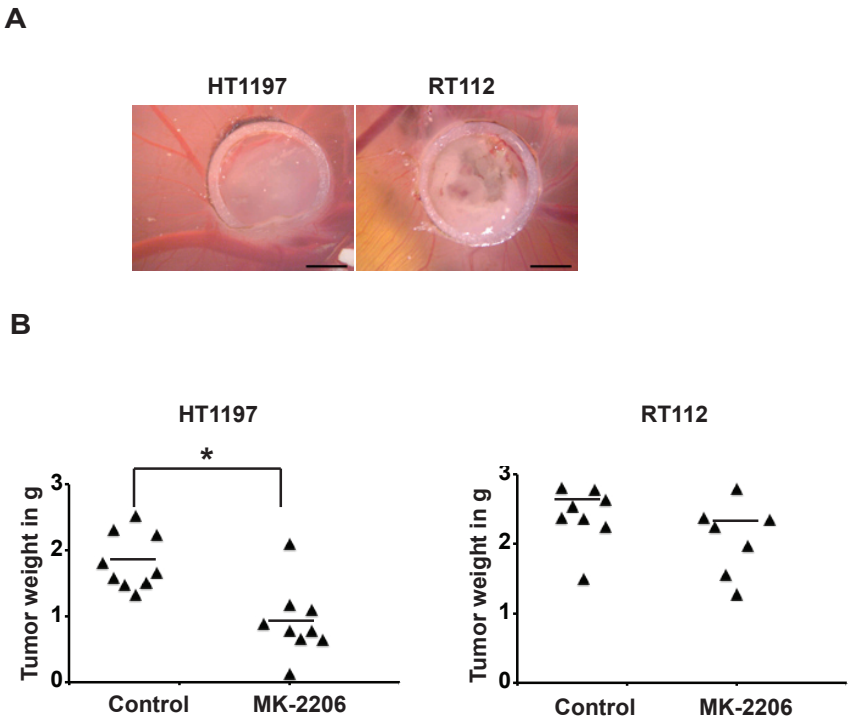

Figure 4.15: ***PIK3CA* mutant cells are sensitive to MK-2206 *in vivo*.** (A) Representative images of HT1197 and RT112 cells show tumour formation on the CAM inside a silicone ring, 6 days after seeding of cells. Scale bar equals 2 mm. (B) Tumours from indicated cell lines were harvested and weighed after MK-2206 or control treatment. * indicates $p < 0.05$. Results are representative of at least two independent experiments.

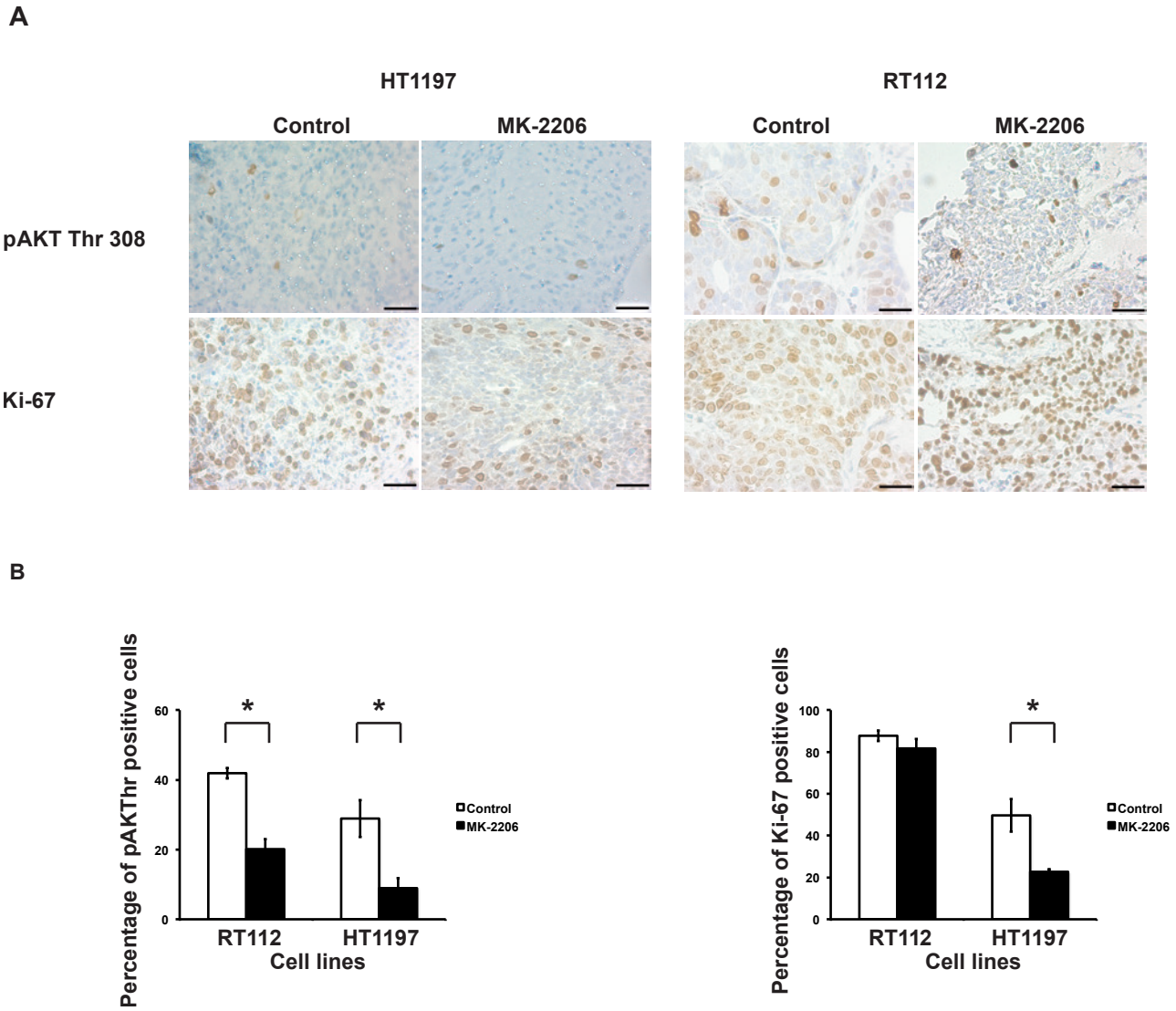

Figure 4.16: **MK-2206 reduces the proliferation of *PIK3CA* mutant cells *in vivo*** (A) Representative images and (B) staining quantification from tumors, which were analyzed with IHC using the indicated antibodies. Scale bar equals 20 µm. * indicates $p < 0.05$. All results are representative of at least two independent experiments.

Similar to the *in vitro* experiment (Figure 4.11), we compared RT112 WT *PIK3CA* cells to those that express the recombinant *PIK3CA* E545K mutation in the CAM model (Figure 4.17 A). A 56% reduction in tumor weight was seen only in the cells containing the mutation. Although an 80% reduction in AKT phosphorylation was seen in both situations, only the *PIK3CA* mutant cells showed a 55% reduced Ki-67 expression (Figure 4.17 B).

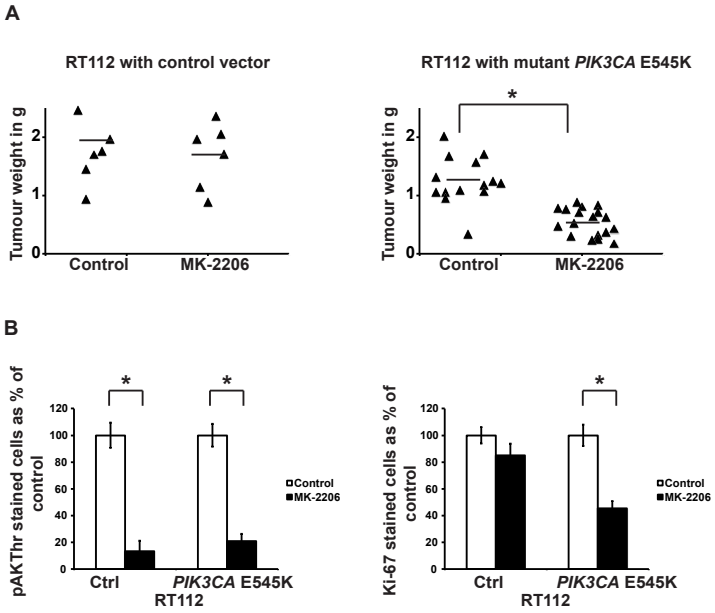

Figure 4.17: **HD mutant *PIK3CA* confers sensitivity to MK-2206 *in vivo*.** (A) RT112 tumours transfected with either control vector or mutant PIK3CA E545K were harvested after control or MK-2206 treatment and weighed. (B) Tumors were analyzed with IHC using the indicated antibodies and staining was quantified.* indicates $p < 0.05$.

4.3 Characterizing CDK 4/6 as a therapeutic target

For characterizing the potential of CDK 4/6 as a target in BLCA, we examined the alterations in the CDK 4/6-RB network in BLCA. We next analyzed the effects of a selective CDK 4/6 inhibitor on cell signaling, viability, apoptosis and cell cycle proliferation and also determined the molecular alterations conferring response to treatment.

4.3.1 Molecular alterations in the CDK 4/6-RB pathway

We analyzed data from the TCGA cohort for genomic alterations in the CDK 4/6-RB signaling pathway (The Cancer Genome Atlas Research, 2014, Gao et al., 2013) (www.cbioportal.org) (Figure 4.18). Loss of function mutations in *RB1* (encoding RB) were present in 21%. *CDKN2A* and *CDKN2B* were deleted or mutated in 40% and 37% tumors respectively. 2-12% tumors had alterations in *CDK 4*, *CDK 6* or *CCND1* (encoding cyclin D1). Overall, the CDK 4/6-RB pathway was deregulated in 64.9% of the tumors. Moreover, the molecular alterations in *CDKN2A* and *CDKN2B* had a significant tendency towards co-occurrence. Conversely, molecular alterations in *RB1* occurred

exclusively as compared to those in either *CDKN2A* or *CDKN2B*. Presence of alterations in CDK 4/6-RB signaling was not associated with any significant changes in either OS or disease free survival (DFS). The presence of molecular alterations in *RB1* and *CDKN2A* have previously been linked to the response to CDK 4/6 inhibition in several cancers (Asghar et al., 2015). The results of our TCGA analysis demonstrated a high frequency of *RB1* and *CDKN2A* alterations in BLCA. Hence, we characterized their influence on the response to CDK 4/6 inhibition in greater detail.

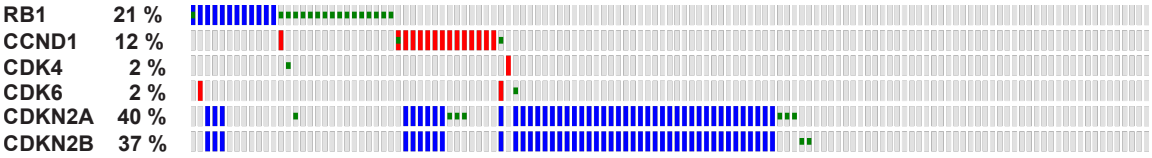

Figure 4.18: **The RB network is altered in 64.9% of BLCA.** Data from 131 muscle invasive BLCA tumors from the Cancer Genome Atlas was analyzed using the cBioPortal and an Oncoprint was generated. Values denote percentage of tumors altered with mutations (green), homozygous deletion (blue) or amplification (red).

4.3.2 Molecular correlates of sensitivity to PD-0332991

For further experiments, we selected a panel of cell lines that are similar to the TCGA cohort for alterations in *CDKN2A* and *RB1* using the CCLE (www.broadinstitute.org/ccle) and COSMIC (cancer.sanger.ac.uk/cosmic) databases. UMUC3, RT112 and VmCUB1 cells have loss of expression of CDKN2A, while 5637, 647V and 639V cells have loss of function mutations in *RB1*. No alterations of functional significance are present in the HT1197, T24, 253J and J82 cells. The pattern of RB expression and phosphorylation was analyzed in these cell lines (Figure 4.19), confirming previously published data (Rieger et al., 1995).

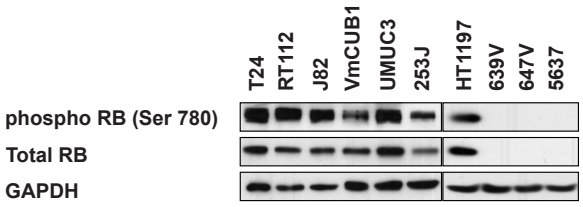

Figure 4.19: **Expression and phosphorylation of RB.** Respective cell lines were analyzed for their RB expression and phosphorylation by immunoblotting.

We tested the dose-response effect of PD-0332991, a selective CDK 4/6 inhibitor, on the viability of this panel of BLCA cell lines (Figure 4.20). While seven cell lines

(HT1197, 253J, T24, J82, UMUC3, RT112 and VmCUB1) responded to treatment, three cell lines (5637, 647V, 639V) remained resistant. The absolute IC50 concentrations of PD-0332991 required to inhibit cell viability clustered these cell lines into three distinct groups. The first group of cell lines were the most sensitive with IC50s in a range of 401 to 523 nM. The second group consisted of intermediate responders with IC50s from 1059 to 1390 nM, while no IC50 was reached in the third group consisting of resistant cell lines. Correlating this response to the presence of alterations in *CDKN2A* and *RB* showed that the sensitive cells had no alterations in either *CDKN2A* or *RB1* (table 4.2). The intermediate responders expressed RB but possessed loss of function mutations or deletions in *CDKN2A*. All the resistant cell lines had loss of function mutations in *RB1*. PD-0332991 treatment is thus effective in reducing the viability of only RB expressing cells.

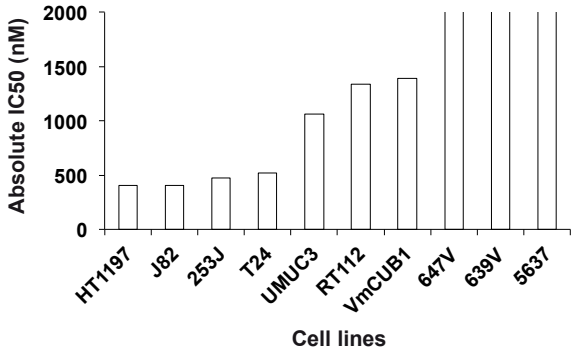

Figure 4.20: **PD-0332991 reduces the viability of selected BLCA cell lines.** Respective cell lines were treated with PD-0332991 for 72 hours and the effect on cell viability was determined. Absolute IC50 (nM) was then calculated from an average of three such experiments.

Cell line	*RB1*	*CDKN2A*	Sensitivity to PD-0332991
HT1197	WT	WT	High
J82	Mutant, amino acid position and functional impact not assessed	WT	High
253J	WT	WT	High
T24	WT	WT	High
UMUC3	WT	WT, copy number loss	Intermediate
RT112	WT	WT, copy number loss	Intermediate
VmCUB1	WT	Mutant, nonsense substitution	Intermediate
647V	Mutant, nonsense substitution	WT	Resistant
639V	Mutant, nonsense substitution	WT	Resistant
5637	Mutant, nonsense substitution	WT	Resistant

Table 4.2: **Genetic background of BLCA cell lines and their response to PD-0332991.** WT *RB1* cells are sensitive to PD-0332991. Loss of *CDKN2A* expression correlates with an intermediate response.

4.3.3 Combination of PD-0332991 and chemotherapy

The clinical application of PD-0332991 is likely to be in combination with conventional chemotherapy regimens. Hence, we assessed the combined effect of PD-0332991 and cisplatin on the viability of representative RT112 cells (Figure 4.21). Individual treatments with 500, 1200 and 2000 nM of PD-0332991 led to a 25%, 50% and 50% reduction in the number of viable cells. 1500 nM of cisplatin when used alone produced a 50% decrease in viability. However, a greater reduction in cell viability between 75-80% was observed after combining this concentration of cisplatin with the varying doses of PD-0332991. We then applied the Chou-Talalay CI theorem to analyze these data. According to this theorem, CI values less than 1 indicate a synergistic mechanism of action , while values equal to or greater than 1 indicate additive or antagonistic effects respectively (Chou, 2010). The combination of cisplatin and varying concentrations of PD-0332991 corresponded to CI values between 0.59 to 0.68 (table 4.3) indicating a synergistic effect. Additionally all the combinations had DRI values greater than 1. This signifies that a dose reduction of both drugs is possible when combined, while maintaining the therapeutic effect obtained from using higher concentrations of a single drug. Hence, using this combination also has the potential to lower concentration associated toxicities.

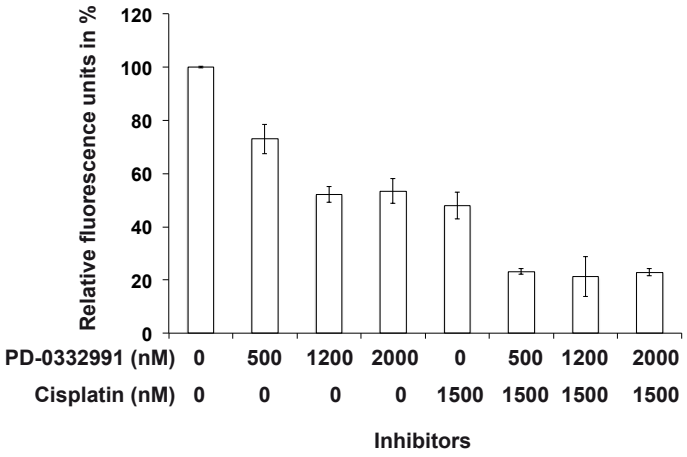

Figure 4.21: **PD-0332991 and cisplatin are an effective drug combination.** RT112 cells were treated with indicated concentrations of PD-0332991 and/or cisplatin for 72 hours and the effect on cell viability was determined.

4.3.4 Biochemical effects of PD-0332991

In order to understand the biochemical effects of PD-0332991 treatment, we examined different downstream substrates by immunoblotting (Figure 4.22)[1]. Increasing concentrations of PD-0332991 led to a dose dependent reduction in the phosphorylation of

[1]Figure 4.22 provided by Ms. Nicole Koshy, Experimental Urology, Klinikum rechts der Isar, TUM.

PD-0332991 (nM)	Cisplatin (nM)	CI	DRI (PD-0332991)	DRI (Cisplatin)
500	1500	0.59	24.55	1.81
1200	1500	0.59	12.18	1.93
2000	1500	0.68	6.69	1.87

Table 4.3: **PD-0332991 and cisplatin are synergistic.** CI and DRI values were calculated using the Chou-Talalay CI theorem.

RB at serine 780 in all the RB expressing cell lines. However, this was accompanied by a parallel reduction in total RB. The reduction in RB expression and phosphorylation correlated with the concentrations of PD-0332991 that impacted cell viability (figure 4.20). Additionally, all cell lines showed an increase in the expression of cyclin D1 after PD-0332991 treatment. These results demonstrate that CDK 4/6 inhibition in RB expressing cells leads to a reduction of both phosphorylated and total RB.

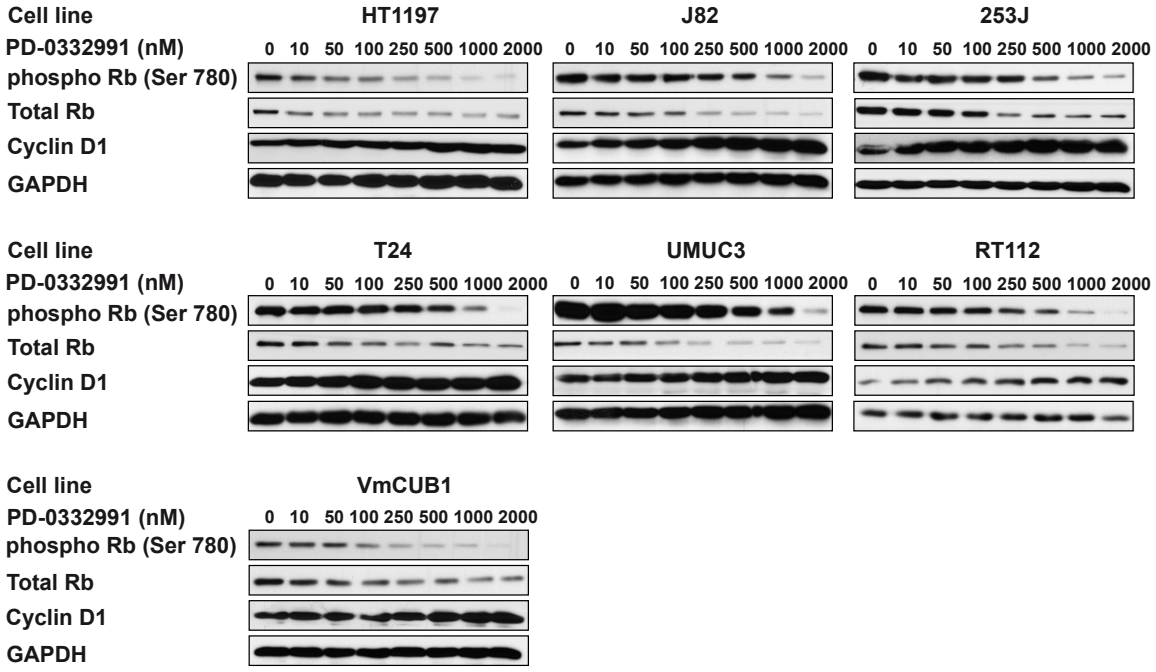

Figure 4.22: **PD-0332991 reduces RB expression.** Respective cell lines were treated for 24 hours with indicated concentrations of PD-0332991 and protein expression was analyzed by immunoblotting.

4.3.5 Effects of CDK 4/6 inhibition on cell cycle progression

E2F target genes such as *CCNA2* and *CCNE2* are major downstream effectors of RB function (Giacinti and Giordano, 2006). RB expressing HT1197 and RT112 cells showed

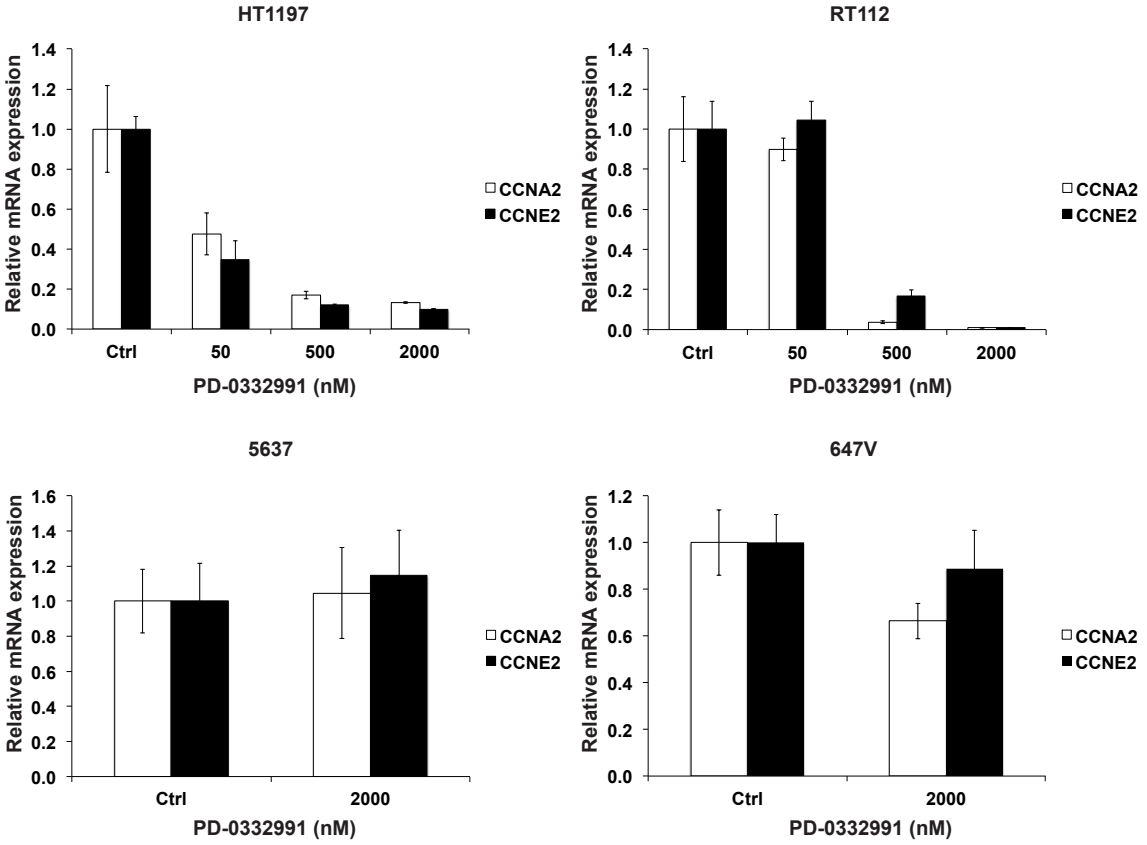

Figure 4.23: **PD-0332991 reduces the expression of E2F target genes in RB expressing cells.** Respective cell lines were treated with the indicated concentrations of PD-0332991 for 24 hours. Graphs indicate the mean relative mRNA expression of *CCNA2* or *CCNE2* in arbitrary units ± S.D normalized to Actin or GAPDH expression using the comparative CT method.

a down regulation of expression of both *CNNA2* and *CCNE2* mRNA transcripts to 90-99% with increasing concentrations of PD-0332991 (Figure 4.23). In the resistant 5637 cells, no such decrease was observed. In 647V cells, no change was observed in *CCNE2* expression and a 34% decrease was observed in *CCNA2* expression.

This pattern of *CCNA2* and *CCNE2* expression after PD-0332991 treatment also correlated with the cell cycle progression in these cell lines, which was analyzed by monitoring the incorporation of EdU by flow cytometry (Figure 4.24). In the HT1197 cells 50, 500 and 2000 nM of PD-0332991 treatment led to a 27%, 37% and 51% increase in the G0/G1 phase of the cell cycle respectively accompanied by a 22%, 27% and 50% decrease in cells in the S phase. RT112 cells showed a 19%, 127% and 127% increase in the G0/G1 resting phase and a 25%, 98.5% and 99.8% reduction in the S phase respectively. Cell cycle progression in the RB negative 5637 and 647V cells remained unaltered after PD-0332991 treatment. No increase in caspase 3/7 activity, indicative of apoptosis, was observed in either the RB positive or negative cells (Figure 4.25).

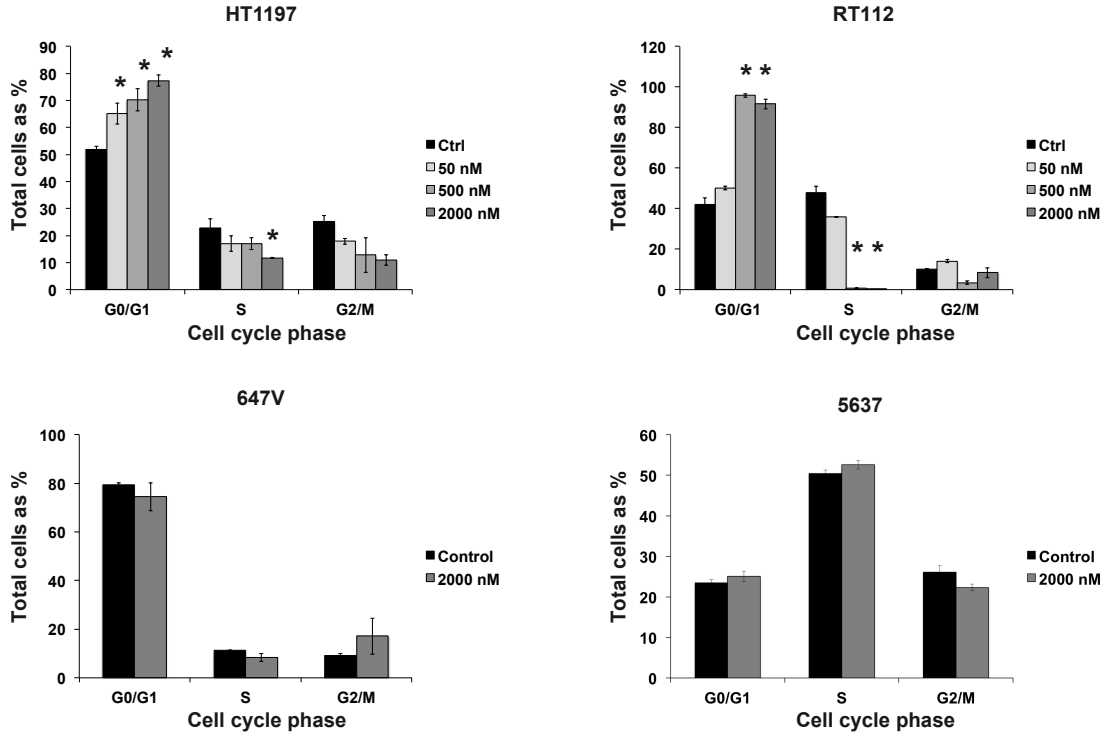

Figure 4.24: **PD-0332991 reduces cell cycle progression of RB expressing cells.** Respective cell lines were treated with indicated concentrations of PD-0332991 for 24 hours and cell cycle was assessed by EdU incorporation. * indicates $p < 0.05$.

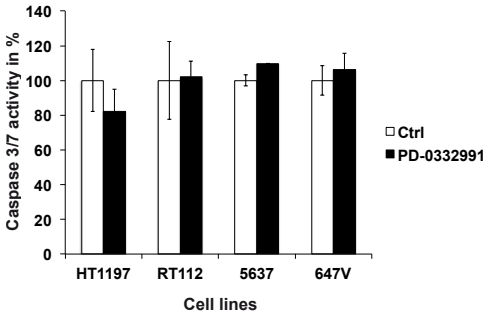

Figure 4.25: **PD-0332991 does not influence apoptosis.** Respective cell lines were treated with 2000 nM of PD-0332991 for 24 hours and caspase 3/7 activity was assessed.

4.3.6 Molecular mechanism of sensitivity to CDK 4/6 inhibition

PD-0332991 has been designed as an ATP-competitive CDK 4/6 inhibitor and should lead to a dephosphorylation of RB (Fry et al., 2001). The observation that it leads to a

reduction in total RB in the RB positive cell lines was unexpected and we investigated it further. We reconstituted RB negative cell lines 647V and 639V with recombinant RB, whose expression is controlled by a CMV promoter (Figure 4.26 A). When these cells were treated with PD-0332991 there was a reduction in phosphorylation of this recombinant protein. However, the expression of total RB protein remained unchanged. Despite the observed reduction in phosphorylated RB, both cell lines remained resistant to PD-0332991 (Figure 4.26 B).

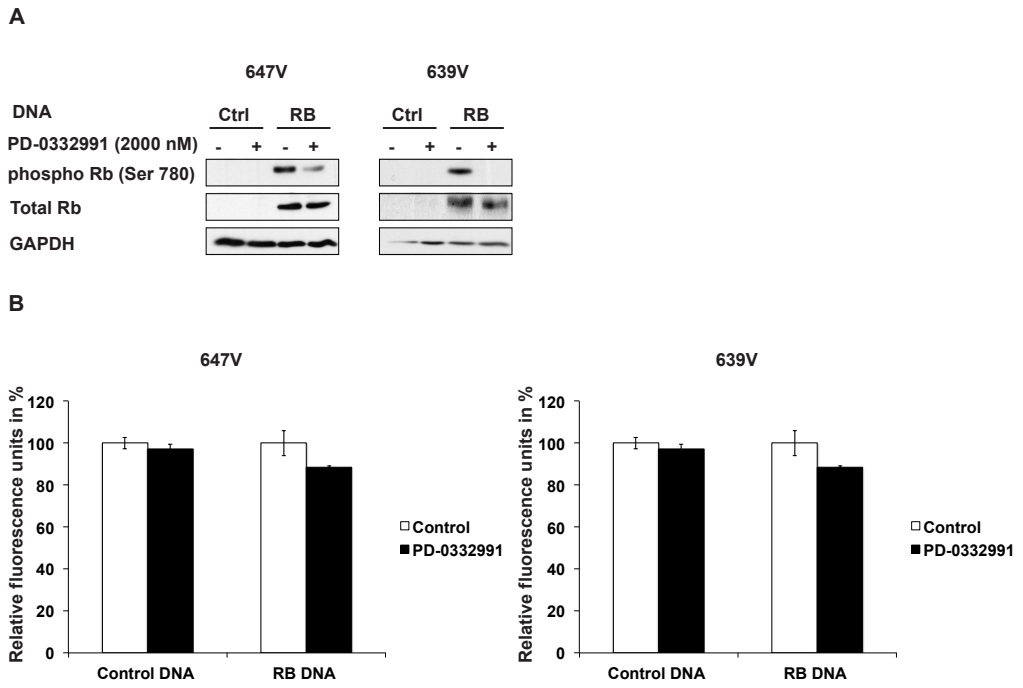

Figure 4.26: **Recombinant RB expression in RB negative cells is not regulated by PD-0332991.** (A) 647V or 639V cells transfected with control (ctrl) or RcCMV/RB cDNA for 30 hours were treated with 2000 nM of PD-0332991 for a further 24 hours and protein expression was analyzed by immunoblotting. '+' indicates present and '-' indicates absent. (B) Transfected cells were treated with 2000 nM of PD-0332991 for a further 72 hours and cell viability was assessed.

PD-0332991 treatment led to different effects on total RB in two experimental setups. While all RB expressing cells showed a reduction in total RB after treatment (Figure 4.22), this effect was not observed in the reconstituted RB in the RB negative cells (Figure 4.26 A). These two situations differ in the promoter that controls *RB1* gene expression. Unlike the RB positive cells containing the intrinsic *RB1* promoter, reconstituted RB was under the control of an independent CMV promoter. We thus speculated that the observed effect on total RB in RB positive cells might be dependent on the *RB1* gene promoter and the cell intrinsic transcriptional machinery that it regulates. Indeed, a dose dependent reduction in the mRNA transcript of *RB1* was ob-

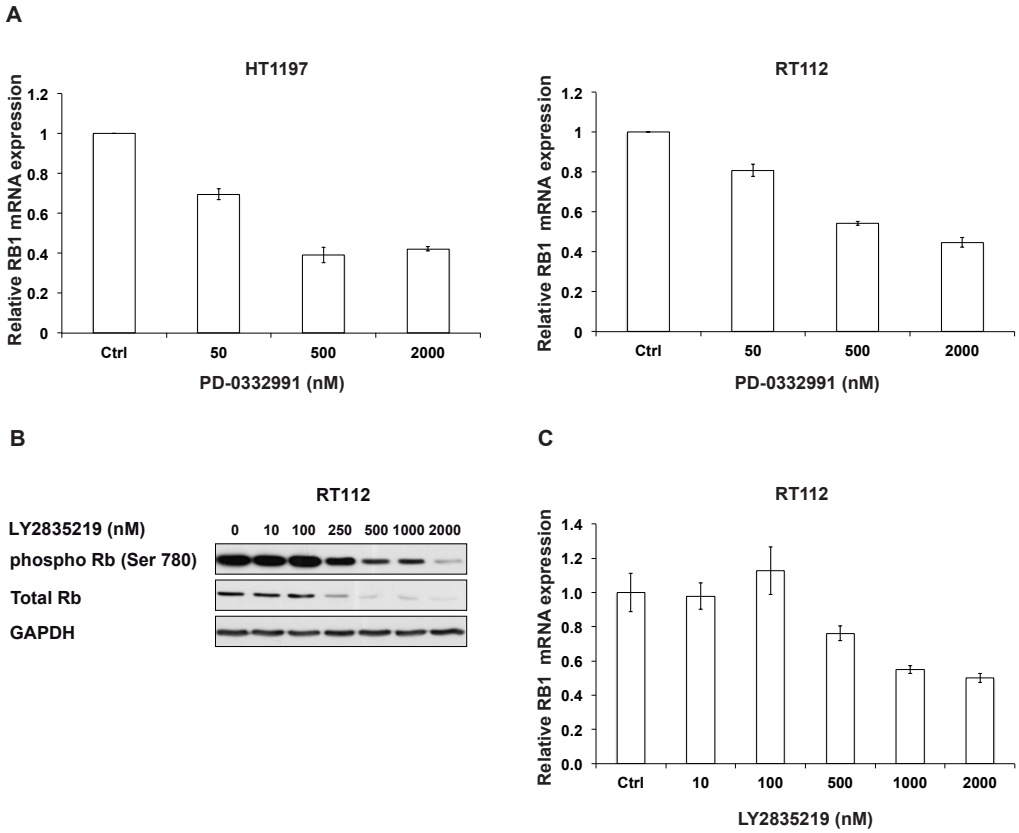

Figure 4.27: **PD-0332991 regulates the transcription of *RB1*.** (A) Respective cell lines were treated with indicated concentrations of PD-0332991 for 24 hours and *RB1* mRNA expression was analyzed. RT112 cells were treated with indicated concentrations of LY2835219 for 24 hours and (B) protein expression was analyzed by immunoblotting or (C) mRNA expression of *RB1* was determined. Graphs indicate the mean relative *RB1* mRNA expression in arbitrary units ± S.D normalized to Actin or GAPDH expression using the comparative CT method.

served in both the HT1197 and RT112 cells after PD-0332991 treatment (Figure 4.27 A). We additionally treated RT112 cells with LY2835219, another CDK 4/6 inhibitor (Gelbert et al., 2014). LY2835219 also led to a parallel reduction in phosphorylated and total RB protein in the RT112 cells (Figure 4.27 B). This corresponded with a reduction in the mRNA transcript of *RB1* in these cells (Figure 4.27 C), suggesting that CDK 4/6 inhibition via different inhibitors leads to a negative regulation of *RB1* mRNA expression.

4.3.7 CDK 4/6 inhibition in a three-dimensional xenograft model

Finally, we wanted to extrapolate our data to the three-dimensional xenograft CAM model. HT1197 and 639V cells were seeded on the developing CAM as representatives of RB positive and negative cells respectively. When treated with PD-0332991, the HT1197 cells showed a 60% reduction in tumor weight (Figure 4.28 A). This was accompanied by a 65% decrease in the expression of Ki-67 (Figure 4.28 B and C), indicating a reduction in proliferation. 639V cells did not respond to PD-0332991 treatment as indicated by no significant changes in either tumor weight or Ki-67 expression (Figure 4.28 A, B and D). Hence, similar to our *in vitro* results, RB positive cells were sensitive to PD-0332991 in a three-dimensional xenograft model.

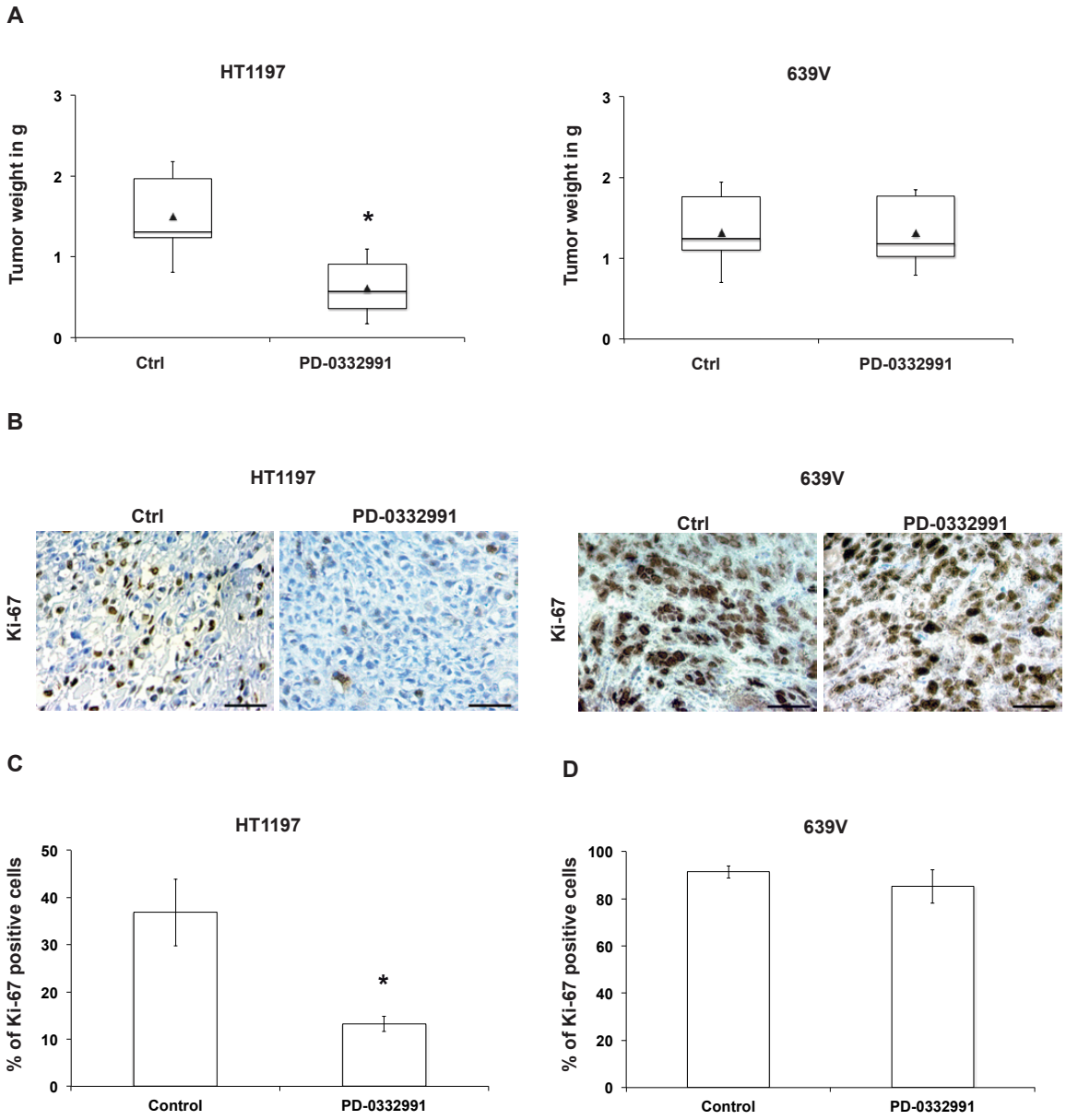

Figure 4.28: **Three-dimensional RB expressing xenografts are sensitive to PD-0332991.** (A) Tumors from indicated cell lines were harvested and weighed after PD-0332991 or control treatment. Horizontal line indicates the median. Triangle indicates the mean. Upper whisker indicates the difference between the maximum and the first quartile; lower whisker denotes the difference between the minimum and the third quartile of distribution. * indicates $p < 0.05$. (B) Representative images and (C), (D) staining quantification of tumors from respective cell lines, which were analyzed with IHC for Ki-67 expression. Scale bar equals 50 µm. * indicates $p < 0.05$. Results are representative of at least two independent experiments, with 8-10 tumors per condition.

5 Discussion

In this thesis, we have assessed the potential of targeting relevant signal transduction pathways as a treatment strategy in BLCA. Specifically, we have characterized AKT and CDK 4/6 as novel targets. We have also determined potential stratifying biomarkers that can predict treatment response.

5.1 Assessment of cell viability

A number of cell viability assays are available to enable high throughput drug screening. We have shown here that the Celltiter-blue cell viability assay can act as a surrogate for counting the number of living cells, only when cells are cultured in a sub-confluent condition. Ignoring this effect can lead to greatly underestimating the effect of an inhibitor. This assay is based on the principle that only viable cells can reduce resazurin to a fluorescent product resorufin (Riss et al., 2004). Hence, it is actually a measure of the reducing potential and metabolic capacity of cells. We can speculate that at higher cell densities, contact inhibition negatively affects cell metabolism, which results in a decreased production of the fluorescent product. It was recently demonstrated that the results of two independent studies that investigated the pharmacogenomics of drug sensitivity using high throughput inhibitor screening , had different results for several small molecule inhibitors. Rather than discrepancies in genetic data, this was mainly attributed to differences in the results of cell viability assays (Haibe-Kains et al., 2013). It is thus imperative that a particular viability assay is directly compared with the number of living cells as a readout, with proper optimization of the assay conditions.

5.2 Characterizing AKT as a target for therapy

The frequent alterations in the PI3K signaling pathway provide a rationale for its therapeutic targeting in BLCA. Previous data from our group has indicated that using either PI3K/mTOR or mTOR inhibitors leads to AKT rephosphorylation (Nawroth et al., 2011). Hence, we characterized the potential of directly targeting AKT in BLCA.

5.2.1 Relative contribution of AKT isoforms

It has been demonstrated before that AKT isoforms display functional non-redundancy, depending on the cellular context. In prostate cancer cells, inhibiting AKT1 and AKT2

with specific small molecule inhibitors resulted in an induction of apoptosis, while AKT3 inhibition had no such effect (DeFeo-Jones et al., 2005). In glioma cell lines, siRNA mediated silencing of AKT2 and AKT3 resulted in a decrease in cell growth and an increase in apoptosis (Mure et al., 2010). shRNA mediated selective silencing of all the three isoforms in PTEN deficient prostate cancer or glioma cells resulted in the highest inhibition of cell growth (Degtyarev et al.,2008). Only AKT2 was responsible for regulation of cell migration in ovarian and breast cell line xenografts (Arboleda et al., 2003). Similar results for AKT2 mediated control of cell migration were obtained in three-dimensional models of breast cancer (Irie et al., 2005). Moreover, in this model system AKT1 silencing led to an increase in cell migration and acquisition of EMT features. Our data demonstrate that in BLCA, the AKT isoforms contribute heterogeneously to AKT phosphorylation and cell viability. The greatest effect in the reduction of cell viability was observed when silencing all three isoforms. Hence, AKT inhibitors that target all three isoforms are likely to have the most benefit for BLCA treatment. While amplifications were observed in all three isoforms in the TCGA cohort, 3% of tumors also showed deletions in AKT1. It has been previously demonstrated in mouse models of lung and breast cancer that AKT1 deletions prevent or delay tumor initiation (Hollander et al., 2011, Watson and Moorehead, 2013). Thus, it is possible that the deletions in AKT1 reflect its role during the pathogenesis of these tumors.

5.2.2 Effects of MK-2206 on mTORC1 signaling

For characterization of AKT as a molecular target in BLCA therapy, we used the inhibitor MK-2206. When analyzing biochemical effects on downstream targets, treatment resulted in the dephosphorylation of S6K1 that correlated with the decrease in AKT phosphorylation, in all of the BLCA cell lines that we examined. This effect was also observed in the RT4 cells although no phosphorylated AKT could be detected in these cells with immunoblotting. This potentially indicates that they contain low levels of phosphorylated AKT that cannot be detected by immunoblotting, or that MK-2206 can directly affect S6K1 phosphorylation. No effect on different phosphorylation residues in 4E-BP1 was observed with MK-2206 treatment in any of the cell lines, demonstrating that the regulation of 4E-BP1 is independent of AKT. This extends previous data where the silencing of all three AKT isoforms in the RT112 and T24 cells led to a decrease in only S6K1 but not in 4E-BP1 phosphorylation (Nawroth et al., 2011). In this publication, it was also demonstrated that inhibiting mTOR alone had a similar effect, where only S6K1 phosphorylation was regulated, with no effect on 4E-BP1. However, dual inhibition of PI3K and mTOR using a small molecule inhibitor was able to dephosphorylate both S6K1 and 4E-BP1. Based on our data, the current model of 4E-BP1 regulation in BLCA supports a mechanism in which mTORC1 is a direct downstream target of AKT but regulates only S6K1 and not 4E-BP1. Our results now extend previous findings that the PI3K mediated regulation of 4E-BP1 occurs independently from AKT. Since 4E-BP1 is a major modulator of BLCA proliferation (Nawroth et al., 2011), further experiments are necessary to clarify its regulation.

5.2.3 Mutant *PIK3CA* is a stratifying and predictive biomarker for AKT inhibition

MK-2206 effectively reduced the viability of only *PIK3CA* mutant cell lines. This correlation was also described independently by another group (Iyer et al., 2013). We have extended this data by extensively characterizing the downstream functional effects and molecular mechanism. Importantly, we have directly manipulated the *PIK3CA* gene using two different strategies to confirm its role in conferring sensitivity to MK-2206. Additionally, we have also described a novel molecular mechanism responsible for this sensitivity. According to our results, in the presence of an HD mutant *PIK3CA* , AKT inhibition results in an increase in DUSP1 expression that leads to ERK 1/2 dephosphorylation and sensitivity to inhibition via an induction of apoptosis. The opposite response is seen in cells with WT *PIK3CA* and these cells remain resistant to inhibition (Figure 5.1).

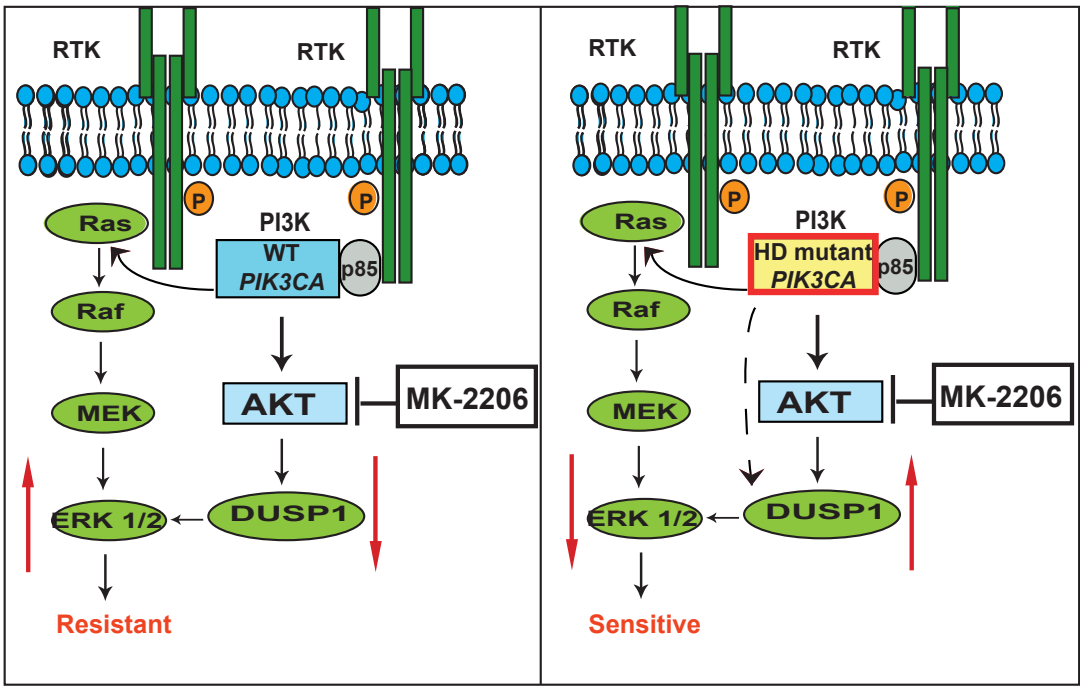

Figure 5.1: **Mutant *PIK3CA* predicts response to MK-2206.** Inhibition of AKT in the presence of hotspot HD mutations in *PIK3CA* results in upregulation of DUSP1 expression leading to reduction in ERK 1/2 phosphorylation and sensitivity to MK-2206.

A modest reduction in cell cycle progression was observed in our cells after MK-2206 treatment as described previously in breast cancer and leukemia (Sangai et al., 2012, Simioni et al., 2012, She et al., 2008). However, the response to MK-2206 in the presence of mutant *PIK3CA* was mediated via an induction of apoptosis. *PIK3CA* mutations have correlated with the response to MK-2006 in thyroid and breast cancer

(Liu et al., 2011, Sangai et al., 2012). However in both cases sensitivity also correlated with the loss of *PTEN* expression, as well as *RAS* mutations in thyroid cancer. In non-small cell lung cancer, no correlations were found between the response to MK-2206 and alterations in *PIK3CA*, *PTEN* or *RAS* (Meng et al., 2010). These data indicate that the molecular determinants of response to inhibitors differ between various tumor entities. In our study alterations in *PTEN* and *RAS* had no influence on sensitivity to MK-2206. Our data indicates that in BLCA response to MK-2206 is solely dependent on specific mutations in *PIK3CA*.

Another report has previously examined AKT inhibition in BLCA (Dickstein et al., 2012). This study used AZ7328, an ATP-competitive AKT inhibitor. Although there was a tendency between the presence of *PIK3CA* mutations and sensitivity to AZ7328, no robust association was present. Additionally, no apoptosis could be detected in sensitive cell lines. To our knowledge, no literature is available regarding the specificity of AZ7328. Being an ATP-competitive AKT inhibitor, it also led to hyperphosphorylation of AKT in all cell lines tested (Okuzumi et al., 2009). Further, apoptosis was determined by PI staining that is indicative of DNA fragmentation occurring in the late phase of apoptosis. However, this fragmentation might also be seen in cells undergoing necrosis, differentiation or alterations in chromatin structure (Riccardi and Nicoletti, 2006). The direct association between *PIK3CA* mutations and sensitivity to MK-2206 that we observed can possibly be explained by the difference in the mechanism of action of the two inhibitors and their specificity.

Unlike other cancers which possess mutations predominantly in the KD of *PIK3CA*, about 75% of *PIK3CA* mutations in BLCA occur in the HD. It has been demonstrated that HD or KD mutants confer gain of function by different mechanisms. With HD mutations, *PIK3CA* function is independent of interaction with the p85 sub-unit, but requires RAS-GTP. The opposite occurs with KD mutants that are dependent on p85 but independent from RAS activation (Zhao and Vogt, 2008). In BLCA, HD mutations led to more proliferation under conditions of nutrient depletion as compared to KD mutations. HD mutant cells were also more resistant to anoikis (Ross et al., 2013a). This may confer a selection advantage that explains their higher frequency in BLCA. Rare mutants in BLCA were found to lead to a lesser degree of AKT activation and did not confer sensitivity to MK-2206. According to our data, the presence of hotspot HD *PIK3CA* mutations can serve as a stratifying biomarker for MK-2206 treatment and also predict treatment response. 20 to 25% of muscle invasive BLCA patients stand to benefit from this novel therapeutic strategy.

5.2.4 Cross talk between PI3K and MAPK signaling

The PI3K and MAPK pathways operate in response to similar external stimuli and regulate processes such as cell growth, proliferation and apoptosis. They also have molecular cross-talk at multiple levels. An increase in RAF-1 phosphorylation at serine 338 was observed in all representative cell lines treated with MK-2206. This indicates an activation of the RAS/RAF/MEK/ERK signaling pathway. The feedback activation of various RTKs after AKT inhibition that has been described previously might explain

this observation (Cen et al., 2013, Chandarlapaty et al., 2011). We did not observe any effect at the RAF-1 serine 259 site, which has been shown to be negatively regulated by AKT in some model systems (Zimmermann, 1999). The increase in ERK 1/2 phosphorylation in the presence of mutant *PIK3CA* and a decrease in the presence of the WT *PIK3CA*, confirms a recent report that demonstrated direct activation of RAS via PI3K (Will et al., 2014). We have described the down regulation of ERK 1/2 phosphorylation, that is mediated via DUSP1 in the presence of a mutant *PIK3CA*, as a novel biochemical signature of response to AKT inhibition. This response was mediated by an increase in apoptosis. In keeping with these findings, it was recently shown that the reduction in ERK phosphorylation after PI3K inhibition is necessary to promote apoptosis in cells (Will et al., 2014). DUSP1 is expressed at higher levels in early stages of BLCA (Loda et al., 1996). DUSP mediated reduction in ERK phosphorylation was also demonstrated to be responsible for the tumor suppressor role of Notch in a BLCA mouse model, confirming its importance in the regulation of cell proliferation (Rampias et al., 2014). The mechanism by which AKT inhibition controls DUSP1 expression in the presence of mutant *PIK3CA* remains to be examined. We have confirmed that it does not depend on CREB mediated transcriptional control. The regulation of DUSP1 expression might be the result of multiple downstream signaling events in the PI3K and MAPK pathways that are initiated by the *PIK3CA* mutation. Conversely, it could also be related to physical properties of the mutation.

5.3 CDK 4/6 inhibition in BLCA

Frequent alterations in cell cycle regulation in BLCA indicate its importance in tumorigenesis. CDK 4/6 is a target within this regulatory mechanism that has been successfully investigated in several tumor entities. We have examined the utility of CDK 4/6 as a target for BLCA treatment. We have demonstrated the first pre-clinical evidence that CDK 4/6 inhibition is an effective therapeutic strategy in RB positive BLCA and that it acts by reducing *RB1* transcription. RB expression can be used as a stratifying biomarker for the clinical application of PD-0332991 and up to 75-80% of BLCA patients stand to benefit from it.

5.3.1 RB expression is a stratifying biomarker for CDK 4/6 inhibition

Correlation between selected biomarker expression and sensitivity to PD-0332991 has been previously examined in several preclinical cancer models including glioblastoma, melanoma, breast, ovarian and renal cell cancer (Young et al., 2014, Cen et al., 2012, Konecny et al., 2011, Finn et al., 2009, Dean et al., 2010, Logan et al., 2013, Wiedemeyer et al., 2010, Rivadeneira et al., 2010). Similar to our results in BLCA, these studies have also shown that PD-0332991 is effective only in RB expressing cells and results in a reduction in cell viability and cell cycle progression. We have also shown a correlation between the reduction in cell cycle progression and a down regulation of

E2F target genes. No increase in apoptotic activity was observed in the cell lines that we examined, indicating that PD-0332991 has a cytostatic mechanism of action.

The loss of *CDKN2A* expression was associated with an increase in sensitivity to PD-0332991 in melanoma, glioblastoma, rhabdoid, ovarian and renal cell cancer (Young et al., 2014, Cen et al., 2012, Konecny et al., 2011, Finn et al., 2009, Logan et al., 2013, Wiedemeyer et al., 2010, Katsumi et al., 2011). This sensitivity pattern is contrary to our observations in BLCA where the loss of *CDKN2A* was associated with an intermediate response requiring higher IC50s. However, at these higher does, these cells responded with a greater reduction in E2F downstream targets and cell cycle progression as compared to cells that express *CDKN2A*. Since *CDKN2A* loss is a frequent event in muscle invasive BLCA occurring in 40% patients, this association warrants further investigation including by direct genetic manipulation of *CDKN2A*. It would also be interesting to test the effect of CDK 2 inhibitors in these cells since one can hypothesize that they are more reliant on the cyclin E/CDK 2 axis in the absence of *CDKN2A*.

5.3.2 PD-0332991 and cisplatin are a rational drug combination

PD-0332991 is being examined in over 60 clinical trials against different cancers, mostly as single agent chemotherapy (www.clinicaltrials.gov). It was successful in combination with hormone therapy in ER positive breast cancer in the PALOMA-1 clinical trial. In this trial, the combination of PD-0332991 with letrozole, an aromatase inhibitor, significantly improved the progression free survival (PFS) to 20.2 months as compared to 10.2 months with letrozole alone (Finn et al., 2015). Since chemotherapeutic agents act in different cell cycle phases, the combination of PD-0332991 with chemotherapy can have synergistic, additive or antagonistic effects. We have shown that PD-0332991 is synergistic in combination with cisplatin. Cells that are blocked in the G1 phase have previously been demonstrated to be more sensitive to cisplatin induced DNA damage mediated cytotoxicity (Shah and Schwartz, 2001). We can speculate that the PD-0332991 mediated G0/G1 accumulation of cells sensitizes them to cisplatin. This is relevant as cisplatin based chemotherapy is the standard of care in the treatment of BLCA. The synergistic combination of PD-0332991 and cisplatin thus has the potential to improve therapeutic efficacy. Moreover, a DRI more than 1 obtained for both the drugs indicates that their doses can be lowered in combination as compared to single agents, while maintaining the anti-tumor effect. Hence, this combination also has the potential to lower the dose dependent toxicities of both the drugs.

5.3.3 CDK 4/6 inhibition reduces *RB1* transcription

Treatment with PD-0332991 led to a parallel reduction in phosphorylated and total RB in all the cell lines that we examined. This observation has also been made previously in most studies with PD-0332991 both *in vitro* and *in vivo*, with few exceptions (Fry et al., 2001, Konecny et al., 2011, Dean et al., 2010, Fry et al., 2004, Marzec et al., 2006). However, it has not been elucidated in further detail and interpreted as a reduction in

phosphorylated RB due to inhibition of the kinase activity of CDK 4/6. We have demonstrated here a novel mechanism where CDK 4/6 inhibition leads to a reduction in total RB protein via a reduction in the *RB1* transcript. We have also confirmed these results using another CDK 4/6 inhibitor LY2835219. Previous data has also demonstrated a reduction in RB total protein after silencing CDK4 or CDK6 expression using shRNAs (Li et al., 2014). Hence, the reduction in total RB expression might be a universal downstream effect of CDK 4/6 inhibition using different methods. Since this reduction in RB was not observed in recombinant RB under the control of an independent CMV promoter, it is likely to be *RB1*-promoter dependent. Recombinant RB also failed to sensitize RB negative cells to PD- 0332991 despite the reduction in its phosphorylated form, indicating that the decrease in total RB expression might be required for the response to PD-0332991. The mechanism by which CDK 4/6 inhibition acts on the *RB1* promoter remains to be examined in further detail. One potential mechanism can be via the auto-regulation of the promoter resulting from dephosphorylation of the RB family members after CDK 4/6 inhibition (Burkhart et al., 2010). CDK 4/6 could also be influencing the promoter via epigenetic mechanisms. Although our results using an experimental strategy to reconstitute RB negative cells suggests that the promoter mediated reduction in the *RB1* transcript is the sole mechanism involved in regulating total RB levels, it should be noted that only a 50% reduction in the *RB1* transcript was observed in RB positive cells. This does not correlate completely with the almost total loss of protein expression. Hence, we cannot rule out that additional mechanisms such as protein degradation might regulate the CDK 4/6 mediated inhibition of RB expression in RB positive cells.

5.4 Outlook

The first part of this work has examined the outcomes of AKT inhibition in BLCA in detail. Similarly designed studies with different inhibitors against the key molecules in the PI3K pathway should provide insights into the ideal strategy for its inhibition as well as the molecular determinants of treatment response. The effect of these inhibitors on 4E-BP1 is a potentially crucial determinant of their efficacy and needs further investigation. Specifically, various PI3K inhibitors and genetic manipulation strategies against PI3K can be examined alone and in combination with mTOR inhibition. We have described an association between the presence of mutant *PI3KCA* and regulation of DUSP1 expression. Additional studies into the mechanism underlying this phenomenon can also expand our knowledge of this signaling cascade. Our data indicates that the MAPK signaling pathway contributes to the development of resistance to PI3K pathway inhibition. Understanding of this cross talk in greater detail might generate novel therapy designs.

Our results using CDK 4/6 inhibitors demonstrate that these agents negatively regulate *RB1* transcription. The mechanism underlying this effect should be investigated to further improve our understanding of RB biology. The association between the loss of *CDKN2A* expression and treatment response also deserves further study. Since this is

a frequent molecular alteration in BLCA, these results will not only provide better insights into developing biomarkers for the clinic, but will also provide information about signaling in the RB network. It is also worth examining if these tumors might rely on CDK2 for the regulation of RB and cell cycle progression, in the absence of *CDKN2A*. In this scenario, CDK2 inhibitors might represent an interesting therapeutic modality for them. Recently, CDK 4/6 inhibitors were demonstrated to overcome resistance to PI3K inhibition in *PIK3CA* mutant breast cancer (Vora et al., 2014). This study opens up an interesting avenue for further research, where combined inhibition of PI3K and RB signaling can be analyzed as a treatment strategy in BLCA.

Despite its common occurrence, BLCA research has been under-funded and neglected compared to high profile cancers like breast and prostate cancer. Unlike many epithelial cancers, the patient prognosis and treatment options have remained largely unchanged for over 30 years (DeGraff et al., 2013). The recent advances in the understanding of the molecular biology of BLCA have the potential to change this dismal situation. These are exciting times for translational research into BCLA signaling that can enable the development of effective personalized medicine strategies. Modeling the recently described molecular sub-types of BLCA and examining their influence on target therapies can be a potential next step. Epigenetic alterations have been described as a frequent event in BLCA and deserve further investigation. The combination of target therapy with established chemotherapy, as well as with emerging promising strategies like immunotherapy or virotherapy offers hope to improving treatment success in BLCA.

6 Summary

The prognosis of muscle invasive and metastatic BLCA has remained largely unchanged in over 25 years. Therapeutic targeting of signal transduction pathways in BLCA offers a novel treatment opportunity. However, given the molecular heterogeneity in BLCA, the challenge is not only to identify suitable targets for treatment but also to define biomarkers that can predict treatment response. The PI3K pathway and cell cycle regulation are altered in 72% and 93% of BLCA respectively providing a strong rationale for their therapeutic targeting. In this work, we have investigated the potential of AKT and CDK 4/6 as targets for BLCA treatment and identified the molecular determinants of treatment response.

We have demonstrated in this project that AKT inhibition was most effective in BLCA when inhibiting all three AKT isoforms via siRNA mediated knockdown of AKT. MK-2206, an allosteric pan-AKT inhibitor, fulfills these requirements. When characterizing MK-2206 mediated effects in signaling events within the PI3K pathway, inhibition of only S6K1 phosphorylation but not 4E-BP1 phosphorylation was observed. Thus we extended results from our group that the AKT-mTORC1 axis within the PI3K signaling pathway does not regulate 4E-BP1 activity in BLCA or does so only in combination with PI3K. When analyzing cell growth, MK-2206 was effective in only a subset of cell lines that possess hotspot helical domain (HD) mutations in *PIK3CA* (encoding for the p110α subunit of PI3K) by inducing apoptosis. An increase in DUSP1 expression that led to a reduction in ERK 1/2 phosphorylation was a biochemical signature of reponse in these cells. The causative role of mutant *PIK3CA* in conferring sensitivity was established by direct genetic manipulation strategies involving recombinant protein overexpression or gene silencing. A three-dimensional chicken chorioallantoic membrane xenograft model was used to extrapolate the *in vitro* results.

In this thesis, we also analyzed the potential role of CDK 4/6 as a molecular target for therapy in BLCA. Treatment of different cell lines with the inhibitor PD-0332991 was effective only in cell lines expressing RB. *CDKN2A* loss correlated with intermediate sensitivity to the inhibitor. In sensitive cells, PD-0332991 treatment led to a reduction in the E2F target genes and an accumulation in the G0/G1 phase with a reduction in the S phase, with no increase in apoptosis. A combination of PD-0332991 with cisplatin showed a synergistic effect on cell proliferation. Biochemically, CDK 4/6 inhibition using PD-0332991 or LY2835219 led to a parallel inhibition in both phosphorylated and total RB. This reduction in total RB occurred via a promoter dependent regulation of *RB1* transcription and was necessary for the response to treatment. RB dependent response to CDK 4/6 inhibition was also demonstrated in a three-dimensional chicken chorioallantoic membrane xenograft model.

Overall, we have provided evidence for the efficacy of two novel treatment strategies

in BLCA and examined the molecular mechanisms underlying this response. Our results show that the presence of *PIK3CA* mutations, found in 20-25% muscle invasive BLCA patients, can be used as a predictive biomarker for the response to AKT inhibition. Up to 75% of RB expressing BLCA patients stand to benefit from CDK 4/6 inhibition. In this way, therapeutic targeting of signal transduction pathways can tailor a personalized medicine strategy in muscle invasive and metastatic BLCA and potentially improve patient prognosis.

7 Zusammenfassung

Die Prognose für das muskelinvasive und metastasierte Blasenkarzinom hat sich in den vergangenen 25 Jahren nicht wesentlich verändert. Eine neue Behandlungsmöglichkeit stellt die direkte Inhibierung von Siganltransduktionswegen dar. Aufgrund der molekularen Heterogenität des Blasenkarzinoms stellt die Identifizierung von prädiktiven Biomarkern und geeigneten Molekülen für die Behandlung eine große Herausforderung dar. Der PI3K Signalweg und die Zellzyklus-Regulation sind in 72%, bzw. 93% der Blasenkarzinome verändert und stellen somit potentielle Möglichkeiten für ein therapeutisches Eingreifen dar. In dieser Arbeit haben wir daher das Potential von AKT und CDK 4/6 als therapeutische Zielmoleküle untersucht und molekulare Determinanten für eine Therapieantwort identifiziert.

Für AKT konnte in dieser Arbeit mittels spezifischer siRNAs gezeigt werden, dass alle drei Isoformen inhibiert werden müssen, um eine möglichst gute Therapieantwort zu erhalten. Der Inhibitor MK-2206, ein allosterischer pan-AKT Inhibitor, erfüllt dieses Kriterium. Eine Behandlung mit MK-2206 führt innerhalb des PI3K Signalweges zu einer Inhibition der Phosphorylierung von S6K1, jedoch nicht 4E-BP1. Damit konnten publizierte Daten unserer Gruppe erweitert werden die zeigen, dass die AKT-mTORC1 Achse des PI3K Signalweges nicht, oder nur in Kombination mit PI3K, die Aktivität von 4E-BP1 reguliert. Die Behandlung mit MK-2206 führte nur in den Zelllinien, die eine Mutation in der helikale Domäne des *PIK3CA* Gens (das für die p110α Untereinheit von PI3K kodiert) haben, zu einer Verringerung der Proliferation durch Induktion von Apoptose . In diesen Zellen wurde durch MK-2206 die Expression von DUSP1 erhöht, was zu einer Reduktion der Phosphorylierung von ERK 1/2 führte. Der kausale Zusammenhang dieser biochemischen Signatur mit dem funktionalen Ansprechen wurde mit verschiedenen molekularbiologischen Strategien bestätigt. Dabei wurden Zellen mit dem Wildtyp oder dem mutierten *PIK3CA* Gen transfiziert, bzw. mittels siRNA basierten Methoden die endogene Expression des *PIK3CA* Gens unterdrückt. Diese Ergebnisse wurden in einem 3-Dimensionalen Xenograft-Model auf der Chorioallantois Membran (CAM) des Hühnerembryos bestätigt.

Des Weiteren wurde in dieser Arbeit die potentielle Rolle von CDK 4/6 als molekulares Ziel einer Therapie des Blasenkarzinoms untersucht. Die Behandlung verschiedener Zelllinien mit dem CDK 4/6 Inhibitor PD-0332991 führte dabei nur in RB exprimierenden Zellen zu einer Reaktion . Der Verlust von *CDKN2A* korrelierte mit einer reduzierten Sensitivität gegenüber diesem Inhibitor. In den RB positiven Zellen führte die Behandlung mit PD-0332991 zu einer Reduktion von E2F Target-Genen und einer Akkumulation der Zellen in der G0/G1 Phase des Zellzyklus. Gleichzeitig konnte eine verringerte Progression in die S-Phase, jedoch keine erhöhte Apoptose nachgewiesen werden. Die Kombination von PD-0332991 mit Cisplatin zeigte eine synergistische

Wirkung auf das Wachstum der Zellen. Biochemisch führte die Inhibition von CDK 4/6 durch die Behandlung der Inhibitoren PD-0332991 oder LY2835219 zu einer Reduktion von phosphoryliertem und RB-Gesamtproteingehalt . Die verminderte Expression des RB Proteins wird auf transkriptioneller Ebene über den RB-Promotor reguliert und scheint für eine Therapieantwort von zentraler Bedeutung zu sein. Das RB abhängige Therapieansprechen auf CDK 4/6 Inhibitoren wurde ebenfalls am 3-dimensionalen Tumor-Xenograft Model der CAM des Hühnerembryos bestätigt.

Zusammenfassend konnten in dieser Arbeit zwei neue Behandlungsstrategien für das Blasenkarzinom identifiziert werden. Dabei wurden molekulare Mechanismen untersucht, die zu der Identifikation prädiktiver Marker führten. Diese Ergebnisse zeigen, dass Mutationen in dem *PIK3CA* Gen, die in etwa 20-25% der muskelinvasiven Blasenkarzinome vorliegen, als prädiktive Marker für die Therapieantwort einer AKT Inhibition genutzt werden können. In etwa 75-80% der Patienten mit einem muskelinvasiven Blasenkarzinom wird RB im Tumorgewebe exprimiert womit diese Patienten von einer CDK 4/6 inhibierenden Therapie profitieren sollten. Auf diese Art und Weise können personalisierte Behandlungsstrategien für muskelinvasive und metastasierende Blasentumore durch zielgerichtete Inhibierung von Signaltransduktionswegen angepasst werden und möglicherweise Patientenprognosen verbessert werden.

Bibliography

ABDOLLAH, F., GANDAGLIA, G., THURET, R., SCHMITGES, J., TIAN, Z., JELDRES, C., PASSONI, N. M., BRIGANTI, A., SHARIAT, S. F., PERROTTE, P., MONTORSI, F., KARAKIEWICZ, P. I. & SUN, M. 2013. Incidence, survival and mortality rates of stage-specific bladder cancer in United States: a trend analysis. Cancer Epidemiol, 37, 219-25.

ABEN, K. K., WITJES, J. A., SCHOENBERG, M. P., HULSBERGEN-VAN DE KAA, C., VERBEEK, A. L. & KIEMENEY, L. A. 2002. Familial aggregation of urothelial cell carcinoma. Int J Cancer, 98, 274-8.

ANASTASIADIS, A. & DE REIJKE, T. M. 2012. Best practice in the treatment of non-muscle invasive bladder cancer. Ther Adv Urol, 4, 13-32.

ARBOLEDA, M. J., LYONS, J. F., KABBINAVAR, F. F., BRAY, M. R., SNOW, B. E., AYALA, R., DANINO, M., KARLAN, B. Y. & SLAMON, D. J. 2003. Overexpression of AKT2/protein kinase Bbeta leads to up-regulation of beta1 integrins, increased invasion, and metastasis of human breast and ovarian cancer cells. Cancer Res, 63, 196-206.

ARCARO, A. & GUERREIRO, A. S. 2007. The phosphoinositide 3-kinase pathway in human cancer: genetic alterations and therapeutic implications. Curr Genomics, 8, 271-306.

ASGHAR, U., WITKIEWICZ, A. K., TURNER, N. C. & KNUDSEN, E. S. 2015. The history and future of targeting cyclin-dependent kinases in cancer therapy. Nat Rev Drug Discov, 14, 130-46.

ASKHAM, J. M., PLATT, F., CHAMBERS, P. A., SNOWDEN, H., TAYLOR, C. F. & KNOWLES, M. A. 2010. AKT1 mutations in bladder cancer: identification of a novel oncogenic mutation that can co-operate with E17K. Oncogene, 29, 150-5.

AVEYARD, J. S., SKILLETER, A., HABUCHI, T. & KNOWLES, M. A. 1999. Somatic mutation of PTEN in bladder carcinoma. Br J Cancer, 80, 904-8.

BARNETT, S. F., DEFEO-JONES, D., FU, S., HANCOCK, P. J., HASKELL, K. M., JONES, R. E., KAHANA, J. A., KRAL, A. M., LEANDER, K., LEE, L. L., MALINOWSKI, J., MCAVOY, E. M., NAHAS, D. D., ROBINSON, R. G. & HUBER, H. E. 2005. Identification and characterization of pleckstrin-homology-domain-dependent and isoenzyme-specific Akt inhibitors. Biochem J, 385, 399-408.

BARRETINA, J., CAPONIGRO, G., STRANSKY, N., VENKATESAN, K., MARGOLIN, A. A., KIM, S., WILSON, C. J., LEHAR, J., KRYUKOV, G. V., SONKIN, D., REDDY, A., LIU, M., MURRAY, L., BERGER, M. F., MONAHAN, J. E., MORAIS, P., MELTZER, J., KOREJWA, A., JANE-VALBUENA, J., MAPA, F. A., THIBAULT, J., BRIC-FURLONG, E., RAMAN, P.,

SHIPWAY, A., ENGELS, I. H., CHENG, J., YU, G. K., YU, J., ASPESI, P., JR., DE SILVA, M., JAGTAP, K., JONES, M. D., WANG, L., HATTON, C., PALESCANDOLO, E., GUPTA, S., MAHAN, S., SOUGNEZ, C., ONOFRIO, R. C., LIEFELD, T., MACCONAILL, L., WINCKLER, W., REICH, M., LI, N., MESIROV, J. P., GABRIEL, S. B., GETZ, G., ARDLIE, K., CHAN, V., MYER, V. E., WEBER, B. L., PORTER, J., WARMUTH, M., FINAN, P., HARRIS, J. L., MEYERSON, M., GOLUB, T. R., MORRISSEY, M. P., SELLERS, W. R., SCHLEGEL, R. & GARRAWAY, L. A. 2012. The Cancer Cell Line Encyclopedia enables predictive modelling of anticancer drug sensitivity. Nature, 483, 603-7.

BELLMUNT, J., FOUGERAY, R., ROSENBERG, J. E., VON DER MAASE, H., SCHUTZ, F. A., SALHI, Y., CULINE, S. & CHOUEIRI, T. K. 2013. Long-term survival results of a randomized phase III trial of vinflunine plus best supportive care versus best supportive care alone in advanced urothelial carcinoma patients after failure of platinum-based chemotherapy. Ann Oncol, 24, 1466-72.

BELLMUNT, J. & PETRYLAK, D. P. 2012. New therapeutic challenges in advanced bladder cancer. Semin Oncol, 39, 598-607.

BOTTEMAN, M. F., PASHOS, C. L., REDAELLI, A., LASKIN, B. & HAUSER, R. 2003. The health economics of bladder cancer: a comprehensive review of the published literature. Pharmacoeconomics, 21, 1315-30.

BRENNAN, P., BOGILLOT, O., CORDIER, S., GREISER, E., SCHILL, W., VINEIS, P., LOPEZ-ABENTE, G., TZONOU, A., CHANG-CLAUDE, J., BOLM-AUDORFF, U., JOCKEL, K. H., DONATO, F., SERRA, C., WAHRENDORF, J., HOURS, M., T'MANNETJE, A., KOGEVINAS, M. & BOFFETTA, P. 2000. Cigarette smoking and bladder cancer in men: a pooled analysis of 11 case-control studies. Int J Cancer, 86, 289-94.

BURGER, M., CATTO, J. W., DALBAGNI, G., GROSSMAN, H. B., HERR, H., KARAKIEWICZ, P., KASSOUF, W., KIEMENEY, L. A., LA VECCHIA, C., SHARIAT, S. & LOTAN, Y. 2013. Epidemiology and risk factors of urothelial bladder cancer. Eur Urol, 63, 234-41.

BURKHART, D. L., NGAI, L. K., ROAKE, C. M., VIATOUR, P., THANGAVEL, C., HO, V. M., KNUDSEN, E. S. & SAGE, J. 2010. Regulation of RB transcription in vivo by RB family members. Mol Cell Biol, 30, 1729-45.

CALDERARO, J., REBOUISSOU, S., DE KONING, L., MASMOUDI, A., HERAULT, A., DUBOIS, T., MAILLE, P., SOYEUX, P., SIBONY, M., DE LA TAILLE, A., VORDOS, D., LEBRET, T., RADVANYI, F. & ALLORY, Y. 2014. PI3K/AKT pathway activation in bladder carcinogenesis. Int J Cancer, 134, 1776-84.

CAPPELLEN, D., GIL DIEZ DE MEDINA, S., CHOPIN, D., THIERY, J. P. & RADVANYI, F. 1997. Frequent loss of heterozygosity on chromosome 10q in muscle-invasive transitional cell carcinomas of the bladder. Oncogene, 14, 3059-66.

CARNEIRO, B. A., MEEKS, J. J., KUZEL, T. M., SCARANTI, M., ABDULKADIR, S. A. & GILES, F. J. 2015. Emerging therapeutic targets in bladder cancer. Cancer Treat Rev, 41, 170-8.

CARRACEDO, A., MA, L., TERUYA-FELDSTEIN, J., ROJO, F., SALMENA, L., ALIMONTI, A., EGIA, A., SASAKI, A. T., THOMAS, G., KOZMA, S. C., PAPA, A., NARDELLA, C., CANTLEY, L. C., BASELGA, J. & PANDOLFI, P. P. 2008. Inhibition of mTORC1 leads to MAPK pathway activation through a PI3K-dependent feedback loop in human cancer. J Clin Invest, 118, 3065-74.

CEN, B., MAHAJAN, S., WANG, W. & KRAFT, A. S. 2013. Elevation of receptor tyrosine kinases by small molecule AKT inhibitors in prostate cancer is mediated by Pim-1. Cancer Res, 73, 3402-11.

CEN, L., CARLSON, B. L., SCHROEDER, M. A., OSTREM, J. L., KITANGE, G. J., MLADEK, A. C., FINK, S. R., DECKER, P. A., WU, W., KIM, J. S., WALDMAN, T., JENKINS, R. B. & SARKARIA, J. N. 2012. p16-Cdk4-Rb axis controls sensitivity to a cyclin-dependent kinase inhibitor PD0332991 in glioblastoma xenograft cells. Neuro Oncol, 14, 870-81.

CERAMI, E., GAO, J., DOGRUSOZ, U., GROSS, B. E., SUMER, S. O., AKSOY, B. A., JACOBSEN, A., BYRNE, C. J., HEUER, M. L., LARSSON, E., ANTIPIN, Y., REVA, B., GOLDBERG, A. P., SANDER, C. & SCHULTZ, N. 2012. The cBio cancer genomics portal: an open platform for exploring multidimensional cancer genomics data. Cancer Discov, 2, 401-4.

CHANDARLAPATY, S., SAWAI, A., SCALTRITI, M., RODRIK-OUTMEZGUINE, V., GRBOVIC-HUEZO, O., SERRA, V., MAJUMDER, P. K., BASELGA, J. & ROSEN, N. 2011. AKT inhibition relieves feedback suppression of receptor tyrosine kinase expression and activity. Cancer Cell, 19, 58-71.

CHOI, W., PORTEN, S., KIM, S., WILLIS, D., PLIMACK, E. R., HOFFMAN-CENSITS, J., ROTH, B., CHENG, T., TRAN, M., LEE, I. L., MELQUIST, J., BONDARUK, J., MAJEWSKI, T., ZHANG, S., PRETZSCH, S., BAGGERLY, K., SIEFKER-RADTKE, A., CZERNIAK, B., DINNEY, C. P. & MCCONKEY, D. J. 2014. Identification of distinct basal and luminal subtypes of muscle-invasive bladder cancer with different sensitivities to frontline chemotherapy. Cancer Cell, 25, 152-65.

CHOU, T. C. 2006. Theoretical basis, experimental design, and computerized simulation of synergism and antagonism in drug combination studies. Pharmacol Rev, 58, 621-81.

CHOU, T. C. 2010. Drug combination studies and their synergy quantification using the Chou-Talalay method. Cancer Res, 70, 440-6.

DAMRAUER, J. S., HOADLEY, K. A., CHISM, D. D., FAN, C., TIGANELLI, C. J., WOBKER, S. E., YEH, J. J., MILOWSKY, M. I., IYER, G., PARKER, J. S. & KIM, W. Y. 2014. Intrinsic subtypes of high-grade bladder cancer reflect the hallmarks of breast cancer biology. Proc Natl Acad Sci U S A, 111, 3110-5.

DEAN, J. L., THANGAVEL, C., MCCLENDON, A. K., REED, C. A. & KNUDSEN, E. S. 2010. Therapeutic CDK4/6 inhibition in breast cancer: key mechanisms of response and failure. Oncogene, 29, 4018-32.

DEFEO-JONES, D., BARNETT, S. F., FU, S., HANCOCK, P. J., HASKELL, K. M., LEANDER, K. R., MCAVOY, E., ROBINSON, R. G., DUGGAN, M. E., LINDSLEY, C. W., ZHAO, Z., HUBER, H. E. & JONES, R. E. 2005. Tumor cell sensitization to apoptotic stimuli by selective inhibition of specific Akt/PKB family members. Mol Cancer Ther, 4, 271-9.

DEGRAFF, D. J., ROBINSON, V. L., SHAH, J. B., BRANDT, W. D., SONPAVDE, G., KANG, Y., LIEBERT, M., WU, X. R., TAYLOR, J. A., 3RD & TRANSLATIONAL SCIENCE WORKING GROUP OF THE BLADDER ADVOCACY NETWORK THINK, T. 2013. Current preclinical models for the advancement of translational bladder cancer research. Mol Cancer Ther, 12, 121-30.

DEGTYAREV, M., DE MAZIERE, A., ORR, C., LIN, J., LEE, B. B., TIEN, J. Y., PRIOR, W. W., VAN DIJK, S., WU, H., GRAY, D. C., DAVIS, D. P., STERN, H. M., MURRAY, L. J., HOEFLICH, K. P., KLUMPERMAN, J., FRIEDMAN, L. S. & LIN, K. 2008. Akt inhibition promotes autophagy and sensitizes PTEN-null tumors to lysosomotropic agents. J Cell Biol, 183, 101-16.

DHILLON, S. 2015. Palbociclib: first global approval. Drugs, 75, 543-51.

DICKSTEIN, R. J., NITTI, G., DINNEY, C. P., DAVIES, B. R., KAMAT, A. M. & MCCONKEY, D. J. 2012. Autophagy limits the cytotoxic effects of the AKT inhibitor AZ7328 in human bladder cancer cells. Cancer Biol Ther, 13, 1325-38.

DIENSTMANN, R., RODON, J., SERRA, V. & TABERNERO, J. 2014. Picking the point of inhibition: a comparative review of PI3K/AKT/mTOR pathway inhibitors. Mol Cancer Ther, 13, 1021-31.

DREICER, R., LI, H., STEIN, M., DIPAOLA, R., ELEFF, M., ROTH, B. J. & WILDING, G. 2009. Phase 2 trial of sorafenib in patients with advanced urothelial cancer: a trial of the Eastern Cooperative Oncology Group. Cancer, 115, 4090-5.

DRUKER, B. J. 2008. Translation of the Philadelphia chromosome into therapy for CML. Blood, 112, 4808-17. DU, K. & MONTMINY, M. 1998. CREB is a regulatory target for the protein kinase Akt/PKB. J Biol Chem, 273, 32377-32379.

DUMMLER, B. & HEMMINGS, B. A. 2007. Physiological roles of PKB/Akt isoforms in development and disease. Biochem Soc Trans, 35, 231-5.

ENGELMAN, J. A., LUO, J. & CANTLEY, L. C. 2006. The evolution of phosphatidylinositol 3-kinases as regulators of growth and metabolism. Nat Rev Genet, 7, 606-19.

EPSTEIN, J. I., AMIN, M. B., REUTER, V. R. & MOSTOFI, F. K. 1998. The World Health Organization/International Society of Urological Pathology consensus classification of urothelial (transitional cell) neoplasms of the urinary bladder. Bladder Consensus Conference Committee. Am J Surg Pathol, 22, 1435-48.

FERLAY, J., SOERJOMATARAM, I., DIKSHIT, R., ESER, S., MATHERS, C., REBELO, M., PARKIN, D. M., FORMAN, D. & BRAY, F. 2015. Cancer incidence and mortality worldwide: sources, methods and major patterns in GLOBOCAN 2012. Int J Cancer, 136, E359-86.

FINN, R. S., CROWN, J. P., LANG, I., BOER, K., BONDARENKO, I. M., KULYK, S. O., ETTL, J., PATEL, R., PINTER, T., SCHMIDT, M., SHPARYK, Y., THUMMALA, A. R., VOYTKO, N. L., FOWST, C., HUANG, X., KIM, S. T., RANDOLPH, S. & SLAMON, D. J. 2015. The cyclin-dependent kinase 4/6 inhibitor palbociclib in combination with letrozole versus letrozole alone as first-line treatment of oestrogen receptor-positive, HER2-negative, advanced breast cancer (PALOMA-1/TRIO-18): a randomised phase 2 study. Lancet Oncol, 16, 25-35.

FINN, R. S., DERING, J., CONKLIN, D., KALOUS, O., COHEN, D. J., DESAI, A. J., GINTHER, C., ATEFI, M., CHEN, I., FOWST, C., LOS, G. & SLAMON, D. J. 2009. PD 0332991, a selective cyclin D kinase 4/6 inhibitor, preferentially inhibits proliferation of luminal estrogen receptor-positive human breast cancer cell lines in vitro. Breast Cancer Res, 11, R77.

FORBES, S. A., BEARE, D., GUNASEKARAN, P., LEUNG, K., BINDAL, N., BOUTSELAKIS, H., DING, M., BAMFORD, S., COLE, C., WARD, S., KOK, C. Y., JIA, M., DE, T., TEAGUE, J. W., STRATTON, M. R., MCDERMOTT, U. & CAMPBELL, P. J. 2015. COSMIC: exploring the world's knowledge of somatic mutations in human cancer. Nucleic Acids Res, 43, D805-11.

FRANKE, T. F. 2008. PI3K/Akt: getting it right matters. Oncogene, 27, 6473-88.

FREEDMAN, N. D., SILVERMAN, D. T., HOLLENBECK, A. R., SCHATZKIN, A. & ABNET, C. C. 2011. Association between smoking and risk of bladder cancer among men and women. JAMA, 306, 737-45.

FRUMAN, D. A. & ROMMEL, C. 2014. PI3K and cancer: lessons, challenges and opportunities. Nat Rev Drug Discov, 13, 140-56.

FRY, D. W., BEDFORD, D. C., HARVEY, P. H., FRITSCH, A., KELLER, P. R., WU, Z., DOBRUSIN, E., LEOPOLD, W. R., FATTAEY, A. & GARRETT, M. D. 2001. Cell cycle and biochemical effects of PD 0183812. A potent inhibitor of the cyclin D-dependent kinases CDK4 and CDK6. J Biol Chem, 276, 16617-23.

FRY, D. W., HARVEY, P. J., KELLER, P. R., ELLIOTT, W. L., MEADE, M., TRACHET, E., ALBASSAM, M., ZHENG, X., LEOPOLD, W. R., PRYER, N. K. & TOOGOOD, P. L. 2004. Specific inhibition of cyclin-dependent kinase 4/6 by PD 0332991 and associated antitumor activity in human tumor xenografts. Mol Cancer Ther, 3, 1427-38.

GALLAGHER, D. J., MILOWSKY, M. I., GERST, S. R., ISHILL, N., RICHES, J., REGAZZI, A., BOYLE, M. G., TROUT, A., FLAHERTY, A. M. & BAJORIN, D. F. 2010. Phase II study of sunitinib in patients with metastatic urothelial cancer. J Clin Oncol, 28, 1373-9.

GAO, J., AKSOY, B. A., DOGRUSOZ, U., DRESDNER, G., GROSS, B., SUMER, S. O., SUN, Y., JACOBSEN, A., SINHA, R., LARSSON, E., CERAMI, E., SANDER, C. & SCHULTZ, N. 2013. Integrative analysis of complex cancer genomics and clinical profiles using the cBioPortal. Sci Signal, 6, pl1.

GELBERT, L. M., CAI, S., LIN, X., SANCHEZ-MARTINEZ, C., DEL PRADO, M., LALLENA, M. J., TORRES, R., AJAMIE, R. T., WISHART, G. N., FLACK, R. S., NEUBAUER,

B. L., YOUNG, J., CHAN, E. M., IVERSEN, P., CRONIER, D., KREKLAU, E. & DE DIOS, A. 2014. Preclinical characterization of the CDK4/6 inhibitor LY2835219: in-vivo cell cycle-dependent/independent anti-tumor activities alone/in combination with gemcitabine. Invest New Drugs, 32, 825-37.

GERBER, D. E. 2008. Targeted therapies: a new generation of cancer treatments. Am Fam Physician, 77, 311-9.

GERULLIS, H., ECKE, T. H., JANUSCH, B., ARNDT, C., HEIDARI, M., ONIANI, J. & OTTO, T. 2011. Long-term response in advanced bladder cancer involving the use of temsirolimus and vinflunine after platin resistance. Anticancer Drugs, 22, 940-3.

GIACINTI, C. & GIORDANO, A. 2006. RB and cell cycle progression. Oncogene, 25, 5220-7.

GILLS, J. J. & DENNIS, P. A. 2009. Perifosine: update on a novel Akt inhibitor. Curr Oncol Rep, 11, 102-10.

GONZALEZ, E. & MCGRAW, T. E. 2009. The Akt kinases: isoform specificity in metabolism and cancer. Cell Cycle, 8, 2502-8.

GUO, Y., CHEKALUK, Y., ZHANG, J., DU, J., GRAY, N. S., WU, C. L. & KWIATKOWSKI, D. J. 2013. TSC1 involvement in bladder cancer: diverse effects and therapeutic implications. J Pathol, 230, 17-27.

HAHN, N. M., STADLER, W. M., ZON, R. T., WATERHOUSE, D., PICUS, J., NATTAM, S., JOHNSON, C. S., PERKINS, S. M., WADDELL, M. J., SWEENEY, C. J. & HOOSIER ONCOLOGY, G. 2011. Phase II trial of cisplatin, gemcitabine, and bevacizumab as first-line therapy for metastatic urothelial carcinoma: Hoosier Oncology Group GU 04-75. J Clin Oncol, 29, 1525-30.

HAIBE-KAINS, B., EL-HACHEM, N., BIRKBAK, N. J., JIN, A. C., BECK, A. H., AERTS, H. J. & QUACKENBUSH, J. 2013. Inconsistency in large pharmacogenomic studies. Nature, 504, 389-93.

HANAHAN, D. & WEINBERG, R. A. 2011. Hallmarks of cancer: the next generation. Cell, 144, 646-74.

HAUTMANN, R. E., DE PETRICONI, R. C., PFEIFFER, C. & VOLKMER, B. G. 2012. Radical cystectomy for urothelial carcinoma of the bladder without neoadjuvant or adjuvant therapy: long-term results in 1100 patients. Eur Urol, 61, 1039-47.

HIRAI, H., SOOTOME, H., NAKATSURU, Y., MIYAMA, K., TAGUCHI, S., TSUJIOKA, K., UENO, Y., HATCH, H., MAJUMDER, P. K., PAN, B. S. & KOTANI, H. 2010. MK-2206, an allosteric Akt inhibitor, enhances antitumor efficacy by standard chemotherapeutic agents or molecular targeted drugs in vitro and in vivo. Mol Cancer Ther, 9, 1956-67.

HOLLANDER, M. C., MAIER, C. R., HOBBS, E. A., ASHMORE, A. R., LINNOILA, R. I. & DENNIS, P. A. 2011. Akt1 deletion prevents lung tumorigenesis by mutant K-ras. Oncogene, 30, 1812-21.

HUANG, B. X. & KIM, H. Y. 2006. Interdomain conformational changes in Akt activation revealed by chemical cross-linking and tandem mass spectrometry. Mol Cell Proteomics, 5, 1045-53.

HUDIS, C. A. 2007. Trastuzumab–mechanism of action and use in clinical practice. N Engl J Med, 357, 39-51.

HUSSAIN, M. H., MACVICAR, G. R., PETRYLAK, D. P., DUNN, R. L., VAISHAMPAYAN, U., LARA, P. N., JR., CHATTA, G. S., NANUS, D. M., GLODE, L. M., TRUMP, D. L., CHEN, H., SMITH, D. C. & NATIONAL CANCER, I. 2007. Trastuzumab, paclitaxel, carboplatin, and gemcitabine in advanced human epidermal growth factor receptor-2/neu-positive urothelial carcinoma: results of a multicenter phase II National Cancer Institute trial. J Clin Oncol, 25, 2218-24.

IRIE, H. Y., PEARLINE, R. V., GRUENEBERG, D., HSIA, M., RAVICHANDRAN, P., KOTHARI, N., NATESAN, S. & BRUGGE, J. S. 2005. Distinct roles of Akt1 and Akt2 in regulating cell migration and epithelial-mesenchymal transition. J Cell Biol, 171, 1023-34.

IYER, G., AL-AHMADIE, H., SCHULTZ, N., HANRAHAN, A. J., OSTROVNAYA, I., BALAR, A. V., KIM, P. H., LIN, O., WEINHOLD, N., SANDER, C., ZABOR, E. C., JANAKIRAMAN, M., GARCIA-GROSSMAN, I. R., HEGUY, A., VIALE, A., BOCHNER, B. H., REUTER, V. E., BAJORIN, D. F., MILOWSKY, M. I., TAYLOR, B. S. & SOLIT, D. B. 2013. Prevalence and co-occurrence of actionable genomic alterations in high-grade bladder cancer. J Clin Oncol, 31, 3133-40.

IYER, G., HANRAHAN, A. J., MILOWSKY, M. I., AL-AHMADIE, H., SCOTT, S. N., JANAKIRAMAN, M., PIRUN, M., SANDER, C., SOCCI, N. D., OSTROVNAYA, I., VIALE, A., HEGUY, A., PENG, L., CHAN, T. A., BOCHNER, B., BAJORIN, D. F., BERGER, M. F., TAYLOR, B. S. & SOLIT, D. B. 2012. Genome sequencing identifies a basis for everolimus sensitivity. Science, 338, 221.

KANDOTH, C., MCLELLAN, M. D., VANDIN, F., YE, K., NIU, B., LU, C., XIE, M., ZHANG, Q., MCMICHAEL, J. F., WYCZALKOWSKI, M. A., LEISERSON, M. D., MILLER, C. A., WELCH, J. S., WALTER, M. J., WENDL, M. C., LEY, T. J., WILSON, R. K., RAPHAEL, B. J. & DING, L. 2013. Mutational landscape and significance across 12 major cancer types. Nature, 502, 333-9.

KATSUMI, Y., IEHARA, T., MIYACHI, M., YAGYU, S., TSUBAI-SHIMIZU, S., KIKUCHI, K., TAMURA, S., KUWAHARA, Y., TSUCHIYA, K., KURODA, H., SUGIMOTO, T., HOUGHTON, P. J. & HOSOI, H. 2011. Sensitivity of malignant rhabdoid tumor cell lines to PD 0332991 is inversely correlated with p16 expression. Biochem Biophys Res Commun, 413, 62-8.

KIND, C. 1975. The development of the circulating blood volume of the chick embryo. Anat Embryol (Berl), 147, 127-32.

KLEMPNER, S. J., MYERS, A. P. & CANTLEY, L. C. 2013. What a tangled web we weave: emerging resistance mechanisms to inhibition of the phosphoinositide 3-kinase pathway. Cancer Discov, 3, 1345-54.

KNOWLES, M. A., HABUCHI, T., KENNEDY, W. & CUTHBERT-HEAVENS, D. 2003. Mutation spectrum of the 9q34 tuberous sclerosis gene TSC1 in transitional cell carcinoma of the bladder. Cancer Res, 63, 7652-6.

KNOWLES, M. A. & HURST, C. D. 2015. Molecular biology of bladder cancer: new insights into pathogenesis and clinical diversity. Nat Rev Cancer, 15, 25-41.

KNOWLES, M. A., PLATT, F. M., ROSS, R. L. & HURST, C. D. 2009. Phosphatidylinositol 3-kinase (PI3K) pathway activation in bladder cancer. Cancer Metastasis Rev, 28, 305-16.

KNUDSEN, E. S. & WANG, J. Y. 2010. Targeting the RB-pathway in cancer therapy. Clin Cancer Res, 16, 1094-9.

KONECNY, G. E., WINTERHOFF, B., KOLAROVA, T., QI, J., MANIVONG, K., DERING, J., YANG, G., CHALUKYA, M., WANG, H. J., ANDERSON, L., KALLI, K. R., FINN, R. S., GINTHER, C., JONES, S., VELCULESCU, V. E., RIEHLE, D., CLIBY, W. A., RANDOLPH, S., KOEHLER, M., HARTMANN, L. C. & SLAMON, D. J. 2011. Expression of p16 and retinoblastoma determines response to CDK4/6 inhibition in ovarian cancer. Clin Cancer Res, 17, 1591-602.

KUMAR, C. C. & MADISON, V. 2005. AKT crystal structure and AKT-specific inhibitors. Oncogene, 24, 7493-501.

LAPLANTE, M. & SABATINI, D. M. 2009. mTOR signaling at a glance. J Cell Sci, 122, 3589-94.

LI, C., QI, L., BELLAIL, A. C., HAO, C. & LIU, T. 2014. PD-0332991 induces G1 arrest of colorectal carcinoma cells through inhibition of the cyclin-dependent kinase-6 and retinoblastoma protein axis. Oncol Lett, 7, 1673-1678.

LINDSLEY, C. W., ZHAO, Z., LEISTER, W. H., ROBINSON, R. G., BARNETT, S. F., DEFEO-JONES, D., JONES, R. E., HARTMAN, G. D., HUFF, J. R., HUBER, H. E. & DUGGAN, M. E. 2005. Allosteric Akt (PKB) inhibitors: discovery and SAR of isozyme selective inhibitors. Bioorg Med Chem Lett, 15, 761-4.

LIU, R., LIU, D., TRINK, E., BOJDANI, E., NING, G. & XING, M. 2011. The Akt-specific inhibitor MK2206 selectively inhibits thyroid cancer cells harboring mutations that can activate the PI3K/Akt pathway. J Clin Endocrinol Metab, 96, E577-85.

LIVAK, K. J. & SCHMITTGEN, T. D. 2001. Analysis of relative gene expression data using real-time quantitative PCR and the 2(-Delta Delta C(T)) Method. Methods, 25, 402-8.

LODA, M., CAPODIECI, P., MISHRA, R., YAO, H., CORLESS, C., GRIGIONI, W., WANG, Y., MAGI-GALLUZZI, C. & STORK, P. J. 1996. Expression of mitogen-activated protein kinase phosphatase-1 in the early phases of human epithelial carcinogenesis. Am J Pathol, 149, 1553-64.

LOGAN, J. E., MOSTOFIZADEH, N., DESAI, A. J., E, V. O. N. E., CONKLIN, D., KONKANKIT, V., HAMIDI, H., ECKARDT, M., ANDERSON, L., CHEN, H. W., GINTHER, C.,

TASCHEREAU, E., BUI, P. H., CHRISTENSEN, J. G., BELLDEGRUN, A. S., SLAMON, D. J. & KABBINAVAR, F. F. 2013. PD-0332991, a potent and selective inhibitor of cyclin-dependent kinase 4/6, demonstrates inhibition of proliferation in renal cell carcinoma at nanomolar concentrations and molecular markers predict for sensitivity. Anticancer Res, 33, 2997-3004.

MALUMBRES, M. & BARBACID, M. 2009. Cell cycle, CDKs and cancer: a changing paradigm. Nat Rev Cancer, 9, 153-66.

MAMANE, Y., PETROULAKIS, E., LEBACQUER, O. & SONENBERG, N. 2006. mTOR, translation initiation and cancer. Oncogene, 25, 6416-22.

MANNING, B. D. & CANTLEY, L. C. 2007. AKT/PKB signaling: navigating downstream. Cell, 129, 1261-74. MARZEC, M., KASPRZYCKA, M., LAI, R., GLADDEN, A. B., WLODARSKI, P., TOMCZAK, E., NOWELL, P., DEPRIMO, S. E., SADIS, S., ECK, S., SCHUSTER, S. J., DIEHL, J. A. & WASIK, M. A. 2006. Mantle cell lymphoma cells express predominantly cyclin D1a isoform and are highly sensitive to selective inhibition of CDK4 kinase activity. Blood, 108, 1744-50.

MATTMANN, M. E., STOOPS, S. L. & LINDSLEY, C. W. 2011. Inhibition of Akt with small molecules and biologics: historical perspective and current status of the patent landscape. Expert Opin Ther Pat, 21, 1309-38.

MENDOZA, M. C., ER, E. E. & BLENIS, J. 2011. The Ras-ERK and PI3K-mTOR pathways: cross-talk and compensation. Trends Biochem Sci, 36, 320-8.

MENG, J., DAI, B., FANG, B., BEKELE, B. N., BORNMANN, W. G., SUN, D., PENG, Z., HERBST, R. S., PAPADIMITRAKOPOULOU, V., MINNA, J. D., PEYTON, M. & ROTH, J. A. 2010. Combination treatment with MEK and AKT inhibitors is more effective than each drug alone in human non-small cell lung cancer in vitro and in vivo. PLoS One, 5, e14124.

MILOWSKY, M. I., IYER, G., REGAZZI, A. M., AL-AHMADIE, H., GERST, S. R., OSTROVNAYA, I., GELLERT, L. L., KAPLAN, R., GARCIA-GROSSMAN, I. R., PENDSE, D., BALAR, A. V., FLAHERTY, A. M., TROUT, A., SOLIT, D. B. & BAJORIN, D. F. 2013. Phase II study of everolimus in metastatic urothelial cancer. BJU Int, 112, 462-70.

MOSTAFA, M. H., SHEWEITA, S. A. & O'CONNOR, P. J. 1999. Relationship between schistosomiasis and bladder cancer. Clin Microbiol Rev, 12, 97-111.

MUKHERJEE, S. 2010. The emperor of all maladies : a biography of cancer, New York, Scribner.

MURANEN, T., SELFORS, L. M., WORSTER, D. T., IWANICKI, M. P., SONG, L., MORALES, F. C., GAO, S., MILLS, G. B. & BRUGGE, J. S. 2012. Inhibition of PI3K/mTOR leads to adaptive resistance in matrix-attached cancer cells. Cancer Cell, 21, 227-39.

MURE, H., MATSUZAKI, K., KITAZATO, K. T., MIZOBUCHI, Y., KUWAYAMA, K., KAGEJI, T. & NAGAHIRO, S. 2010. Akt2 and Akt3 play a pivotal role in malignant gliomas. Neuro Oncol, 12, 221-32.

NAWROTH, R., STELLWAGEN, F., SCHULZ, W. A., STOEHR, R., HARTMANN, A., KRAUSE, B. J., GSCHWEND, J. E. & RETZ, M. 2011. S6K1 and 4E-BP1 are independent regulated and control cellular growth in bladder cancer. PLoS One, 6, e27509.

NETWORK, T. C. G. A. R. 2014. Comprehensive molecular characterization of urothelial bladder carcinoma. Nature, 507, 315-22.

NIEGISCH, G., RETZ, M., THALGOTT, M., BALABANOV, S., HONECKER, F., OHLMANN, C. H., STOCKLE, M., BOGEMANN, M., VOM DORP, F., GSCHWEND, J., HARTMANN, A., OHMANN, C. & ALBERS, P. 2015. Second-Line Treatment of Advanced Urothelial Cancer with Paclitaxel and Everolimus in a German Phase II Trial (AUO Trial AB 35/09). Oncology.

OHNISHI, Y., TAMURA, Y., YOSHIDA, M., TOKUNAGA, K. & HOHJOH, H. 2008. Enhancement of allele discrimination by introduction of nucleotide mismatches into siRNA in allele-specific gene silencing by RNAi. PLoS One, 3, e2248.

OKUZUMI, T., FIEDLER, D., ZHANG, C., GRAY, D. C., AIZENSTEIN, B., HOFFMAN, R. & SHOKAT, K. M. 2009. Inhibitor hijacking of Akt activation. Nat Chem Biol, 5, 484-93.

PHILIPS, G. K., HALABI, S., SANFORD, B. L., BAJORIN, D., SMALL, E. J., CANCER & LEUKAEMIA GROUP, B. 2008. A phase II trial of cisplatin, fixed dose-rate gemcitabine and gefitinib for advanced urothelial tract carcinoma: results of the Cancer and Leukaemia Group B 90102. BJU Int, 101, 20-5.

PLATT, F. M., HURST, C. D., TAYLOR, C. F., GREGORY, W. M., HARNDEN, P. & KNOWLES, M. A. 2009. Spectrum of phosphatidylinositol 3-kinase pathway gene alterations in bladder cancer. Clin Cancer Res, 15, 6008-17.

RADER, J., RUSSELL, M. R., HART, L. S., NAKAZAWA, M. S., BELCASTRO, L. T., MARTINEZ, D., LI, Y., CARPENTER, E. L., ATTIYEH, E. F., DISKIN, S. J., KIM, S., PARASURAMAN, S., CAPONIGRO, G., SCHNEPP, R. W., WOOD, A. C., PAWEL, B., COLE, K. A. & MARIS, J. M. 2013. Dual CDK4/CDK6 inhibition induces cell-cycle arrest and senescence in neuroblastoma. Clin Cancer Res, 19, 6173-82.

RAMPIAS, T., VGENOPOULOU, P., AVGERIS, M., POLYZOS, A., STRAVODIMOS, K., VALAVANIS, C., SCORILAS, A. & KLINAKIS, A. 2014. A new tumor suppressor role for the Notch pathway in bladder cancer. Nat Med, 20, 1199-205.

RAYASAM, G. V., TULASI, V. K., SODHI, R., DAVIS, J. A. & RAY, A. 2009. Glycogen synthase kinase 3: more than a namesake. Br J Pharmacol, 156, 885-98.

RIBATTI, D. 2014. The chick embryo chorioallantoic membrane as a model for tumor biology. Exp Cell Res, 328, 314-24.

RICCARDI, C. & NICOLETTI, I. 2006. Analysis of apoptosis by propidium iodide staining and flow cytometry. Nat Protoc, 1, 1458-61.

RIEGER, K. M., LITTLE, A. F., SWART, J. M., KASTRINAKIS, W. V., FITZGERALD, J. M., HESS, D. T., LIBERTINO, J. A. & SUMMERHAYES, I. C. 1995. Human bladder

carcinoma cell lines as indicators of oncogenic change relevant to urothelial neoplastic progression. Br J Cancer, 72, 683-90.

RISS, T. L., MORAVEC, R. A., NILES, A. L., BENINK, H. A., WORZELLA, T. J. & MINOR, L. 2004. Cell Viability Assays. In: SITTAMPALAM, G. S., GAL-EDD, N., ARKIN, M., AULD, D., AUSTIN, C., BEJCEK, B., GLICKSMAN, M., INGLESE, J., LEMMON, V., LI, Z., MCGEE, J., MCMANUS, O., MINOR, L., NAPPER, A., RISS, T., TRASK, O. J. & WEIDNER, J. (eds.) Assay Guidance Manual. Bethesda (MD).

RIVADENEIRA, D. B., MAYHEW, C. N., THANGAVEL, C., SOTILLO, E., REED, C. A., GRANA, X. & KNUDSEN, E. S. 2010. Proliferative suppression by CDK4/6 inhibition: complex function of the retinoblastoma pathway in liver tissue and hepatoma cells. Gastroenterology, 138, 1920-30.

ROSENBERG, J. E., CARROLL, P. R. & SMALL, E. J. 2005. Update on chemotherapy for advanced bladder cancer. J Urol, 174, 14-20.

ROSS, R. L., ASKHAM, J. M. & KNOWLES, M. A. 2013a. PIK3CA mutation spectrum in urothelial carcinoma reflects cell context-dependent signaling and phenotypic outputs. Oncogene, 32, 768-76.

ROSS, R. L., BURNS, J. E., TAYLOR, C. F., MELLOR, P., ANDERSON, D. H. & KNOWLES, M. A. 2013b. Identification of mutations in distinct regions of p85 alpha in urothelial cancer. PLoS One, 8, e84411.

SANGAI, T., AKCAKANAT, A., CHEN, H., TARCO, E., WU, Y., DO, K. A., MILLER, T. W., ARTEAGA, C. L., MILLS, G. B., GONZALEZ-ANGULO, A. M. & MERIC-BERNSTAM, F. 2012. Biomarkers of response to Akt inhibitor MK-2206 in breast cancer. Clin Cancer Res, 18, 5816-28.

SATHE, A., GUERTH, F., CRONAUER, M. V., HECK, M. M., THALGOTT, M., GSCHWEND, J. E., RETZ, M. & NAWROTH, R. 2014. Mutant PIK3CA controls DUSP1-dependent ERK 1/2 activity to confer response to AKT target therapy. Br J Cancer, 111, 2103-13.

SCHWARZ, D. S., HUTVAGNER, G., DU, T., XU, Z., ARONIN, N. & ZAMORE, P. D. 2003. Asymmetry in the assembly of the RNAi enzyme complex. Cell, 115, 199-208.

SCHWARZ, D. S., DING, H., KENNINGTON, L., MOORE, J. T., SCHELTER, J., BURCHARD, J., LINSLEY, P. S., ARONIN, N., XU, Z. & ZAMORE, P. D. 2006. Designing siRNA that distinguish between genes that differ by a single nucleotide. PLoS Genet, 2, e140.

SEBAUGH, J. L. 2011. Guidelines for accurate EC50/IC50 estimation. Pharm Stat, 10, 128-34.

SERONT, E., PINTO, A., BOUZIN, C., BERTRAND, L., MACHIELS, J. P. & FERON, O. 2013. PTEN deficiency is associated with reduced sensitivity to mTOR inhibitor in human bladder cancer through the unhampered feedback loop driving PI3K/Akt activation. Br J Cancer, 109, 1586-92.

SERONT, E., ROTTEY, S., SAUTOIS, B., KERGER, J., D'HONDT, L. A., VERSCHAEVE, V., CANON, J. L., DOPCHIE, C., VANDENBULCKE, J. M., WHENHAM, N., GOEMINNE, J. C., CLAUSSE, M., VERHOEVEN, D., GLORIEUX, P., BRANDERS, S., DUPONT, P.,

SCHOONJANS, J., FERON, O. & MACHIELS, J. P. 2012. Phase II study of everolimus in patients with locally advanced or metastatic transitional cell carcinoma of the urothelial tract: clinical activity, molecular response, and biomarkers. Ann Oncol, 23, 2663-70.

SHAH, M. A. & SCHWARTZ, G. K. 2001. Cell cycle-mediated drug resistance: an emerging concept in cancer therapy. Clin Cancer Res, 7, 2168-81. SHARMA, S., KS-HEERSAGAR, P. & SHARMA, P. 2009. Diagnosis and treatment of bladder cancer. Am Fam Physician, 80, 717-23.

SHE, Q. B., CHANDARLAPATY, S., YE, Q., LOBO, J., HASKELL, K. M., LEANDER, K. R., DEFEO-JONES, D., HUBER, H. E. & ROSEN, N. 2008. Breast tumor cells with PI3K mutation or HER2 amplification are selectively addicted to Akt signaling. PLoS One, 3, e3065.

SIMIONI, C., NERI, L. M., TABELLINI, G., RICCI, F., BRESSANIN, D., CHIARINI, F., EVANGELISTI, C., CANI, A., TAZZARI, P. L., MELCHIONDA, F., PAGLIARO, P., PESSION, A., MCCUBREY, J. A., CAPITANI, S. & MARTELLI, A. M. 2012. Cytotoxic activity of the novel Akt inhibitor, MK-2206, in T-cell acute lymphoblastic leukemia. Leukemia, 26, 2336-2342.

SJODAHL, G., LAUSS, M., LOVGREN, K., CHEBIL, G., GUDJONSSON, S., VEERLA, S., PATSCHAN, O., AINE, M., FERNO, M., RINGNER, M., MANSSON, W., LIEDBERG, F., LINDGREN, D. & HOGLUND, M. 2012. A molecular taxonomy for urothelial carcinoma. Clin Cancer Res, 18, 3377-86.

SLAMON, D., EIERMANN, W., ROBERT, N., PIENKOWSKI, T., MARTIN, M., PRESS, M., MACKEY, J., GLASPY, J., CHAN, A., PAWLICKI, M., PINTER, T., VALERO, V., LIU, M. C., SAUTER, G., VON MINCKWITZ, G., VISCO, F., BEE, V., BUYSE, M., BENDAHMA-NE, B., TABAH-FISCH, I., LINDSAY, M. A., RIVA, A., CROWN, J. & BREAST CANCER INTERNATIONAL RESEARCH, G. 2011. Adjuvant trastuzumab in HER2-positive breast cancer. N Engl J Med, 365, 1273-83.

STERNBERG, C. N. & VOGELZANG, N. J. 2003. Gemcitabine, paclitaxel, pemetrexed and other newer agents in urothelial and kidney cancers. Crit Rev Oncol Hematol, 46 Suppl, S105-15.

THE CANCER GENOME ATLAS RESEARCH, N. 2014. Comprehensive molecular characterization of urothelial bladder carcinoma. Nature.

TSURUTA, H., KISHIMOTO, H., SASAKI, T., HORIE, Y., NATSUI, M., SHIBATA, Y., HAMADA, K., YAJIMA, N., KAWAHARA, K., SASAKI, M., TSUCHIYA, N., ENOMOTO, K., MAK, T. W., NAKANO, T., HABUCHI, T. & SUZUKI, A. 2006. Hyperplasia and carcinomas in Pten-deficient mice and reduced PTEN protein in human bladder cancer patients. Cancer Res, 66, 8389-96.

VAN DEN HEUVEL, S. 2005. Cell-cycle regulation. WormBook, 1-16.

VON DER MAASE, H., SENGELOV, L., ROBERTS, J. T., RICCI, S., DOGLIOTTI, L., OLIVER, T., MOORE, M. J., ZIMMERMANN, A. & ARNING, M. 2005. Long-term survival results of a randomized trial comparing gemcitabine plus cisplatin, with methotrexate,

vinblastine, doxorubicin, plus cisplatin in patients with bladder cancer. J Clin Oncol, 23, 4602-8.

VORA, S. R., JURIC, D., KIM, N., MINO-KENUDSON, M., HUYNH, T., COSTA, C., LOCKERMAN, E. L., POLLACK, S. F., LIU, M., LI, X., LEHAR, J., WIESMANN, M., WARTMANN, M., CHEN, Y., CAO, Z. A., PINZON-ORTIZ, M., KIM, S., SCHLEGEL, R., HUANG, A. & ENGELMAN, J. A. 2014. CDK 4/6 inhibitors sensitize PIK3CA mutant breast cancer to PI3K inhibitors. Cancer Cell, 26, 136-49.

WAGLE, N., GRABINER, B. C., VAN ALLEN, E. M., HODIS, E., JACOBUS, S., SUPKO, J. G., STEWART, M., CHOUEIRI, T. K., GANDHI, L., CLEARY, J. M., ELFIKY, A. A., TAPLIN, M. E., STACK, E. C., SIGNORETTI, S., LODA, M., SHAPIRO, G. I., SABATINI, D. M., LANDER, E. S., GABRIEL, S. B., KANTOFF, P. W., GARRAWAY, L. A. & ROSENBERG, J. E. 2014. Activating mTOR mutations in a patient with an extraordinary response on a phase I trial of everolimus and pazopanib. Cancer Discov, 4, 546-53.

WATSON, K. L. & MOOREHEAD, R. A. 2013. Loss of Akt1 or Akt2 delays mammary tumor onset and suppresses tumor growth rate in MTB-IGFIR transgenic mice. BMC Cancer, 13, 375.

WIEDEMEYER, W. R., DUNN, I. F., QUAYLE, S. N., ZHANG, J., CHHEDA, M. G., DUNN, G. P., ZHUANG, L., ROSENBLUH, J., CHEN, S., XIAO, Y., SHAPIRO, G. I., HAHN, W. C. & CHIN, L. 2010. Pattern of retinoblastoma pathway inactivation dictates response to CDK4/6 inhibition in GBM. Proc Natl Acad Sci U S A, 107, 11501-6.

WILL, M., QIN, A. C., TOY, W., YAO, Z., RODRIK-OUTMEZGUINE, V., SCHNEIDER, C., HUANG, X., MONIAN, P., JIANG, X., DE STANCHINA, E., BASELGA, J., LIU, N., CHANDARLAPATY, S. & ROSEN, N. 2014. Rapid induction of apoptosis by PI3K inhibitors is dependent upon their transient inhibition of RAS-ERK signaling. Cancer Discov, 4, 334-347.

WITJES, J. A., COMPERAT, E., COWAN, N. C., DE SANTIS, M., GAKIS, G., LEBRET, T., RIBAL, M. J., VAN DER HEIJDEN, A. G. & SHERIF, A. 2013. EAU Guidelines on Muscle-invasive and Metastatic Bladder Cancer: Summary of the 2013 Guidelines. Eur Urol.

WITJES, J. A., COMPERAT, E., COWAN, N. C., DE SANTIS, M., GAKIS, G., LEBRET, T., RIBAL, M. J., VAN DER HEIJDEN, A. G., SHERIF, A. & EUROPEAN ASSOCIATION OF, U. 2014. EAU guidelines on muscle-invasive and metastatic bladder cancer: summary of the 2013 guidelines. Eur Urol, 65, 778-92.

WOLFF, E. M., CHIHARA, Y., PAN, F., WEISENBERGER, D. J., SIEGMUND, K. D., SUGANO, K., KAWASHIMA, K., LAIRD, P. W., JONES, P. A. & LIANG, G. 2010. Unique DNA methylation patterns distinguish noninvasive and invasive urothelial cancers and establish an epigenetic field defect in premalignant tissue. Cancer Res, 70, 8169-78.

WU, X. R. 2005. Urothelial tumorigenesis: a tale of divergent pathways. Nat Rev Cancer, 5, 713-25.

XU, W., KASPER, L. H., LERACH, S., JEEVAN, T. & BRINDLE, P. K. 2007. Individual CREB-target genes dictate usage of distinct cAMP-responsive coactivation mechanisms. EMBO J, 26, 2890-2903.

YAP, T. A., YAN, L., PATNAIK, A., FEAREN, I., OLMOS, D., PAPADOPOULOS, K., BAIRD, R. D., DELGADO, L., TAYLOR, A., LUPINACCI, L., RIISNAES, R., POPE, L. L., HEATON, S. P., THOMAS, G., GARRETT, M. D., SULLIVAN, D. M., DE BONO, J. S. & TOLCHER, A. W. 2011. First-in-man clinical trial of the oral pan-AKT inhibitor MK-2206 in patients with advanced solid tumors. J Clin Oncol, 29, 4688-95.

YOUNG, R. J., WALDECK, K., MARTIN, C., FOO, J. H., CAMERON, D. P., KIRBY, L., DO, H., MITCHELL, C., CULLINANE, C., LIU, W., FOX, S. B., DUTTON-REGESTER, K., HAYWARD, N. K., JENE, N., DOBROVIC, A., PEARSON, R. B., CHRISTENSEN, J. G., RANDOLPH, S., MCARTHUR, G. A. & SHEPPARD, K. E. 2014. Loss of CDKN2A expression is a frequent event in primary invasive melanoma and correlates with sensitivity to the CDK4/6 inhibitor PD0332991 in melanoma cell lines. Pigment Cell Melanoma Res, 27, 590-600.

ZHAO, J. J., LIU, Z., WANG, L., SHIN, E., LODA, M. F. & ROBERTS, T. M. 2005. The oncogenic properties of mutant p110alpha and p110beta phosphatidylinositol 3-kinases in human mammary epithelial cells. Proc Natl Acad Sci U S A, 102, 18443-8.

ZHAO, L. & VOGT, P. K. 2008. Helical domain and kinase domain mutations in p110alpha of phosphatidylinositol 3-kinase induce gain of function by different mechanisms. Proc Natl Acad Sci U S A, 105, 2652-7.

ZIMMERMANN, S. 1999. Phosphorylation and Regulation of Raf by Akt (Protein Kinase B). Science, 286, 1741-1744.

Publications

SATHE, A., GUERTH, F., CRONAUER, M. V., HECK, M. M., THALGOTT, M., GSCHWEND, J. E., RETZ, M. & NAWROTH, R. 2014. Mutant PIK3CA controls DUSP1-dependent ERK 1/2 activity to confer response to AKT target therapy. Br J Cancer, 111, 2103-13.

SATHE, A., KOSHY, N., SCHMID, S. C., THALGOTT, M., SCHWARZENBOCK, S. M., KRAUSE, B. J., HOLM, P. S., GSCHWEND, J. E., RETZ, M. & NAWROTH, R. 2015. CDK4/6-inhibition controls proliferation of bladder cancer and transcription of RB1. J Urol.